

AD-765 354

THEORETICAL STUDIES OF HIGH-POWER  
INFRARED WINDOW MATERIALS

M. Sparks

Xonics, Incorporated

Prepared for:

Advanced Research Projects Agency  
Defense Supply Service

30 June 1973

DISTRIBUTED BY:

**NTIS**

National Technical Information Service  
U. S. DEPARTMENT OF COMMERCE  
5285 Port Royal Road, Springfield Va. 22151

AD-765 354

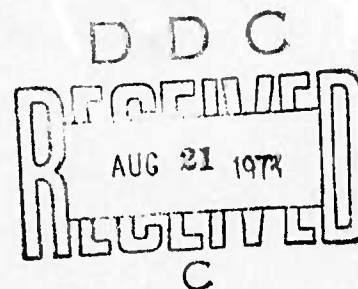
THEORETICAL STUDIES OF HIGH-POWER  
INFRARED WINDOW MATERIALS

M. Sparks, Principal Investigator, 213/787-7380

Xonics, Incorporated  
Van Nuys, California 91406

First Technical Report

30 June 1973



Contract No. DAHC15-73-C-0127

Effective Date of Contract: 7 December 1972

Contract Expiration Date: 6 December 1973

Reproduced by  
NATIONAL TECHNICAL  
INFORMATION SERVICE  
U S Department of Commerce  
Springfield VA 22151

Prepared for  
Defense Supply Service - Washington, D. C.

Sponsored by Advanced Research Projects Agency  
ARPA Order No. 1969, Amendment No. 1; Program Code No. 3D10

"This research was supported by the Advanced Research Projects Agency of the Department of Defense and was monitored by the Defense Supply Service-Washington, D.C. under Contract No. DAHC15-73-C-0127. The views and conclusions contained in this document are those of the authors and should not be interpreted as necessarily representing the official policies, either expressed or implied, of the Advanced Research Projects Agency or the U. S. Government."

DISTRIBUTION STATEMENT A

Approved for public release;  
Distribution Unlimited

185

## TABLE OF CONTENTS

|  | <u>Page</u> |
|--|-------------|
| Preface . . . . .  | vi          |
| Summary . . . . .  | 1           |
| A. Introduction . . . . .  | 4           |
| B. Theory of Infrared Absorption and Material Failure in Crystals<br>Containing Inclusions . . . . .                         | 9           |
| I. Introduction . . . . .  | 10          |
| II. Analysis of Absorption Cross Sections . . . . .  | 12          |
| III. Absorption Efficiencies for Various Types of Inclusions . . . . .   | 18          |
| IV. Material Failure from Local Heating . . . . .  | 22          |
| V. Conclusions . . . . .   | 38          |
| C. Theory of Multiphonon Absorption in Insulating Crystals . . . . .   | 42          |
| I. Introduction . . . . .  | 43          |
| II. Anharmonic Contribution to the Absorption Coefficient . . . . .  | 48          |
| III. Asymptotic Approximation for Absorption by a Large Number<br>of Phonons . . . . .                                       | 55          |
| IV. The Confluence Processes . . . . .   | 58          |
| V. Vertex Corrections . . . . .  | 59          |
| VI. Frequency and Temperature Dependence of the Absorption<br>Coefficient . . . . .  | 71          |
| VII. Assumptions and Approximations . . . . .  | 84          |
| D. Temperature Dependence of Multiphonon Infrared Absorption . . . . .   | 89          |
| E. Theory of Infrared Absorption by Crystals in the High Frequency<br>Wing of Their Fundamental Lattice Absorption . . . . . | 101         |
| I. Introduction . . . . .  | 103         |
| II. General Theory . . . . .   | 109         |

## TABLE OF CONTENTS (Cont'd)

|   | <u>Page</u> |
|---|-------------|
| III. Applications of the Formalism to the Study of Multiphonon<br>Absorption for Some Specific Potentials . . . . . | 123         |
| IV. General Discussion . . . . .  | 137         |
| F. Temperature Dependence of the Absorption Coefficient of Alkali<br>Halides in the Multiphonon Regime . . . . .    | 153         |
| G. Temperature and Frequency Dependence of Infrared Absorption<br>as a Diagnostic Tool . . . . .                    | 167         |
| H. Short-Pulse Operation of Infrared Windows without Thermal<br>Defocusing . . . . .                                | 173         |

# LIST OF ILLUSTRATIONS

| <u>Section</u> | <u>Figure</u> | <u>Title</u>   | <u>Page</u> |
|----------------|---------------|--|-------------|
| B              | 1             | Absorption efficiency of a spherical metallic inclusion as a function of radius  | 16          |
|                | 2             | Temperature at the center of a spherical inclusion as a function of time in the case of volume heating   | 26          |
|                | 3             | Temperature at the surface of a spherical inclusion as a function of time in the case of surface heating   | 30          |
|                | 4             | Temperature at the surface of a metallic inclusion as a function of radius for various pulse durations   | 33          |
|                | 5             | Temperature of a dielectric inclusion as a function of radius  | 36          |
| C              | 1             | Experimental frequency dependence of the infrared absorption coefficient $\beta$ for NaCl  | 44          |
|                | 2             | n-phonon summation and confluence processes  | 46          |
|                | 3             | Various kinds of vertices  | 60          |
|                | 4             | Three-phonon summation processes   | 61          |
|                | 5             | The n-phonon absorption vertices   | 65          |
|                | 6             | The 4-phonon absorption vertices   | 68          |
|                | 7             | The 5-phonon absorption vertices   | 69          |
|                | 8             | The 6-phonon absorption vertices   | 70          |
|                | 9             | Phonon density of states in NaCl and the Debye approximation   | 75          |
|                | 10            | Theoretical estimates of $\beta_n$ at room temperature for NaCl  | 77          |
|                | 11            | Phonon self-energy terms of order $\epsilon^2$   | 79          |
| D              | 1             | Comparison of experimental points of Harrington and Hoss (NaF, $943\text{ cm}^{-1}$ ) and Barker (KBr, $418\text{ cm}^{-1}$ ) with theoretical curves fit to the data at 300 K | 95          |

# LIST OF ILLUSTRATIONS (Cont'd)

| <u>Section</u> | <u>Figure</u> | <u>Title</u>   | <u>Page</u> |
|----------------|---------------|--|-------------|
| E              | 1             | Comparison between the multiphonon data in KCl, and the non-interacting oscillator model, for the case where the motion of the oscillator is governed by the Morse potential | 140         |
| F              | 1             | Frequency dependence of the absorption coefficient for a Morse potential oscillator at $T = 300^\circ\text{K}$ and $900^\circ\text{K}$ , with a $D$ chosen for NaCl          | 158         |
|                | 2             | Temperature dependence of the absorption coefficient at $10.6\mu$ in (a) NaCl and (b) NaF  | 162         |

## PREFACE

This First Technical Report describes the work performed on Contract DAHC15-73-C-0127 on Theoretical Studies of High-Power Infrared Window Materials during the period from December 7, 1972 through June 30, 1973. The work on the present contract is a continuation of that of the previous Contract DAHC15-72-C-0129.

The following investigators contributed to this report:

Mr. H. C. Chow, research associate

Dr. C. J. Duthler, principal research scientist

Dr. A. M. Karo, consultant, Lawrence Livermore Laboratory,  
Livermore, California

Dr. A. A. Maradudin, consultant, University of California, Irvine, California

Dr. D. L. Mills, consultant, University of California, Irvine, California

Mr. A. Moreira, research associate

Dr. L. J. Sham, consultant, University of California, San Diego, California

Dr. M. Sparks, principal investigator

The material in this report constitutes the final results on the subjects covered. The preliminary discussions of the theory of infrared absorption and material failure in crystals containing inclusions and of the theory of multiphonon infrared absorption presented in the reports of the preceding contract DAHC15-72-C-0129 are superseded by the results of the present report. In particular, the section on the effect of inclusion of optical absorption in the previous Final Report contained an error, which fortunately is not of practical consequence. The appropriate value of reflection is the average value  $\langle R \rangle$  rather than the perpendicular incidence value  $R_{\perp}$ .

## SUMMARY

Theory of Infrared Absorption and Material Failure in Crystals Containing Inclusions. Two effects of inclusions in or on the surface of infrared-transmitting materials are to increase the average value of the optical absorption coefficient  $\beta$  and to cause localized heating that could lead to material failure at high-power levels. Volume fractions as low as  $10^{-7}$  to  $10^{-8}$  of such inclusions can give rise to a value of the optical absorption coefficient  $\beta$  of  $10^{-4} \text{ cm}^{-1}$ , a typical value of current interest. For various types of inclusions, the frequency dependence of  $\beta$  ranges from increasing as  $\omega^2$ , to independent of  $\omega$ , to exponentially decreasing with  $\omega$ . The temperature dependence ranges from independent of  $T$ , to increasing as  $T^p$  in the high-temperature limit, where  $p \approx 2-4$  typically. Simple expressions for the absorption cross section are derived for various cases of practical interest. The cross sections are used to derive expressions for  $\beta$  for the four cases of large inclusions of strong and weak absorbers and of small inclusions of dielectric and metallic particles. The material failure resulting from local heating of inclusions is a far greater problem in high-intensity short-pulse systems than in low-intensity long-pulse or cw systems having the same average intensity. Microsecond pulses with energy densities as low as a few joules per square centimeter can cause material failure.

Theory of Multiphonon Absorption in Insulating Crystals. The nearly exponential frequency dependence of the infrared absorption coefficient  $\beta$  recently observed in fifteen crystals up to several times the reststrahl frequency is explained in terms of multiphonon absorption processes. The central-limit theorem is used to reduce the multiphonon contribution to a simple closed form. The theoretical estimates for the magnitude of the absorption coefficient, with no adjustable

parameters, are also in good agreement with experiment. The temperature dependence of  $\beta$  at a fixed frequency is shown to be considerably weaker than  $\beta \sim T^{n-1}$ , where  $n$  is the number of created phonons. Higher-order processes in the perturbation expansion are shown to be negligible for small  $n$ , to be comparable to that of the lowest-order, single-vertex terms for  $n \approx 5$ , and to dominate for large  $n$  in a typical case. Difference processes, in which some thermally excited phonons are annihilated, are shown to be negligible with respect to the summation processes in the nearly exponential region. An explanation involving finite phonon lifetimes is proposed to explain the fact that the alkali halides show less structure in the  $\beta - \omega$  curves than do the semiconductor crystals.

Temperature Dependence of Multiphonon Infrared Absorption. Measurements of Harrington and Hass and of Barker indicate that the temperature dependence of the infrared absorption coefficient  $\beta$  in the  $n$ -phonon region is considerably weaker than  $\beta \sim T^{n-1}$ , which had been predicted for the high-temperature limit of multiphonon absorption. This discrepancy is resolved by taking into account the temperature dependence of the phonon frequencies and the lattice constant. The agreement between the experimental and theoretical results with no adjustable parameters is good. A new evaluation of the multiphonon sums yields  $\beta \sim \exp(-\omega \tau)$  directly, rather than as a sum on  $n$ .

Theory of Infrared Absorption by Crystals in the High Frequency Wing of Their Fundamental Lattice Absorption. We have calculated the frequency dependence of infrared absorption in the classical limit for an exactly soluble model of a lattice of noninteracting diatomic molecules, each bound internally by a potential for which the classical equation of motion can be solved in closed form. Four potentials have been used: a Morse potential, a potential of the form  $V(x) = (a/x^2) + bx^2$ ,

an infinite square well potential, and a triangular well potential. The analytic results we obtain show that the absorption coefficient for large frequencies associated with potentials which admit an harmonic approximation decreases nearly exponentially over the frequency region covered by recent experiments, with significant deviations from exponential behavior at higher frequencies. For the square and triangular well potentials, the absorption decreases like  $\omega^{-2}$  for frequencies large compared to a characteristic frequency.

Temperature Dependence of the Absorption Coefficient of Alkali Halides in the Multiphonon Regime. The theory of infrared absorption by an array of independent, anharmonic oscillators is discussed. When the oscillator potential is the Morse potential, the theory provides an excellent description of the temperature dependence of the absorption coefficient at  $10.6\mu$  in NaCl and NaF reported by Harrington and Hass.

Temperature and Frequency Dependence of Infrared Absorption as a Diagnostic Tool. Recent developments render untenable a proposed method of distinguishing between intrinsic and extrinsic infrared absorption on the basis of the proposed temperature dependence. However, when the proper temperature dependence of multiphonon absorption is accounted for and the possibility of other intrinsic processes is taken into account, the temperature and frequency dependence of the absorption of both the best available and intentionally imperfect crystals should be useful in studying extrinsic processes.

Short-Pulse Operation of Infrared Windows without Thermal Defocusing. The possibility of transmitting short infrared pulses through materials with little thermally induced optical distortion is shown to exist. For sufficiently short pulses, of the order of  $10^{-8}$  -  $10^{-9}$  sec, the absorbed energy does not have time to thermalize. Thus, the thermally induced optical distortion is greatly reduced.

## A. INTRODUCTION

The motivation for this program on theoretical studies of high-power infrared window materials, which is a continuation of a previous contract DAHC15-72-C-0129, was the availability of high-power infrared lasers for current Department of Defense programs and the realization that lack of transparent materials for windows may limit the usefulness of many laser systems. Values of the optical absorption coefficient  $\beta$  of candidate window materials were needed in order to evaluate the potential performance of the materials. There had been no previous calculations of the numerical values of  $\beta$  in the highly transparent regions for materials of interest (such as KBr and ZnSe at  $10.6\mu\text{m}$ ), and the currently available corresponding experimental values were of questionable efficacy since they were believed to be extrinsic (i.e., caused by imperfections that can be removed in principle.).

The paucity of experimental and theoretical information on the values of  $\beta$  was one of the most pressing problems in the present Department of Defense high-power-window programs. It was especially important to know if the values of  $\beta$  were intrinsic or extrinsic and to have reliable estimates of the intrinsic value of  $\beta$  before undertaking imperfection-identification and sample-purification programs since there were many candidate materials and these expensive programs should be undertaken only if there were a good chance of reducing  $\beta$  to the required value.

During the early stages of the previous contract it became increasingly apparent that in order to obtain this information on  $\beta$ , theoretical and experimental values of  $\beta$  were needed not only at  $10.6\mu\text{m}$ , but also over a large range of values of frequencies and temperature. In the intervening eighteen months there has been considerable progress in our theoretical program and in experimental and theoretical

## Sec. A

programs at other laboratories. We have explained quantitatively the nearly exponential frequency dependence of the optical absorption frequency  $\beta$  observed by Rupprecht and by Deutsch and the substantial deviations from the expected temperature dependence observed by Harrington and Hass. The calculations are based on a reasonable model of the lattice with the Born-Mayer interaction potential. They include the dispersion relations of the phonons, and the approximations made were shown to be reasonable. The theory of intrinsic multiphonon absorption now appears to be complete, and the emphasis of the program has shifted to extrinsic and nonlinear and other high-power absorption mechanisms. Although no attempt will be made to review the progress of other laboratories, it should be mentioned that the Raytheon measurements of  $\beta(\omega)$  and our theoretical prediction that there should be no drastic deviations from the extrapolations of the measured  $\beta(\omega)$  have settled the question of whether the values of  $\beta$  measured at  $10.6\mu\text{m}$  are intrinsic or extrinsic for most materials of interest and have afforded estimates of the intrinsic values. With the exception of KCl, the estimated intrinsic values of  $\beta_{10.6}$  for candidate  $10.6\mu\text{m}$  window materials are well below the lowest measured values.

A study (Sec. C) of the effects of macroscopic inclusions in crystals, including the increase in absorption and damage thresholds, has been completed. A study of a proposed quasi-selection rule for absorption and the first phase of a study of the effects on absorption of parametric processes are nearing completion, and a number of other problems, listed below, are under investigation. The following publications and reports have been prepared under this and the previous contract:

Sec. A

M. Sparks and T. Azzarelli, "Theoretical Studies of High-Power Infrared Window Materials," Xonics Quarterly Technical Progress Report No. 1, Contract DAHC15-72-C-0129, March 1972.

M. Sparks, "Recent Developments in High-Power Infrared Window Research," Invited Talk, 4th ASTM Damage in Laser Materials Symposium, Boulder, Colorado, June 14-15, 1972.

M. Sparks and T. Azzarelli, "Theoretical Studies of High-Power Infrared Window Materials," Xonics Quarterly Technical Progress Report No. 2, Contract DAHC15-72-C-0129, June 1972.

M. Sparks and L. J. Sham, "Theory of Multiphonon Infrared Absorption," AFCRL Conference on High-Power Infrared Laser Window Materials, Hyannis, Massachusetts, Oct. 30-Nov. 1, 1972.

M. Sparks and M. Cottis, "Pressure-Induced Optical Distortion in Infrared Windows," AFCRL Conference on High Power Infrared Laser Window Materials, Hyannis, Massachusetts, Oct. 30-Nov. 1, 1972.

M. Sparks and L. J. Sham, "Exponential Frequency Dependence of Multiphonon Summation Infrared Absorption," Solid State Commun. 11, 1451 (1972).

M. Sparks, "Theoretical Studies of High-Power Infrared Window Materials," Xonics Final Report, Contract DAHC15-72-C-0129, December 1972.

M. Sparks and M. Cottis, "Pressure-Induced Optical Distortion in Laser Windows," J. Appl. Phys. 44, 787 (1973).

M. Sparks, "Stress and Temperature Analysis for Surface Cooling or Heating of Laser Window Materials," J. Appl. Phys., in press, September 1973.

M. Sparks and C. J. Duthler, "Theory of Infrared Absorption and Material Failure in Crystals Containing Inclusions," J. Appl. Phys., in press, July 1973.

M. Sparks and L. J. Sham, "Theory of Multiphonon Absorption in Insulating Crystals," Phys. Rev., in press.

M. Sparks, "Short-Pulse Operation of Infrared Windows without Thermal Defocusing," Appl. Opt., in press.

## Sec. A

M. Sparks and L. J. Sham, "Temperature Dependence of Infrared Absorption," submitted to Phys. Rev. Letters.

C. J. Duthler and M. Sparks, "Theory of Material Failure in Crystals Containing Infrared Absorbing Inclusions," ASTM 1973 Symposium on Damage in Laser Materials, Boulder, Colorado, May 15-16, 1973.

M. Sparks, "Temperature and Frequency Dependence of Infrared Absorption as a Diagnostic Tool," submitted to Appl. Phys. Letters.

D. L. Mills and A. A. Maradudin, "Theory of Infrared Absorption by Crystals in the High Frequency Wing of Their Fundamental Lattice Absorption," Phys. Rev., in press.

A. A. Maradudin and D. L. Mills, "Temperature Dependence of the Absorption Coefficient of Alkali Halides in the Multiphonon Regime," submitted to Phys. Rev. Letters.

C. J. Duthler and M. Sparks, "Quasi-Selection Rule for Infrared Absorption by NaCl-Structure Crystals," to be published.

C. J. Duthler and R. Hellwarth, "Mechanism for Surface Damage in Laser Window Materials," to be published.

M. Sparks and H. C. Chow, "Nonlinear Infrared Absorption: Parametric Instabilities of Phonons," to be published.

L. J. Sham and M. Sparks, "Explicit Exponential Frequency Dependence of Multiphonon Infrared Absorption," to be published.

The following topics will be covered in the final report:

- Parametric processes in infrared absorption
- Infrared absorption by imperfections in crystals; ionic impurities, dislocations, band-mode plus impurity mode absorption, and surface imperfections
- Quasi-selection rule for infrared absorption
- Explicit exponential frequency dependence of multiphonon infrared absorption
- Numerical evaluation of multiphonon absorption coefficients

## Sec. A

- Explanation of surface damage cones observed in high-power laser experiments
- Explanation of well known anomalies in stimulated Raman and Brillouin scattering and moving focus filaments
- Relative strengths of anharmonic interaction and higher-order-dipole interaction in infrared absorption
- Ultraviolet-induced infrared absorption.

B. THEORY OF INFRARED ABSORPTION AND MATERIAL  
FAILURE IN CRYSTALS CONTAINING INCLUSIONS

M. Sparks and C. J. Duthler

Xonics, Incorporated, Van Nuys, California 91406

Two effects of inclusions in or on the surface of infrared-transmitting materials are to increase the average value of the optical absorption coefficient  $\beta$  and to cause localized heating that could lead to material failure at high-power levels. Volume fractions as low as  $10^{-7}$  to  $10^{-8}$  of such inclusions can give rise to a value of the optical absorption coefficient  $\beta$  of  $10^{-4} \text{ cm}^{-1}$ , a typical value of current interest. For various types of inclusions, the frequency dependence of  $\beta$  ranges from increasing as  $\omega^2$ , to independent of  $\omega$ , to exponentially decreasing with  $\omega$ . The temperature dependence ranges from independent of  $T$ , to increasing as  $T^p$  in the high-temperature limit, where  $p \approx 2 - 4$  typically. Simple expressions for the absorption cross section are derived for various cases of practical interest. The cross sections are used to derive expressions for  $\beta$  for the four cases of large inclusions of strong and weak absorbers and of small inclusions of dielectric and metallic particles. The material failure resulting from local heating of inclusions is a far greater problem in high-intensity short-pulse systems than in low-intensity long-pulse or cw systems having the same average intensity. Microsecond pulses with energy densities as low as a few joules per square centimeter can cause material failure.

## I. INTRODUCTION

The problem of obtaining highly transparent window materials for high-power infrared laser systems is of considerable interest.<sup>1,2</sup> In particular, there is great interest in lowering the value of  $\beta$  for candidate materials such as ZnSe, CdTe, KCl, KBr, and TI 1173 glass ( $\text{Ge}_{28}\text{Sb}_{12}\text{Se}_{60}$ ). Materials having values of  $\beta$  at least as low as  $10^{-4} \text{ cm}^{-1}$  are needed. It has been shown<sup>3</sup> that the absorption with  $\beta$  decaying exponentially with frequency  $\omega$ , observed in a number of materials,<sup>4</sup> is intrinsic and results from multiphonon absorption.

The present investigation is concerned with another aspect of the problem -- that of extrinsic absorption by macroscopic inclusions either in the bulk of the crystals or on their surfaces. The results of this investigation are of practical interest since it is believed the current experimental values of  $\beta$  for all candidate window materials for high-power  $10.6 \mu\text{m}$  systems are extrinsic.<sup>5-7</sup> The temperature and frequency dependence of  $\beta$  derived in Sec. III should be useful in experiments to determine whether  $\beta$  is intrinsic or extrinsic, especially as improved materials become available.

Two aspects of optical absorption by inclusions are considered. First, the spatial average of  $\beta$  is increased, thus increasing the overall heating of the material. Second, the local heating in the region of an inclusion can lead to material failure. The overall increase in the value of  $\beta$  can cause either irreversible system failure, such as thermally induced fracture, or reversible failure, such as thermal defocusing of the laser beam by the heated window.<sup>5-7</sup>

## Sec. B

For sufficiently large concentrations of inclusions, the localized heating can also cause considerable optical degradation of the beam. In the present study it is assumed that the concentration of inclusions is so small that this localized-heating type of optical distortion is negligible. However, it should be mentioned that scattering may be considerably greater at high-power levels than at low levels as a result of the scattering by the heated host material near the inclusion. This effect should be greatest for scattering near the forward angle.

Local material failure at discrete inclusion sites has been observed and studied by others.<sup>8,9</sup> In these treatments, which were concerned with metallic inclusions in glass hosts, the absorption cross section  $\sigma_{\text{abs}} = \epsilon_{\lambda} \pi a^2$  was used, where  $\epsilon_{\lambda}$  is the bulk emissivity of the inclusion material and  $a$  is the inclusion radius. The resulting errors in  $\sigma_{\text{abs}}$  can be large, especially for inclusions with diameters less than the laser wavelength. The heating in transparent hosts of both dielectric and metallic spherical inclusions will be considered as a function of inclusion radius and laser pulse length, using more realistic models for the absorption cross section and for the heat transfer from the inclusion to the host.

Absorption is of greater interest than scattering in the study of high-power infrared windows. A value of  $\beta = 10^{-4} \text{ cm}^{-1}$  for the absorption coefficient can cause sufficient heating for the system to fail, for example, by thermal defocusing or by window fracture. But an equal amount of scattering  $\beta_{\text{scat}} = 10^{-4} \text{ cm}^{-1}$  may be tolerable. Thus, scattering will be neglected here, except to mention that observation of the associated scattering may help to identify the absorption mechanism in some cases. Winsor<sup>10</sup> has shown theoretically that scattering, especially in conjunction with total internal reflection at the host-crystal boundaries, may increase the measured value of  $\beta$  by increasing the path lengths of the rays in the crystal.

## II. ANALYSIS OF ABSORPTION CROSS SECTIONS

In this section, the absorption cross section of an individual spherical inclusion of radius  $a$  will be considered. The absorption cross section is not generally equal to the geometrical cross section  $\pi a^2$ . For  $ka \ll 1$ , where  $k = 2\pi/\lambda_H$ , with  $\lambda_H$  the wavelength of the radiation in the host material, the value of  $\sigma_{\text{abs}}$  typically is small ( $\sigma_{\text{abs}} \ll \pi a^2$ ). In the case of  $ka \gg 1$  and  $|\epsilon| \gg 1$ , where  $\epsilon = \epsilon_I/\epsilon_H$ , with  $\epsilon_I$  and  $\epsilon_H$  the dielectric constants of the inclusion and host, respectively, the reflection at the surface of the sphere is great, which again makes  $\sigma_{\text{abs}} \ll \pi a^2$ . Exact absorption cross sections for spheres of arbitrary size can be obtained from the classic result of Mie.<sup>11, 12</sup> The Mie solutions are complicated in general, but reduce to simple results in the limits  $ka \gg 1$  and  $ka \ll 1$ .

For small spheres ( $ka \ll 1$ ), the Mie series is well approximated by the first term, which yields

$$\sigma_{\text{abs}} \cong \frac{12 \epsilon_g ka}{(\epsilon_R + 2)^2 + \epsilon_g^2} \pi a^2, \quad \text{for } ka \ll 1, \quad (2.1)$$

where  $\epsilon = \epsilon_R + i \epsilon_g$ . Two limiting cases of (2.1) are of interest. For  $\epsilon_g \ll \epsilon_R$ , which is satisfied for nonmetals at frequencies not too near the fundamental resonance frequency or the high-frequency absorption edge,  $\beta_I$  and  $\epsilon_g$  are related by the expression

$$\beta_I = 2 n_g k \cong \frac{\epsilon_g k}{n_R}, \quad (2.2)$$

where  $n = n_R + i n_g$ . Using this result to eliminate  $\epsilon_g k$  in (2.1) gives

$$\sigma_{\text{abs}} = \frac{12 n_R}{(\epsilon_R + 2)^2} (\beta_I a) \pi a^2, \quad \epsilon_g \ll \epsilon. \quad (2.3)$$

The second limiting case of (2.1) is that of small metallic inclusions. The Drude expression for the dielectric constant is<sup>13</sup>

$$\epsilon = \epsilon_\infty - \frac{\omega_p^2}{\epsilon_H(\omega^2 + i\omega\Gamma)}, \quad (2.4)$$

where  $\Gamma$  is the electron relaxation frequency (often written as  $1/\tau$ ),  $\epsilon_\infty$  is the contribution to  $\epsilon$  from the core electrons, and  $\omega_p = (4\pi Ne^2/m)^{1/2}$  is the plasma frequency, which has a typical value of  $\omega_p = 5 \times 10^{15} \text{ sec}^{-1}$ . At  $10.6 \mu\text{m}$ ,  $\omega \approx 1.9 \times 10^{14} \text{ sec}^{-1}$ . There are two contributions to the relaxation frequency  $\Gamma$ :  $\Gamma = \Gamma_{\text{Bu}} + \Gamma_{\text{Su}}$ , where the bulk contribution  $\Gamma_{\text{Bu}}$  has a typical value<sup>13</sup> of  $\Gamma_{\text{Bu}} \approx 5 \times 10^{13} \text{ sec}^{-1}$ . The value of the surface scattering contribution<sup>14</sup>  $\Gamma_{\text{Su}}$  is  $\sim v_F/a$ , where the Fermi velocity  $v_F$  has the value  $v_F \approx 10^8 \text{ cm/sec}$  for many metals. With  $\Gamma_{\text{Bu}} \approx 5 \times 10^{13} \text{ sec}^{-1}$  and  $v_F \approx 10^8 \text{ cm/sec}$ ,  $\Gamma_{\text{Su}} > \Gamma_{\text{Bu}}$  for  $a < a_\Gamma \approx 200 \text{ \AA}$ .

For typical metals at  $10.6 \mu\text{m}$ ,  $\omega_p^2 \gg |\omega^2 + i\omega\Gamma|$ , and (2.4) gives

$$\epsilon \epsilon_H \approx - \frac{\omega_p^2}{\omega^2 + i\omega\Gamma} = - \frac{\omega_p^2}{\omega^2 + \Gamma^2} \left( 1 - i \frac{\Gamma}{\omega} \right), \quad \epsilon_R + 2 \approx \epsilon_R. \quad (2.5)$$

Both the real and imaginary parts of the dielectric constant are large in magnitude for small particles of typical metals at  $10.6 \mu\text{m}$ . Substituting (2.5) into (2.1) gives

$$\sigma_{\text{abs}} = 12 \epsilon_H^{3/2} \frac{\omega^2}{\omega_p^2} \frac{\Gamma a}{c} \pi a^2 ; \quad \omega_p^2 \gg |\omega^2 + i\omega\Gamma| , \quad (2.6)$$

for metals with  $ka \ll 1$ .

Next consider the case of large spheres ( $ka \gg 1$ ). Using geometrical optics and the identity  $1 + x + x^2 + \dots = (1 - x)^{-1}$ , where  $x \equiv R_i \exp(-\beta_I d)$ , with  $R_i$  the internal reflection coefficient and  $d$  the distance the ray travels in traversing the sphere once, gives

$$\sigma_{\text{abs}} = \pi a^2 \int_0^1 d(\cos^2 \theta) (1 - R) \left( 1 - e^{-\beta_I d} \right) \left( 1 - R_i e^{-\beta_I d} \right)^{-1} \quad (2.7)$$

where  $R = (|r_p|^2 + |r_n|^2)/2$ , with  $r_p$  and  $r_n$  the Fresnel reflection coefficients for the two polarizations,  $d$  the distance that the refracted ray travels through the sphere, and  $\theta$  the angle of incidence.

There are two limiting cases of (2.7) of interest. First, for  $\beta_I a \gg 1$ , which is typically satisfied for metals and strongly absorbing dielectrics, (2.7) yields

$$\sigma_{\text{abs}} \cong \pi a^2 (1 - \langle R \rangle) \quad (2.8)$$

where the average reflection coefficient  $\langle R \rangle$  is defined as

$$\langle R \rangle = \int_0^1 R d(\cos^2 \theta) .$$

For  $\beta_I a \ll 1$ , in the limit of small index of refraction, using  $|n_I - 1| \ll 1$ ,  $R \cong R_i \cong 0$ , and  $d \cong a \cos \theta$  in (2.7) yields

$$\sigma_{\text{abs}} \approx \frac{4}{3} \beta_I \pi a^3. \quad (2.9)$$

As  $n_R$  departs from 1,  $\sigma_{\text{abs}}$  first increases slightly for small  $|n-1|$  and eventually goes to zero when  $R$  goes to one. Notice that (2.9) has the same functional dependence on  $a$  as (2.3), but with a slightly different coefficient.

For metallic inclusions, a schematic illustration of the absorption efficiency  $\sigma_{\text{abs}}/\pi a^2$ , obtained by sketching the results (2.6) and (2.8), is shown in Fig. 1. The dashed line represents the asymptotic values obtained from (2.6) with  $\Gamma \sim a^{-1}$  (for  $a \ll a_\Gamma$ ), from (2.6) with  $\Gamma \sim a^0$  (for  $a_\Gamma \ll a \ll k^{-1}$ ), and from (2.8) (for  $a \gg k^{-1}$ ). The extrapolated dashed curve from (2.6) with  $a \gg a_\Gamma$  intersects the dashed curve from (2.8) at

$$a_k = \frac{\omega_p^2 c (1 - \langle R \rangle)}{12 \epsilon_H^{3/2} \omega^2 \Gamma_{\text{Bu}}} \quad (2.10)$$

which occurs near  $k^{-1}$  for many metals in the infrared. The solid curve schematically illustrates the results in the intermediate regions  $a \sim a_\Gamma$  and  $a \sim a_k$ . The dashed curve will be sufficient for the order-of-magnitude estimates of overall absorption and failure intensity in Secs. III and IV.

In dielectric inclusions,  $\beta_I a \ll 1$  typically is satisfied except for very strong absorbers with rather large radii. (For example,  $\beta_I a = 1$  for  $\beta_I = 10^4 \text{ cm}^{-1}$  and  $a = 1 \mu\text{m}$ .) For  $\beta_I a \ll 1$ , the absorption cross section is given by (2.3) for  $ka \ll 1$  and by (2.9) for  $ka \gg 1$ . Since these two limiting results both are of the form  $\sigma_{\text{abs}} \sim \beta_I a^3$ , with only slightly different coefficients, the approximation  $\sigma_{\text{abs}} = A \beta_I a^3$ , with  $A$  the average of the two coefficients, will be used for all values of  $ka$ .

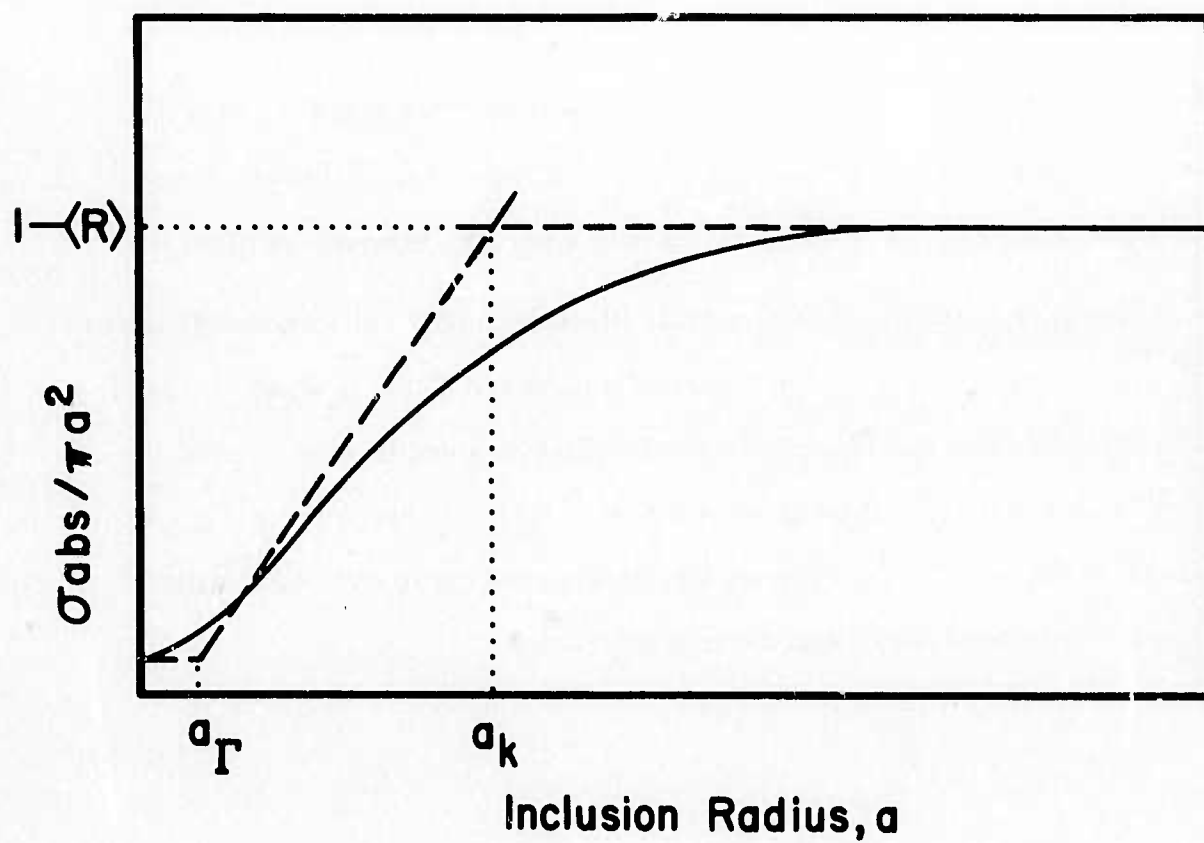


Figure 1. Absorption efficiency of a spherical metallic inclusion as a function of radius.

## Sec. B

The absorption efficiency for dielectric inclusions is qualitatively similar to that sketched in Fig. 1 for metallic inclusions, with two exceptions. First, for  $ka \ll 1$ , (2.3) indicates that  $\sigma_{\text{abs}}/\pi a^2 \propto a$ , and the constant region at small  $a$  does not occur for dielectrics. Second, the extrapolated linear region crosses the large  $a$  asymptotic region near  $\beta_1^{-1}$ , rather than  $k^{-1}$ . This can be seen from (2.8) and (2.9), which are valid for  $a > \beta_1^{-1}$  and  $a < \beta_1^{-1}$ , respectively. In some cases with  $n_R^{-1}$  and  $n_I$  small, the exact Mie solution yields  $\sigma_{\text{abs}} > \pi a^2$  near  $ka = 1$ .

For large-bandgap semiconductors, such as AlP, SiC, and ZnS, the dielectric-inclusion results above can be applied. The absorption by small-bandgap semiconductors is more complicated than that by dielectrics and metals in general, and will not be considered explicitly. Problems can occur involving temperature dependence of the electrical conductivity, increased absorption caused by free carriers that are created in the absorption process, and the resulting thermal runaway.<sup>4</sup>

### III. ABSORPTION EFFICIENCIES FOR VARIOUS TYPES OF INCLUSIONS

The above cross sections will now be used to calculate properties of the absorption coefficient for crystals containing various types of inclusions. The volume fraction  $f$  of inclusions required to make  $\beta = 10^{-4} \text{ cm}^{-1}$ , a value of current interest, will be determined.

Consider a sample consisting of a nonabsorbing host material of dielectric constant  $\epsilon_H$  (real) containing  $N_I$  inclusions per unit volume, each inclusion having absorption cross section  $\sigma_{\text{abs}}$ . Multiple scattering will be neglected -- a reasonable approximation for the present case of small impurity concentrations. The well known result for the absorption coefficient  $\beta$  of the sample is then

$$\beta = \sigma_{\text{abs}} N_I . \quad (3.1)$$

For small dielectric inclusions,  $\sigma_{\text{abs}}$  is given by (2.1), which when substituted into (3.1) yields

$$\beta \cong \left[ \frac{9n_R}{(\epsilon_R + 2)^2 + \epsilon_I^2} \right] \beta_I f , \quad \text{for } ka \ll 1, \epsilon_I \ll 1, \quad (3.2)$$

where the factor in the bracket typically has a value near unity. The absorption coefficient in (3.2) is independent of  $a$ , but is strongly temperature and frequency dependent in general. If  $\beta_I$  is controlled by, say, the  $n$ -phonon summation process, then  $\beta \sim T^{n-1}$  in the high-temperature limit, and  $\beta$  decays exponentially with frequency. Using  $\beta_I = 10$  to  $10^4 \text{ cm}^{-1}$  for strongly absorbing inclusions, (3.2) gives  $\beta = 10^{-4} \text{ cm}^{-1}$  for volume fractions of  $f = 10^{-5}$  to  $10^{-8}$ .

In the case of large dielectric inclusions, there are two possibilities. First, for  $ka \gg 1$  and  $\beta_I a \ll 1$ , using the geometrical-optics absorption cross section (2.9) yields  $\beta \propto \beta_I f$  with a numerical factor near unity, as in (3.2). For  $ka \gg 1$  and  $\beta_I a \ll 1$ , (2.8) and (3.1) give

$$\beta = \pi a^2 (1 - \langle R \rangle) N_I = 3(1 - \langle R \rangle) f / 4a, \quad ka \gg 1, \quad \beta_I a \ll 1. \quad (3.3)$$

The absorption coefficient in (3.3) is proportional to  $a^{-1}$  for a given value of  $f$  and is generally temperature independent, except near the reststrahl region where  $\langle R \rangle$  is strongly temperature dependent. For  $1 - \langle R \rangle \cong 1$  and  $a \cong 10^{-2}$  to  $10^{-3}$  cm, (3.3) gives  $\beta = 10^{-4}$  cm for  $f$  in the range from  $10^{-6}$  to  $10^{-7}$ .

For large metallic inclusions, the value of  $(1 - \langle R \rangle)$  in (3.3) is small ( $< 1/10$ ), since the reflectivity of metals in the infrared is great. As a result, the volume fraction of inclusions for  $\beta = 10^{-4}$  cm is increased by a factor of at least ten over the corresponding dielectric case.

Next consider the case of small metallic inclusions. From (2.6) and (3.1),

$$\beta \cong \frac{9 \epsilon_H^{3/2} \omega^2 \Gamma f}{c \omega_p^2} \quad (3.4)$$

This expression shows that  $\beta$  increases quadratically with frequency. For temperatures greater than room temperature, the electron relaxation frequency  $\Gamma_{Bu}$  and hence  $\beta$  increases linearly with temperature having a typical fractional increase of  $10^{-2}$  per degree Kelvin. With  $\epsilon_H^{3/2} = 10$ ,  $\omega = \omega_p / 25$ , and  $\Gamma = 5 \times 10^{14} \text{ sec}^{-1}$ , an inclusion volume fraction of  $f = 4 \times 10^{-8}$  results in  $\beta = 10^{-4} \text{ cm}^{-1}$ .

## Sec. B

The absorption by small metallic inclusions has a peak that typically lies in the ultraviolet or visible region.<sup>13</sup> The value of  $\beta$  at this peak is much greater than the value in the infrared. Thus, ultraviolet and visible measurements of absorption or scattering can be used to verify the source of absorption by small metallic particles in the infrared.

Consider, as an example, small potassium spheres in KCl or KBr. F centers can be transformed to colloidal potassium (small spheres) by heating the crystal.<sup>15-17</sup> The transformation is enhanced by ultraviolet radiation. The wavelengths  $\lambda_0$  of the peaks for the small potassium spheres in KCl and KBr are 0.730 and 0.770  $\mu\text{m}$ , respectively.<sup>13</sup> In the visible and ultraviolet,  $\Gamma^2 \ll \omega^2$ , and (2.1) and (2.4) give, with  $k = n_H \omega / c$

$$\epsilon \cong \epsilon_\infty - \frac{\omega_p^2}{\epsilon_H \omega^2} + i \frac{\omega_p^2 \Gamma}{\epsilon_H \omega^3},$$

$$\beta \cong \frac{\Gamma^2 \omega^2 \beta_{pk}}{(\omega^2 - \omega_0^2)^2 + (\Gamma \omega_0^2 / \omega)^2}, \quad (3.5)$$

where:

$$\omega_0^2 = \frac{\omega_p^2}{2 \epsilon_H + \epsilon_\infty}, \quad \beta_{pk} = \frac{9 n_H^3 \omega_0^4}{c \omega_p^2 \Gamma} f.$$

Notice that for fairly narrow lines ( $\Gamma \lesssim \omega_0 / 10$ ),  $\beta \cong \beta_{pk}$  at the peak at  $\omega = \omega_0$ , and  $\Gamma$  is the full line width between the points  $\beta = \frac{1}{2} \beta_{pk}$ .

## Sec. B

Dividing  $\beta_{pk}$  by the infrared absorption coefficient in (3.4) gives

$$\frac{\beta_{pk}}{\beta_{IR}} = \frac{\omega_0^4}{\omega_{IR}^2 \Gamma^2} . \quad (3.6)$$

For  $\lambda_0 = 2 \pi c / \omega_0 = 0.75 \mu m$ ,  $\lambda_{IR} = 10.6 \mu m$ , and  $\Gamma = 5 \times 10^{14} \text{ sec}^{-1}$ , (3.6) gives

$$\frac{\beta_{pk}}{\beta_{10.6}} = 6.4 \times 10^3 . \quad (3.7)$$

For  $\beta = 10^{-4} \text{ cm}^{-1}$ , (3.7) gives  $\beta_{pk} = 6.4 \text{ cm}^{-1}$ , which would produce a visibly colored crystal. Uncolored KBr or KCl with  $\beta_{pk} < 10^{-1} \text{ cm}^{-1}$  would have  $\beta_{10.6} < 1.6 \times 10^{-4} \text{ cm}^{-1}$ , and the contribution from potassium colloids to the infrared absorption would be small. Colored crystals could have a greater contribution to  $\beta$  from this source. It should also be mentioned that impurities in the form of F centers, which give rise to strong absorption in the visible region, may not give rise to detectable absorption in the infrared.

## IV. MATERIAL FAILURE FROM LOCAL HEATING

The heating of macroscopic inclusions can give rise to localized regions of high temperature that can cause material failure when the intensity is great. This is not a nonlinear effect, but is usually important only at relatively high intensities. For times short with respect to a characteristic time for heat to diffuse a distance  $a$ , very roughly speaking, most of the energy absorbed by the inclusion remains in the inclusion. Thus, the temperature in the inclusion increases linearly with time. For times large with respect to the characteristic time, part of the absorbed energy has diffused into the host crystal, and the temperature rise in the inclusion is considerably less than the value obtained by neglecting diffusion. Thus, a given amount of energy will cause a greater temperature rise if it is deposited in a time that is short with respect to the characteristic time than if deposited in a time long with respect to the characteristic time; the local heating of macroscopic inclusions is a more severe problem in high-intensity short-pulse systems than in low-intensity long-pulse or cw systems of equal average intensity.

The criterion for failure of the window material depends on the details of the laser system and the type of material and inclusions. Since there is no universal criterion, it will be assumed that a temperature rise of 1,000 K constitutes failure. This is a reasonable choice for the following reasons: This temperature is approximately the correct value for melting temperatures and fracture-inducing temperatures. The latter have typical values of the order of  $^{18-20} \sigma_f / \alpha E$ , where  $\sigma_f$  is the material strength,  $\alpha$  the linear thermal expansion coefficient, and  $E$  the Young's modulus. For  $\sigma_f = 10^5$  psi,  $\alpha = 10^{-5}$  and

$E = 10^7$  psi, the temperature corresponding to fracture is 1,000 K. Heats of fusion have typical values corresponding to several hundred degrees Kelvin. At 1,000 K above ambient temperature in materials which do not melt, the ionic diffusion may be important. Although order-of-magnitude accuracy in temperature usually is not sufficient, order-of-magnitude accuracy of intensities corresponding to failure is all that can be expected at present, and this is often adequate. Since the present interest is in this failure intensity  $I_f$ , and the failure temperature  $T_f$  is linearly related to  $I_f$ , the value  $T_f = 1,000$  K should be sufficient for present purposes.

Two important features of high-power laser-window failure are that failure of the weakest part of the window can constitute system failure, and that fatigue and other multiple-pulse effects must be considered when repeated pulses must be withstood. Concerning the former, a single inclusion in a window conceivably could cause failure. As an example of the latter, in a single-pulse measurement, a laser glass conceivably could melt locally and recrystallize without leaving detectable damage. For a window in a pulse-operated system, the local absorption coefficient could be changed by the high temperature associated with the first pulse or the first  $n$  pulses, thus causing increased absorption in subsequent pulses with eventual failure.

Bloembergen<sup>21</sup> has suggested that local field enhancement, such as that occurring at the edge of a crack in a material, may give rise to local intensities up to 100 times greater than the nominal external intensity. Thus, if an inclusion is in the high-intensity region, this effect could lower the failure intensities calculated below by a factor of the order of 100. Local field enhancement can also occur when one inclusion is at the focal point of another. Since

## Sec. B

focusing is limited by diffraction when  $ka \lesssim 1$ , the focusing by large, weakly absorbing inclusions is most severe. Focusing by surface imperfections also could occur.

The temperature rise below the melting point can be calculated simply for the following model. The spherical inclusion of radius  $a$  is assumed to have temperature-independent values  $C_I$  and  $K_I$  of heat capacity per unit volume and thermal conductivity. The host crystal is assumed to have temperature-independent values  $C_H$  and  $K_H$ . The boundary between the two is assumed to be thermally perfect; that is, there is no thermal impedance. Heat absorption by the host crystal is assumed negligible. The relaxation time required to transfer energy to heat from the modes that absorb energy is assumed to be much shorter than the laser pulse duration.

Simple solutions to the heat-flow equation

$$-K \nabla^2 T + C \frac{\partial T}{\partial t} = S \quad (4.1)$$

will be derived for a series of limiting times for the cases of uniform heat generation within the volume of the inclusion and of uniform heat generation over the surface of the inclusion. In (4.1),  $S$  is the rate at which heat is generated per unit volume.

First consider the case of spatially uniform heat generation within the inclusion at the rate

$$S = 3 \sigma_{\text{abs}} I / 4 \pi a^3 \quad (4.2)$$

per unit volume, where  $I$  is the incident intensity. This applies for dielectric inclusions with  $\beta_I a \ll 1$  or for metallic inclusions with skin depth  $\delta > a$ .

## Sec. B

Roughly speaking, the thermal time constant

$$\tau = Ca^2/4K \quad (4.3)$$

is the time required for heat to diffuse a distance  $a$  in either the inclusion or the host when the appropriate values of  $C$  and  $K$  are used. Subscripts  $I$  and  $H$  will denote the values of  $\tau$  in the inclusion and in the host crystal, respectively. For short times  $t \ll \tau_H$ , the diffusion of heat out of the inclusion is negligible. The term  $K_I \nabla^2 T$  in (4.1) is then negligible. The temperature at the center of the inclusion is, from (4.1) and (4.2),

$$T_C = 3\sigma_{abs} I t / 4\pi a^3 C_I, \quad \text{for } t \ll \tau_H \quad (4.4)$$

for  $T$  defined as zero at the time the laser is turned on ( $t = 0$ ).

For long times  $t \gg \tau_I, \tau_H$ , equilibrium is reached with the host material conducting heat away from the inclusion at the same rate that it is generated within the inclusion. In this case the temperature is obtained by solving (4.1) with  $\partial T / \partial t = 0$  in both the inclusion and the host. Using  $\nabla^2 r^2 = 6$ ,  $\nabla^2 (1/r) = 0$  for  $r > a$ , and the boundary conditions that the temperature and the heat flow be continuous at the inclusion surface, yields the steady-state value at the inclusion center.

$$T_{C\infty} = \frac{3\sigma_{abs} I}{8\pi a K_{eff}}, \quad \frac{1}{K_{eff}} \equiv \frac{1}{3} \left( \frac{2}{K_H} + \frac{1}{K_I} \right). \quad (4.5)$$

For short and long times, the temperatures are approximated by (4.4) and (4.5), respectively. These are shown as dashed lines in Fig. 2, while the actual

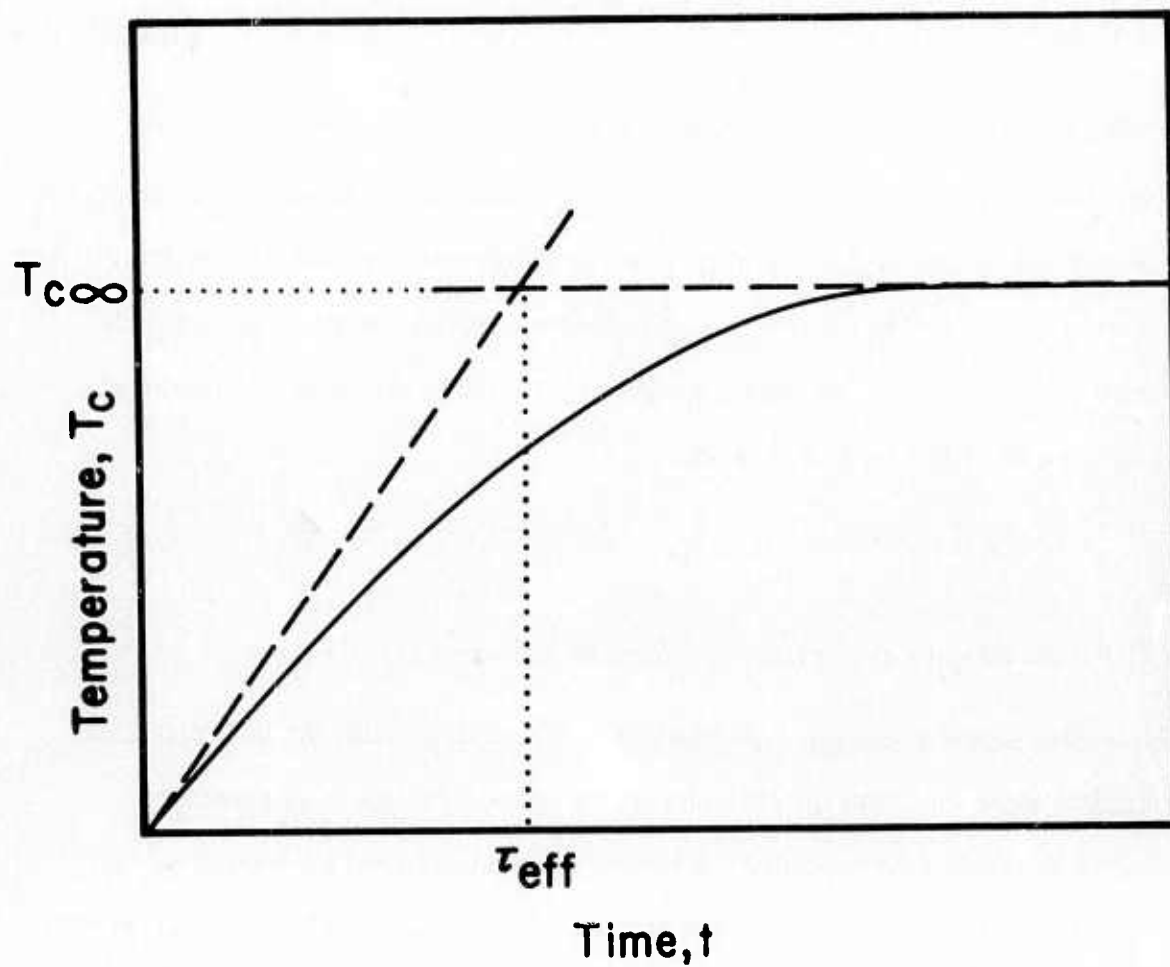


Figure 2. Temperature at the center of a spherical inclusion as a function of time in the case of volume heating.

temperature is sketched as the solid line. The extrapolated short-time curve intersects the steady-state value at the time  $\tau_{\text{eff}} = (2K_I/K_{\text{eff}}) \tau_I$ , which is found by equating (4.4) and (4.5).

Next consider the case in which the heat is generated near the surface of the inclusion, rather than uniformly throughout its volume. Such is the case for metallic inclusions in dielectric hosts, where a typical value for the skin depth  $\delta$  is 40 Å (Cu at  $\lambda = 10.6 \mu\text{m}$ ),<sup>13</sup> or for dielectric inclusions with  $\beta_I a \gg 1$ , where  $1/\beta_I$  is of the order of  $10^{-3}$  cm for strong absorption.

For spherical inclusions with radius  $a \gg \delta$ , it is assumed that heat is generated uniformly within a layer of thickness  $\delta$  over the entire surface of the inclusion. This is a good approximation for  $a \ll \lambda$  because the electric field is nearly constant over distances of the order of  $a$ . In general, there will be local hot spots over the surface -- not only on the front surface, but also on the rear surface.

There are three characteristic times of interest. First,

$$\tau_\delta = 4C_I \delta^2 / \pi K_I \quad (4.6)$$

is roughly the time in which heat diffuses out of the skin depth, assuming negligible diffusion into the host for small time, since  $K_H$  (dielectric)  $\ll K_I$  (metal). Second,

$$\tau_a = 4C_I a^2 / 9\pi K_I \quad (4.7)$$

is the time in which heat diffuses from the inclusion surface to the center, roughly speaking. Third,

## Sec. B

$$\tau_H = C_H a^2 / 3 K_H \quad (4.8)$$

is roughly the time in which heat diffuses a distance equal to the radius of the inclusion into the host. The values of the numerical coefficients in (4.6)-(4.8) are chosen for later convenience.

For  $t \ll \tau_\delta$  and  $\delta \ll a$ , the spherical shape of the inclusion surface is not important, and the solution to the simpler problem of heat generation in a thin plane slab can be used. In this case, the temperature is obtained from the Laplace-transform solution of (4.1).<sup>22</sup> The solution to the transform equation at the inclusion surface is

$$T(x = \delta, p) = \frac{S}{C_I} \frac{\sqrt{C_I K_I}}{\sqrt{C_I K_I} + \sqrt{C_H K_H}} \frac{1 - e^{-q_I a}}{p^2}$$

where  $q_I = (p C_I / K_I)^{1/2}$ . Taking the inverse transform and keeping only the dominant term for  $t$  small yields the temperature at the inclusion surface

$$T_S = \frac{1}{C_I} \frac{\sqrt{C_I K_I}}{(\sqrt{C_I K_I} + \sqrt{C_H K_H})} \frac{I \sigma_{abs}}{4 \pi a^2 \delta} t \cong \frac{I \sigma_{abs}}{4 \pi a^2 \delta C_I} t, \quad t \ll \tau_\delta. \quad (4.9)$$

In (4.9) and in the equations below, the approximate equalities are valid for  $C_I K_I \gg C_H K_H$ . For  $\tau_\delta \ll t \ll \tau_a$ , the heat generation in a plane-slab problem can be approximated by a delta-function source at  $x = 0$ . Using the method of Laplace transforms and keeping the dominant term for small  $t$  yields

$$T_S = \frac{2}{\sqrt{\pi} (\sqrt{C_H K_H} + \sqrt{C_I K_I})} \frac{I \sigma_{abs}}{4 \pi a^2} t^{1/2}, \quad \tau_\delta \ll t \ll \tau_a. \quad (4.10)$$

## Sec. B

When  $t \gg \tau_a$ , the temperature inside the spherical inclusion reaches a spatially uniform value. The present problem then is equivalent to uniform heat generation within an inclusion of infinite conductivity and the previous result (4.4) can be used to obtain

$$T_S = \frac{3I\sigma_{abs}t}{4\pi a^3 C_I}, \quad \tau_a \ll t \ll \tau_H. \quad (4.11)$$

For  $t \gg \tau_H$ , the temperature inside the spherical inclusion reaches an equilibrium value that is spatially uniform. This case is again equivalent to uniform volume heating within an inclusion of infinite conductivity, and (4.5) yields

$$T_{S\infty} = \frac{I\sigma_{abs}}{4\pi a K_H}, \quad t \gg \tau_H. \quad (4.12)$$

The temperature at the surface of the spherical inclusion is sketched in Fig. 3 for the various time regimes in (4.9)-(4.12). The extrapolated low-temperature linear time-dependent section of the curve intersects the  $t^{1/2}$  curve at the time  $t_\delta = \tau_\delta$ , at which time the temperature is

$$T_\delta = \frac{I\delta\sigma_{abs}}{\pi^2 a^2} \frac{1}{K_I} \frac{\sqrt{C_I K_I}}{(\sqrt{C_I K_I} + \sqrt{C_H K_H})} \approx \frac{I\delta\sigma_{abs}}{\pi^2 a^2 K_I} \quad (4.13)$$

At  $t = t_a$ , the extrapolated  $t^{1/2}$  curve intersects the second linear region. The temperature at this intersection has the value

$$T_a = \frac{I\sigma_{abs} C_I}{3\pi^2 a (\sqrt{C_H K_H} + \sqrt{C_I K_I})^2} \approx \frac{I\sigma_{abs}}{3\pi^2 a K_I}, \quad (4.14)$$

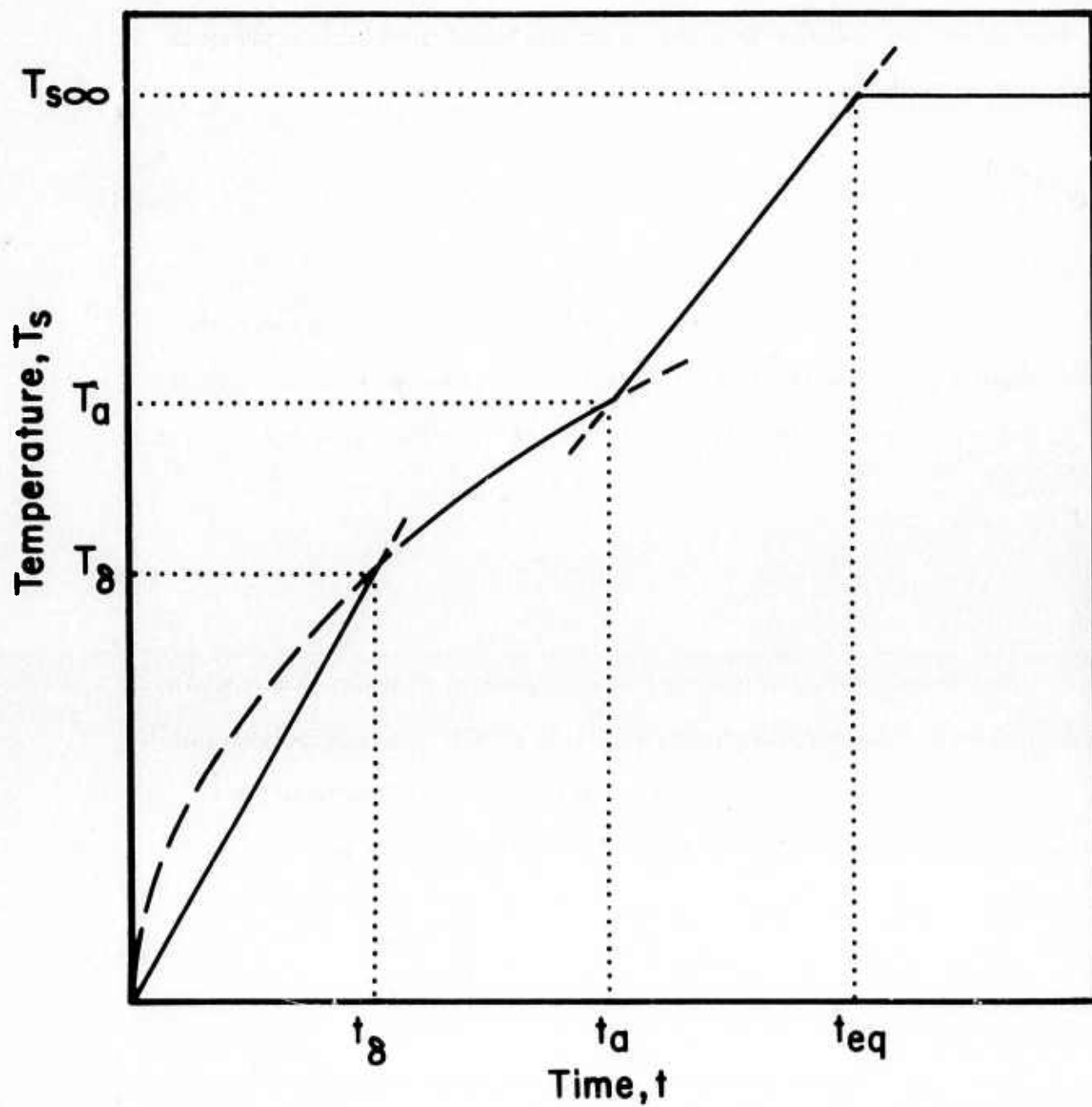


Figure 3. Temperature at the surface of a spherical inclusion as a function of time in the case of surface heating.

and the value of  $t_a$  is

$$t_a = \frac{4a^2 C_1^2}{9\pi (\sqrt{C_H K_H} + \sqrt{C_I K_I})^2} \equiv \tau_a. \quad (4.15)$$

At the time  $t_{eq} = (C_I/C_H) \tau_H$ , the extrapolated linear curve crosses the equilibrium value given in (4.12).

Consider the effect of inclusion size on the failure intensity  $I_f$ . The various time regimes in Fig. 3 depend on inclusion size in such a way that if the pulse length is fixed, long times in the figure are associated with small inclusions. For example, the time  $t_{eq}$  at which the temperature reaches equilibrium is equivalent to an inclusion of radius  $a_{eq} = (3K_H t / C_I)^{1/2}$  for a pulse of duration  $t$ . The temperature is then given by (4.12) for  $a < a_{eq}$ . Similarly, the time  $t_a$  in Fig. 3 corresponds to a size  $a_t \cong (9\pi K_I t / 4C_I)^{1/2}$ , and the temperature is given by (4.11) for  $a_{eq} < a < a_t$ . Next, the time  $t_\delta$  is independent of size and is determined by the skin depth and thermal properties of the inclusion.

In the case of metallic inclusions,  $t_\delta$  is typically of the order of  $10^{-13}$  sec, which is much less than most laser pulse durations of interest. Hence, the first linear region in Fig. 3 given by (4.9) does not occur, in general, and for  $a > a_t$  the temperature is given by (4.10). To determine the temperature in a pulsed system as a function of the inclusion radius, the dependence of  $\sigma_{abs}$  on  $a$  in (4.9)-(4.12) must be included. In the case of metallic inclusions, the dashed curve of Fig. 1 is used as an approximation for  $\sigma_{abs}$ . For a given type of inclusion in a particular host, the radii  $a_\Gamma$  and  $a_k$  at which the functional dependence of the cross section changes are independent of the pulse duration, while the radii  $a_t$  and  $a_{eq}$  are both proportional to  $t^{1/2}$  and decrease with decreasing pulse length.

There are six combinations of the sequence of  $a_{\Gamma}$ ,  $a_k$ ,  $a_t$ ,  $a_{eq}$  which can occur for different pulse lengths. The temperature as a function of inclusion size is sketched for each of these cases in Fig. 4, with the pulse duration decreasing in going from A to F. For a given type of inclusion, the curves C and D cannot both occur. The applicable case will depend on the relative size of ratios  $a_t/a_{eq}$  and  $a_k/a_{\Gamma}$ .

Consider the example of metallic inclusions with the laser wavelength equal to  $10.6 \mu\text{m}$ . Using the typical values  $\omega_p = 5 \times 10^{15} \text{sec}^{-1}$ ,  $\Gamma_{Bu} = 5 \times 10^{13} \text{sec}^{-1}$ ,  $(1 - \langle R \rangle) = 0.1$ , and  $\epsilon_H^{3/2} = 10$  in (2.10) yields  $a_k = 4 \mu\text{m}$ . A typical value of  $a_{\Gamma}$  is  $200 \text{\AA}$ . Using  $C_H \cong C_I \cong 2 \text{J/cm}^3 \text{K}$ ,  $K_I = 2 \text{W/cm K}$  and  $K_H = 10^{-2} \text{W/cm K}$ , these typical values indicate that  $a_{eq} = a_k$  when  $t = 10^{-5} \text{sec}$ ,  $a_t = a_k$  when  $t = 2 \times 10^{-8} \text{sec}$ ,  $a_{eq} = a_{\Gamma}$  when  $t = 3 \times 10^{-10} \text{sec}$ , and  $a_t = a_{\Gamma}$  when  $t = 6 \times 10^{-13} \text{sec}$ . Hence, curve A applies for  $t < 10^{-5} \text{sec}$ , that is, in the range of cw or millisecond pulses. Curve B applies to microsecond pulses, curve C or D to nanosecond pulses, curve E to picosecond pulses, and curve F to subpicosecond pulses.

The maximum temperature for a microsecond duration pulse occurs for  $a_{eq} < a < a_k$  in Fig. 4B, where  $a_{eq} = 1 \mu\text{m}$  using the above parameters. For radii in this range, the temperature is given by (4.11), which is evaluated at  $a = a_k$  using the absorption cross section (2.8). With the above values in (4.11), the failure temperature of  $1,000 \text{K}$  occurs for a pulse energy of  $3 \text{J/cm}^2$  with micron-size inclusions.

With a nanosecond duration pulse, the maximum temperature again occurs near  $a = a_k$  in Fig. 4D and is determined from (4.10). In this case, the failure temperature occurs at a pulse energy of  $2 \text{J/cm}^2$ .

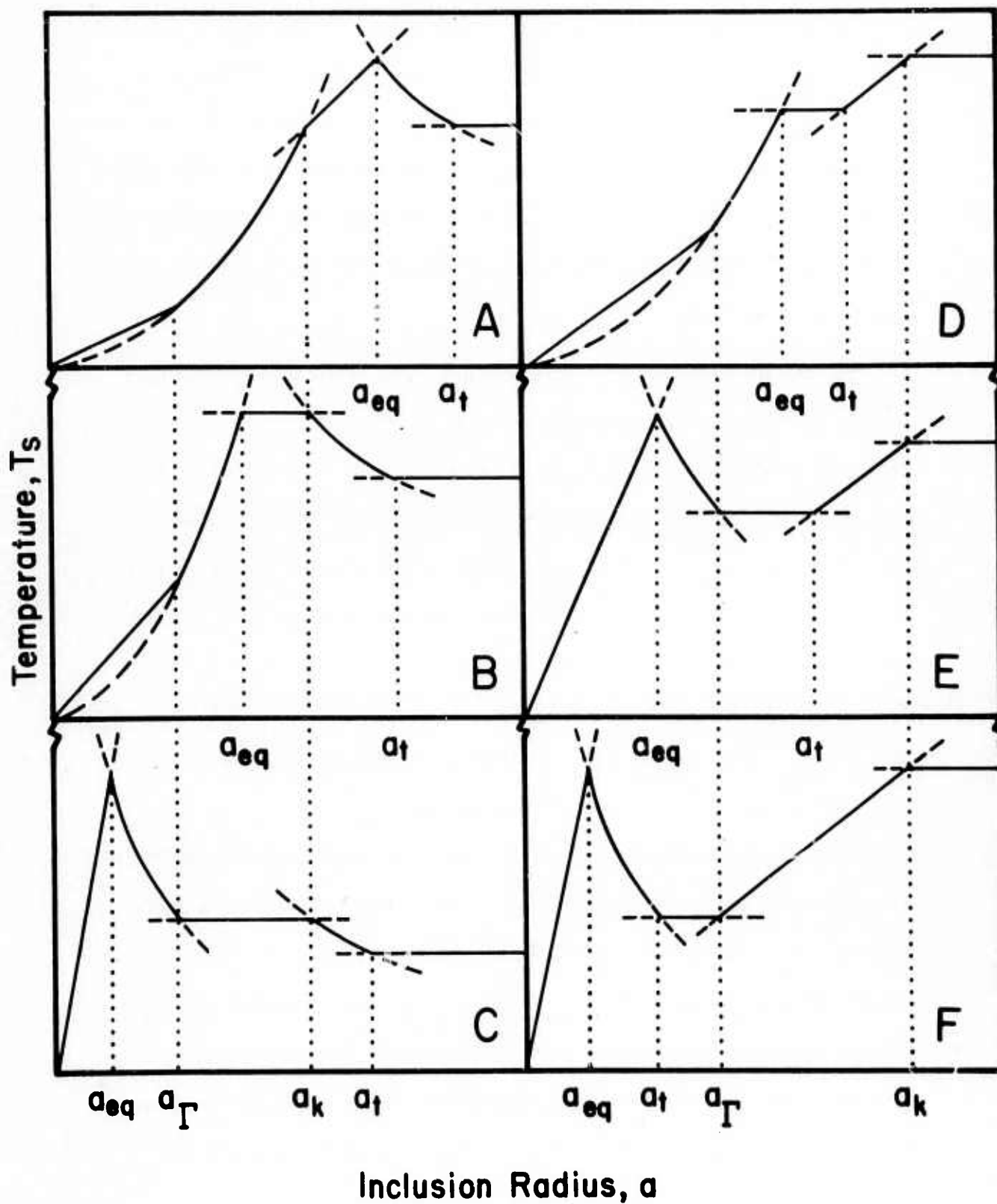


Figure 4. Temperature at the surface of a metallic inclusion as a function of radius for various pulse durations.

Next consider a cw system with  $I = 300 \text{ W/cm}^2$ , an intensity which is equal to the average intensity of a repetitively pulsed system with a pulse energy of  $3 \text{ J/cm}^2$  and a 100 pulse/sec repetition rate. In this cw case, the temperature of an inclusion with  $a = a_k$  is determined by (4.12), which yields a temperature rise of less than 1 K above ambient. Hence, the pulsed system would fail on a single pulse, while the cw system of the same average intensity would have a negligible temperature rise.

At laser wavelengths other than  $10.6 \mu\text{m}$ , the various curves of Fig. 4 correspond to pulse durations different from those listed above. Consider the case of platinum inclusions in a glass host with  $\lambda = 1 \mu\text{m}$ . Fitting the Drude expression (2.4) for the dielectric constant of platinum to tabulated values of the refractive index<sup>23</sup> yields the values for the parameters  $\epsilon_\infty$ ,  $\omega_p$ , and  $\Gamma_{\text{Bu}}$ , which together with  $\epsilon_H^{3/2} = 3$  when substituted into (2.10) gives  $a_k = 400 \text{ \AA}$  for platinum inclusions in a glass host. In this case, using  $K_I = 0.7 \text{ W/cm}^2 \text{ K}$ ,  $K_H = 1.3 \times 10^{-2} \text{ W/cm K}$ ,  $C_I = 2.8 \text{ J/cm}^3 \text{ K}$ , and  $C_H = 3.8 \text{ J/cm}^3 \text{ K}$ ,  $a_{\text{eq}} = a_k$  when  $t = 10^{-9} \text{ sec}$ . Hence, curve A applies for pulses longer than a nano-second duration, and the maximum temperature  $T_{\text{max}}$  occurs at  $a = a_{\text{eq}}$ . This example with a pulse energy of  $20 \text{ J/cm}^2$  and a pulse duration of 30 nsec has been considered previously by Hopper and Uhlmann.<sup>8</sup> With this pulse duration,  $T_{\text{max}}$  occurs at  $a_{\text{eq}} = 0.2 \mu\text{m}$ . Using (2.8) with  $(1 - \langle R \rangle) = 0.2$  at this wavelength, (4.12) yields  $T_{\text{max}} = 5 \times 10^4 \text{ K}$ . These results are in reasonable agreement with results shown in Hopper and Uhlmann's Fig. 3, which presents a plot of  $T$  versus  $a$  that agrees with Fig. 4A only for the region  $a_k < a < a_t = 2.3 \mu\text{m}$ . In their curve, a maximum temperature of  $T = 2.5 \times 10^4$

occurs at  $a = 0.2 \mu\text{m}$ , the difference in temperature resulting from the extrapolations made in curve A. In the region  $a < a_k$ , their results are not valid since the incorrect cross section  $\sigma_{\text{abs}} = \epsilon_\lambda \pi a^2$  was used.

In the case of dielectric inclusions, volume heating is used for  $\beta_I a < 1$ , and surface heating is used for  $\beta_I a > 1$ . The time  $\tau_{\text{eff}}$  separating the two regions of Fig. 2 given by (4.4) and (4.5) corresponds to a radius  $a_{\text{eff}} = (2 K_{\text{eff}} t / C_I)^{1/2}$  for a pulse of duration  $t$ . In the volume heating range with  $\beta_I a < 1$ , the absorption cross section is proportional to  $a^3$  with slightly different coefficients for  $ka \ll 1$  in (2.3) and for  $ka \gg 1$  in (2.9). Using  $\sigma_{\text{abs}} \propto a^3$  with the average of the two coefficients for the entire volume heating region, (4.4) gives  $T_c \propto a^0$  for  $a_{\text{eff}} < a < \beta_I^{-1}$  and (4.5) gives  $T_c \propto a^2$  for  $a < a_{\text{eff}}$  where it is assumed that  $\beta_I < k$ . These results are sketched at the left side of Fig. 5.

For surface heating of strongly absorbing dielectric inclusions with  $\beta = 1/\delta = 10^3 \text{ cm}^{-1}$ ,  $C_I = 2 \text{ J/cm}^3 \text{ K}$  and  $K_I = 10^{-2} \text{ W/cm K}$ ,  $\tau_\delta$  is of the order of  $10^4 \text{ sec}$ . This value is much greater than pulse lengths of interest, and the first linear region of Fig. 3 given by (4.9), which was only of academic interest for metals, is now the only surface heating region that applies. Because  $\beta_I a > 1$  for surface heating and generally  $ka \gg 1$ , the absorption cross section is  $\sigma_{\text{abs}} = (1 - \langle R \rangle) \pi a^2$ , according to (2.8). Substituting (2.8) for  $\sigma_{\text{abs}}$  into (4.9), the surface temperature is independent of  $a$ . This is sketched at the right side of Fig. 5 for  $\beta_I a > 1$ .

In Fig. 5 the maximum temperature occurs for  $a_{\text{eff}} < a < 1/\beta_I$ . Using  $\sigma_{\text{abs}} = 0.8 \beta_I \pi a^3$ ,  $C_I = 2 \text{ J/cm}^3 \text{ K}$ , and  $\beta_I$  ranging from  $10$  to  $10^4 \text{ cm}^{-1}$ , the

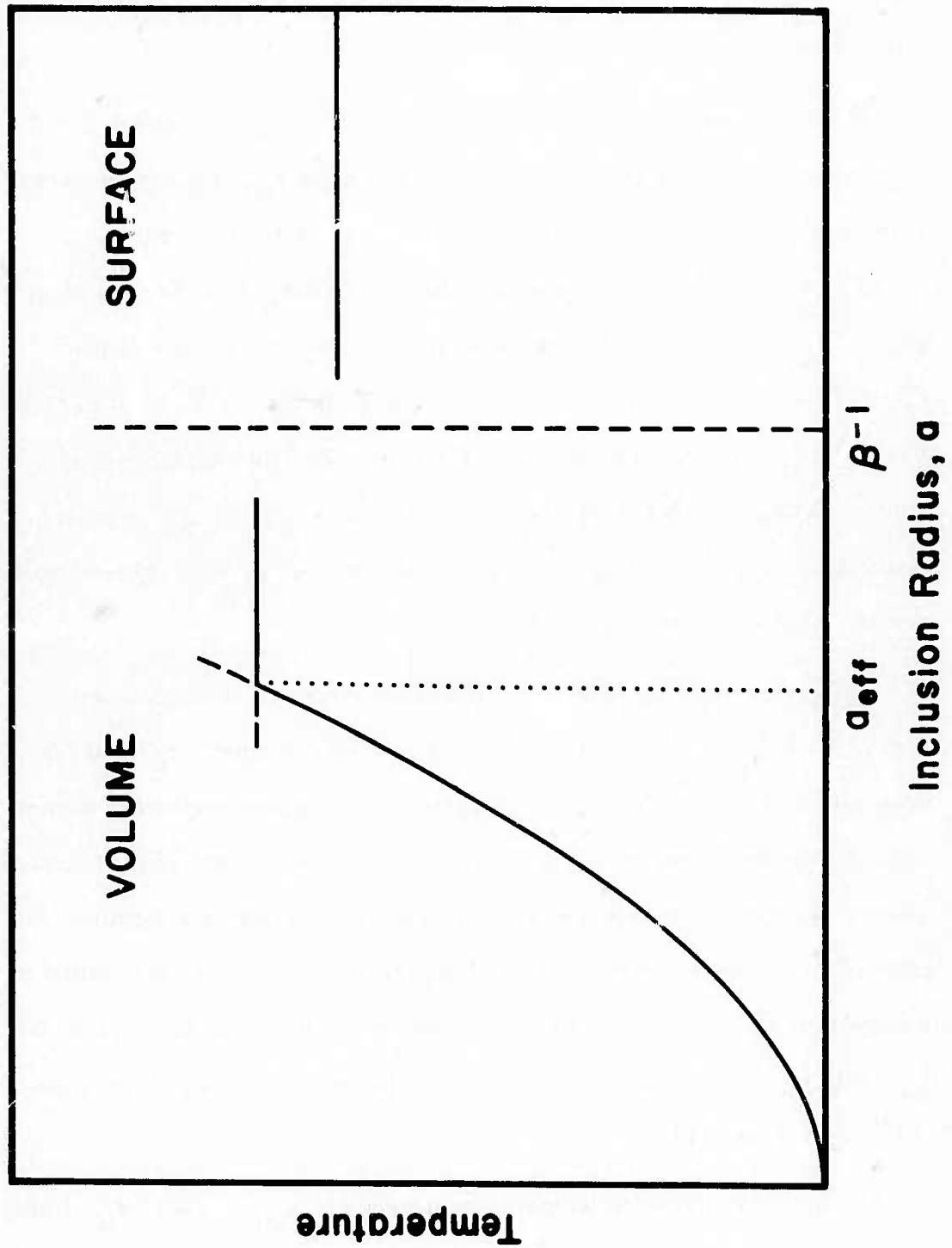


Figure 5. Temperature of a dielectric inclusion as a function of radius.

## Sec. B

failure temperature of 1,000 K occurs for pulse energies ranging from  $0.3 \text{ J/cm}^2$  to  $300 \text{ J/cm}^2$ . For microsecond duration pulses  $a_{\text{eff}}$  is of the order of  $10^{-4} \text{ cm}$ , and for nanosecond pulses is of the order of  $300 \text{ \AA}$ , where  $K_{\text{eff}} = 10^{-2} \text{ W/cm K}$  is used.

Many other examples, in nearly every case of practical interest, could be derived using the simple results developed above. The extrapolations from the simple limiting cases to the intermediate regions, such as using the dashed rather than solid curve in Fig. 1, tend to overestimate the temperature, or underestimate the pulse energy at the damage threshold, but only by factors typically of order 2.

## V. CONCLUSIONS

Simple limiting expressions for the absorption cross sections of inclusions derived in Sec. II are used in Sec. III to obtain expressions for the optical absorption coefficient  $\beta$  for the cases of large ( $ka > 1$ ) and small ( $ka < 1$ ) dielectric and metallic inclusions. For various types of inclusions, the frequency dependence of  $\beta$  ranges from increasing as  $\omega^2$ , to independent of  $\omega$ , to exponentially decreasing with  $\omega$ . The temperature dependence ranges from independent of  $T$  to increasing as  $T^p$  in the high-temperature limit, where  $p \approx 2-4$  typically. The examples in Sec. III illustrate that for strongly absorbing dielectric or metallic inclusions, impurity volume fractions as small as  $f = 10^{-8}$  can result in infrared absorption coefficients of the order of  $10^{-4} \text{ cm}^{-1}$ , which are currently observed. The impurities are not necessarily limited to the bulk of the crystal, but may be on the surface as would occur for a surface contaminated by polishing compounds, which generally have large absorption coefficients.

In Sec. IV failure due to local heating of dielectric and metallic inclusions in pulsed and cw systems is examined, and schematic results are given for many limiting cases. Local heating is a far greater problem in short-pulse systems than in long-pulse or cw systems having the same average intensity as the short-pulse system. In the case of micron-size metallic or dielectric inclusions, pulse energies of a few joules per square centimeter are sufficient to cause local damage. In special cases where the inclusion is adjacent to a crack or other imperfection or near the focal point of another inclusion or other imperfections, the damage thresholds could be lower than our calculated values by as much as two orders of magnitude.

## REFERENCES

\*This research was supported by the Advanced Research Projects Agency of the Department of Defense and was monitored by the Defense Supply Service - Washington, D. C.

1. C. S. Sahagian and C. A. Pitha, Ed., Conference on High-Power Infrared Laser Window Materials, Air Force Cambridge Research Laboratories (1971); C. A. Pitha, Ed., Conference on High-Power Infrared Laser Window Materials, Air Force Cambridge Research Laboratories (1972).
2. M. Sparks, "Recent Developments in High-Power Infrared Window Research," 4th ASTM Damage in Laser Materials Symposium, Boulder, Colorado, June 14-15, 1972.
3. M. Sparks and L. J. Sham, "Exponential Frequency Dependence of Multiphonon-Summation Infrared Absorption," Solid State Commun. **11**, 1451 (1972); M. Sparks and L. J. Sham, "Theory of Multiphonon Infrared Absorption," Conference on High Power Infrared Laser Window Materials, Hyannis, Massachusetts, Oct. 30-Nov. 1, 1972 (proceedings to be published by Air Force Cambridge Research Laboratories, Cambridge, Massachusetts; M. Sparks, "Recent Developments in High-Power Infrared Window Research," 4th ASTM Damage in Laser Materials Symposium, Boulder, Colorado, June 14-15, 1972.
4. F. A. Horrigan and T. F. Deutsch, "Research in Optical Materials and Structures for High-Power Lasers," Raytheon Research Division, Quarterly Technical Reports Nos. 1 and 2, Contract DA-AH01-72-C-0194, January and April 1972.

Sec. B

5. M. Sparks, J. Appl. Phys. 42, 5029 (1971).
6. M. Sparks, "Optical Distortion by Heated Windows in High-Power Laser Systems," Rand Corporation Report No. R-545-PR, September 1971.
7. M. Sparks, "Physical Principles, Materials Guidelines, and Materials List for High-Power 10.6 $\mu$  Windows," Rand Corporation Report No. R-863-PR, August 1971.
8. R. W. Hopper and D. R. Uhlmann, J. Appl. Phys. 41, 4023 (1970).
9. L. I. Van Torne, Phys. Stat. Sol. 16, 171 (1966).
10. H. V. Winsor, Air Force Weapons Laboratory, Kirtland Air Force Base, private communication (1970).
11. G. Mie, Ann. Physik 25, 377 (1908).
12. H. C. Van de Hulst, Light Scattering by Small Particles, (John Wiley and Sons, Inc., New York, 1957).
13. C. Kittel, Introduction to Solid State Physics, 4th ed. (John Wiley and Sons, Inc., New York, 1971).
14. A. Kawabata and R. Kubo, J. Phys. Soc. Jap. 21, 1765 (1966).
15. V. A. Fock, J. Phys. USSR 10, 130 (1946).
16. H. Siedentopf, Z. Physik 6, 855 (1905).
17. A. B. Scott, W. A. Smit, and M. A. Thompson, J. Phys. Chem. 57, 757 (1953).
18. M. Sparks, "Stress and Temperature Analysis for Surface Cooling or Heating of Laser Window Materials," Parke Mathematical Laboratories Report No. 0142-TM-1, July 1971.

Sec. B

19. M. Sparks, "Temperature and Stress Analysis for Bulk- and Surface-Heated Slabs," Parke Mathematical Laboratories Report No. TM-2, August 1971.
20. M. Sparks, "Calculated Temperature Distributions in Slabs Heated in a Thin Surface Layer," Parke Mathematical Laboratories Report No. TM-3, September 1971.
21. N. Bloembergen, Appl. Opt. (to be published).
22. H. S. Carslaw and J. C. Jaeger, Conduction of Heat in Solids, 2nd ed. (Oxford Clarendon Press, London, 1959).
23. AIP Handbook, 2nd ed. (McGraw-Hill Book Co., Inc., 1963).

C. THEORY OF MULTIPHONON ABSORPTION IN INSULATING CRYSTALS\*

M. Sparks

Xonics, Incorporated, Van Nuys, California 91406

and

L. J. Sham

University of California, San Diego, La Jolla, California 92037, and

Xonics, Incorporated, Van Nuys, California 91406

The nearly exponential frequency dependence of the infrared absorption coefficient  $\beta$  recently observed in fifteen crystals up to several times the reststrahl frequency is explained in terms of multiphonon absorption processes. The central-limit theorem is used to reduce the multiphonon contribution to a simple closed form. The theoretical estimates for the magnitude of the absorption coefficient, with no adjustable parameters, are also in good agreement with experiment. The temperature dependence of  $\beta$  at a fixed frequency is shown to be considerably weaker than  $\beta \sim T^{n-1}$ , where  $n$  is the number of created phonons. Higher-order processes in the perturbation expansion are shown to be negligible for small  $n$ , to be comparable to that of the lowest-order, single-vertex terms for  $n \cong 5$ , and to dominate for large  $n$  in a typical case. Difference processes, in which some thermally excited phonons are annihilated, are shown to be negligible with respect to the summation processes in the nearly exponential region. An explanation involving finite phonon lifetimes is proposed to explain the fact that the alkali halides show less structure in the  $\beta$ - $\omega$  curves than do the semiconductor crystals.

## I. INTRODUCTION

The intensity  $I$  of infrared radiation propagating through a solid typically decays according to Beer's law,  $I = I_0 \exp(-\beta z)$ , where  $\beta$  is defined as the optical absorption coefficient. Extensive experimental and theoretical studies have been conducted on the absorption due to phonons in insulating or semi-conducting crystals. Refs. 1-4 represent some recent reviews on this topic. The main interest has been focused on the two-phonon region where  $\beta \gg 1 \text{ cm}^{-1}$ , and particularly on the structure of the frequency dependence that determines the critical points of the phonon spectra.<sup>5</sup> The availability of high-power infrared lasers has shifted attention to higher-order phonon processes, where  $\beta \ll 1 \text{ cm}^{-1}$ . Not only the positions of the multiphonon peaks are of interest, but also the magnitude of  $\beta$  is of great importance now that high intensities are available.

It has been observed<sup>6,7a,7b</sup> that for frequencies  $\omega$  greater than several times the reststrahl frequency  $\omega_f$ , the optical absorption coefficient varies nearly exponentially with frequency,

$$\beta \sim \exp(-A\omega) , \quad (1.1)$$

for a number of crystals including LiF, NaF, NaCl, KCl, KBr,  $\text{MgF}_2$ ,  $\text{CaF}_2$ ,  $\text{BaF}_2$ ,  $\text{SrF}_2$ , MgO,  $\text{Al}_2\text{O}_3$ ,  $\text{SiO}_2$ ,  $\text{TiO}_2$ ,  $\text{BaTiO}_3$ , and  $\text{SrTiO}_3$ . This is true for  $\beta \lesssim 10 \text{ cm}^{-1}$  and  $\omega \gtrsim 2 \omega_f$ , roughly. In NaCl at room temperature, for instance,  $\beta$  decreases nearly exponentially for over four orders of magnitude as the frequency increases from  $2.2 \omega_f$  to  $5.8 \omega_f$ , as shown in Fig. 1.

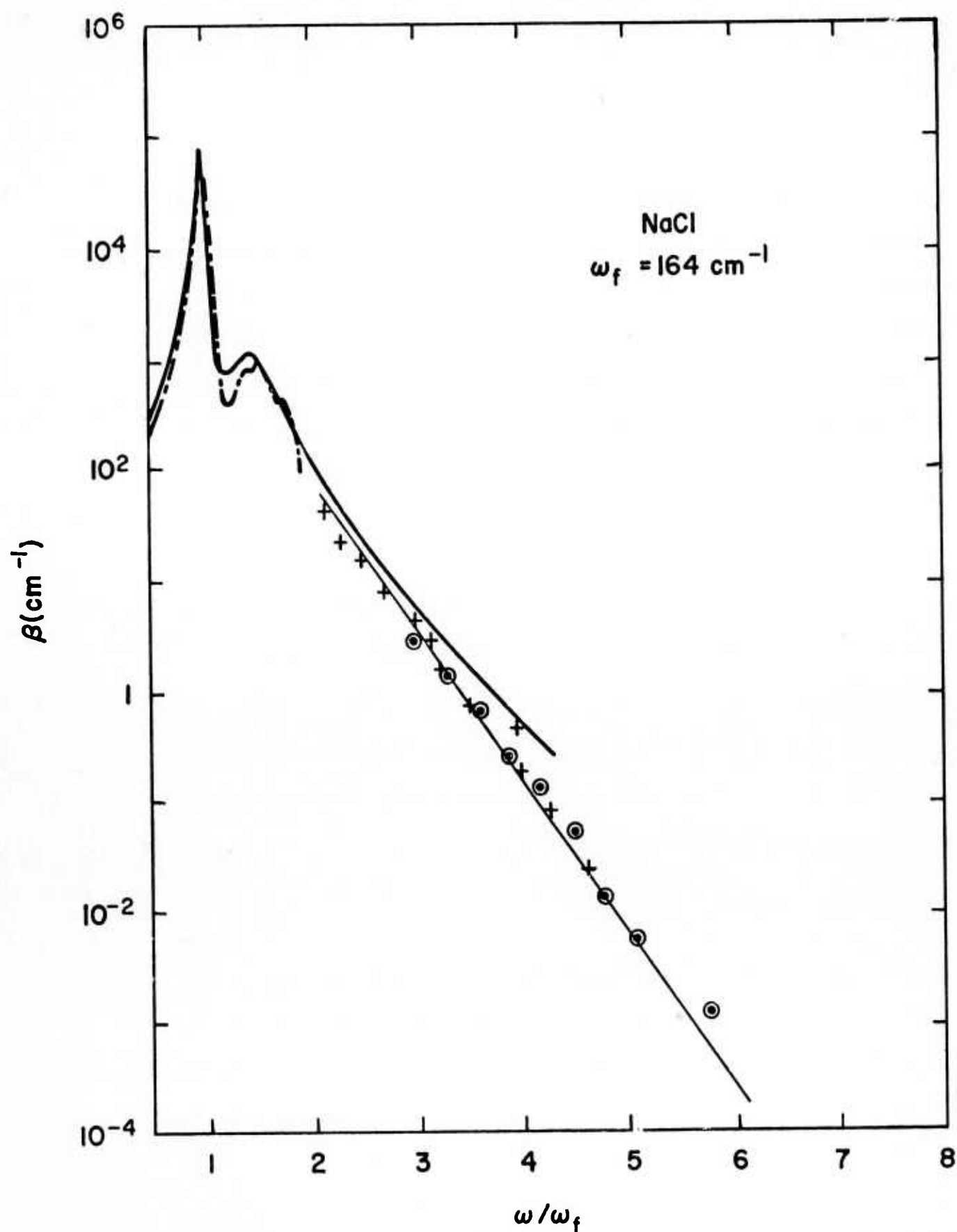


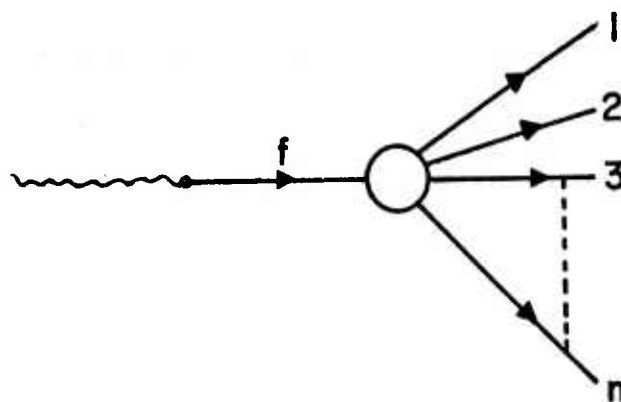
Figure 1. Experimental frequency dependence of the infrared absorption coefficient  $\beta$  for NaCl after Horrigan and Deutsch (+,  $\odot$ ) Ref. 7, Smart, et al (—•—) Ref. 7a, and Genzel (—) Ref. 7b.

At first sight, the nearly exponential behavior might suggest the form  $\beta \sim \exp(-\hbar\omega/k_B T)$ . However, the room-temperature values of the coefficient  $A$  in (1.1) differ by factors of 2 - 4 from the value of  $\hbar/k_B T$ . Furthermore, the temperature dependence<sup>8</sup> of  $\beta$ , though not extensively studied to date, appears to be less strong than  $\exp(-\hbar\omega/k_B T)$ .

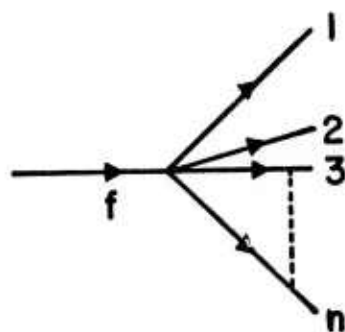
In this paper, an investigation of the optical absorption by multiphonon processes is presented. It is shown that the sum of  $n$ -phonon summation processes is approximately exponentially decreasing with increasing frequency over the frequency range of interest, i. e., about  $2\omega_f - 7\omega_f$ , typically. As illustrated in Fig. 2a, we consider the  $n$ -phonon summation process in which the photon is absorbed by the crystal through the virtual excitation of the fundamental reststrahlen mode which finally emits  $n$  phonons. In other words, the electromagnetic field drives the fundamental mode (off resonance since  $\omega > \omega_f$ ), whose relaxation time is determined by the sum of all possible processes of splitting into  $n$  normal modes of lattice vibrations. The Lax-Burstein-Born higher-order dipole-moment mechanism<sup>9</sup> is not considered explicitly, although most of the analysis still applies to that case.

By energy conservation, the energy  $\hbar\omega$  of the photon absorbed is equal to the sum of the energies of the  $n$  final-state phonons. It follows that the  $n$ -phonon summation process cannot contribute to  $\beta$  when  $\omega > n\omega_{gr}$ , where  $\omega_{gr}$  is the greatest frequency of the phonon spectrum. For  $\omega \ll n\omega_{gr}$ , the contribution  $\beta_n$  of the  $n$ -phonon summation process to  $\beta$  is small because the low frequencies of the final-state phonons greatly restrict the amount of phase space available. Thus,  $\beta_n$  must peak at a frequency not far below  $n\omega_{gr}$ . As  $n$  increases,

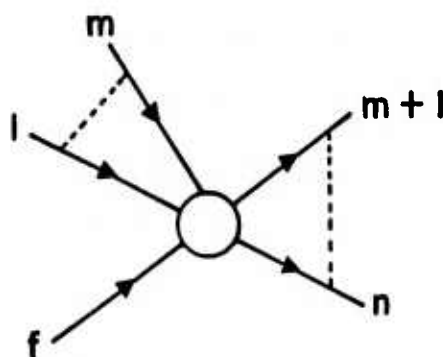
Figure 2.  $n$ -phonon summation and confluence processes.



(a)



(b)



(c)



PHOTON



PHONON

the peak shifts to higher frequencies and decreases in height since higher-order phonon processes involve weaker coupling coefficients. The sum of the  $\beta_n$  then has a frequency dependence nearly exponential in the experimental frequency range. This behavior of the  $\beta_n$  and the sum of the  $\beta_n$  is demonstrated explicitly in Sec. VI.

A preliminary account of these results has been published.<sup>10</sup> Subsequent investigations are discussed in Sec. II. The exponential frequency dependence of the absorption was first suggested by Rupprecht<sup>6</sup> to be due to n-phonon processes, although he did not investigate the theory in detail.

In Sec. II, formal expressions for the contribution to  $\beta$  due to multiphonon processes are given. A practical approximation for the anharmonic coefficient is chosen. In Sec. III, an asymptotic approximation for evaluation of the n-phonon contribution is developed. In Sec. IV, confluence phonon processes are shown to be unimportant in the nearly exponential region. In Sec. V, all possible processes that convert the fundamental phonon to n phonons are examined, and the contributions of vertex corrections are estimated. In Sec. VI, the explicit evaluation of  $\beta_n$  is described, and comparison of theory with experiment is made. In Sec. VII, a summary of all the assumptions and approximations that have gone into the theory is given, and the relation of a computer-calculation program to the present results is discussed.

## II. ANHARMONIC CONTRIBUTION TO THE ABSORPTION COEFFICIENT

The infrared radiation perturbs the insulating crystal by excitation of the dipole moment of the crystal by the oscillating electric field. The absorption coefficient is simply related to the imaginary part of the electric susceptibility by

$$\beta(\omega) = 4\pi\chi_1(\omega) \omega/n_r c, \quad (2.1)$$

where  $c$  is the speed of light and  $n_r$  is the refractive index at frequency  $\omega$ .

The susceptibility, in turn, is just the linear response of the dipole moment.<sup>3, 11</sup>

In an anharmonic crystal, the dipole moment can be expanded in powers of the ionic displacements.<sup>12</sup> For infrared-active crystals, the leading nonzero term is linear in the ionic displacements. The nonlinear terms (the dominant mechanism for infrared absorption in such non-infrared-active crystals as diamond<sup>9</sup>) are probably small in polar crystals, especially in alkali halides,<sup>13, 14</sup> and shall be neglected in this work. However, there are contrary conclusions.<sup>15</sup>

Then, the absorption coefficient is given by the imaginary part of the Green's function of the fundamental mode<sup>3, 13</sup>

$$\beta = \frac{4\pi N e^{*2}}{c m_r n_r \Omega} \frac{\omega \omega_f \Gamma(\omega)}{(\omega^2 - \omega_f^2)^2 + [\omega_f \Gamma(\omega)]^2}, \quad (2.2)$$

where  $N$  is the number of unit cells,  $\Omega$  the volume of the crystal,  $e^*$  is the Born effective charge,  $m_r$  the reduced mass of the two ions in the unit cell, and  $\Gamma$  is the energy relaxation frequency of the fundamental mode (equal to twice the  $\Gamma$  in R. A. Cowley's notation<sup>13</sup>). The real part of the phonon self-energy is understood to have been included in producing the renormalized reststrahl frequency  $\omega_f$ , and its frequency dependence is neglected in Eq. (2.2). A simple classical model of a

harmonic oscillator (the fundamental lattice mode) driven by the applied electric field gives (2.2), but with  $\omega_f \Gamma$  replaced by  $\omega \Gamma$  in the numerator and denominator.<sup>12</sup>

The contribution  $\Gamma_n$  from the  $n$ -phonon summation processes to  $\Gamma$  can be calculated by applying<sup>16</sup> the standard perturbation-theory result that the probability per unit time of a transition between two states is  $2\pi/\hbar$  times the product of the square of the matrix element and the energy conserving delta function, giving

$$\Gamma_n(\omega) = \frac{2\pi}{\hbar^2} (n+1)^2 n! \sum_{Q_1 \cdots Q_n} |\Lambda(fQ_1 \cdots Q_n)|^2 \Delta\left(\sum_{j=1}^n q_j\right) \delta\left(\omega - \sum_{j=1}^n \omega_{Q_j}\right) \tilde{n}_n, \quad (2.3)$$

where  $Q_j$  is the phonon mode with wavevector  $q_j$  and branch  $b_j$ ,  $\Delta$  is the modified Kronecker delta which is unity when the argument is zero or a reciprocal-lattice vector and zero otherwise, and

$$\tilde{n}_n = \prod_{j=1}^n (n_j + 1) / n_{\omega} + 1 \quad (2.4)$$

with

$$n_j = n(Q_j) = 1 / [e^{\omega_{Q_j}/\omega_T} - 1], \quad (2.5)$$

$$n_{\omega} = 1 / (e^{\omega/\omega_T} - 1), \quad (2.6)$$

and

$$\omega_T = k_B T / \hbar. \quad (2.7)$$

Furthermore,  $\Lambda(fQ_1 \cdots Q_n)$  denotes the renormalized  $n+1$  phonon vertex, represented by the circle in Fig. 2a, and is the sum of all possible  $n+1$  phonon vertices. The simplest one is the unrenormalized vertex  $V(fQ_1 \cdots Q_n)$  from the anharmonic Hamiltonian given by<sup>12, 13</sup>

$$\mathcal{K}_{n+1} = \sum_{Q_1} \cdots \sum_{Q_{n+1}} V(Q_1 \cdots Q_{n+1}) \Delta\left(\sum_{j=1}^{n+1} q_j\right) A_{Q_1} \cdots A_{Q_{n+1}}, \quad (2.8)$$

## Sec. C

where

$$A_Q \equiv A_{qb} = a_{qb} + a_{-qb}^\dagger, \quad (2.9)$$

$a^\dagger$  and  $a$  being the phonon creation and annihilation operators normalized to unit commutators, as usual. This simple vertex is represented diagrammatically in Fig. 2b. Other more complicated processes are examined in Sec. V, where we derive an approximate form for the total vertex

$$\Lambda(f Q_1 \cdots Q_n) = \Lambda_n V(f Q_1 \cdots Q_n). \quad (2.10)$$

To obtain a reasonable approximation for the anharmonic coefficients, let us confine our attention to diatomic polar crystals with cubic symmetry, especially NaCl-structure crystals. The model interaction potential<sup>12,17</sup> between ions is composed of a Coulomb potential and a nearest-neighbor overlap exchange repulsion of the form

$$\phi(r) = C \exp(-r/\rho a), \quad (2.11)$$

where  $a$  is the equilibrium nearest-neighbor distance. The Coulomb interaction is used only in determining the constants  $C$  and  $\rho$  in Eq. (2.11) from the equilibrium condition and the value of the bulk modulus,  $B$ , yielding<sup>12,17</sup>

$$C = 3 a^3 B e^{1/\rho} \rho^2 / (1 - 2\rho). \quad (2.12)$$

In the anharmonic coefficients, only the derivatives of the repulsive potential (2.11) are retained. Since  $\rho$  is of the order of 0.1 for NaCl, the derivatives of the Coulomb potential are smaller than the corresponding ones of the repulsive

potential for orders up to at least  $n \cong 10$ . Had we used an inverse power law for the repulsive potential, this would be true to any order. This model, including the neglect of the Coulomb potential in the anharmonic terms, has been used previously<sup>13</sup> with much success.

The anharmonic coefficients can be obtained in a straightforward calculation from this nearest-neighbor exchange repulsion potential.<sup>12</sup> The  $m^{\text{th}}$  order coefficient  $V(Q_1 \cdots Q_m)$  involves derivatives of  $\phi(r)$  up to order  $m$ . From the exponential form (2.11), it is clear that

$$|a \phi^{(m)}(a) / \phi^{(m-1)}(a)| \sim 10 \quad (2.13)$$

Thus, it is a good approximation to retain only the highest-order derivative.

Using these results and assuming central forces yields

$$V(Q_1 \cdots Q_m) = (N/m!) \phi^{(m)}(a) \sum_{\gamma=1}^6 \prod_{j=1}^m U_{\gamma}(Q_j) (\hbar/2Nm_{<} \omega_{Q_j})^{1/2} \quad (2.14)$$

where

$$U_{\gamma}(Q_j) = \hat{x}_{\gamma} \cdot \left[ \tilde{w}_{<Q_j}^{-(m_{<}/m_{>})^{1/2}} \tilde{w}_{>Q_j} e^{i\mathbf{q} \cdot \mathbf{x}_{\gamma}} \right] \quad (2.15)$$

and  $m_{<}$  and  $m_{>}$  denote the smaller and larger ionic masses, respectively.

The positions of nearest neighbors measured from the lighter ion are  $\mathbf{x}_{\gamma}$ , and  $\hat{x}_{\gamma}$  is the unit vector in the same direction. The polarization vector  $\tilde{w}_{<Q}$  is defined in terms of the ionic displacement  $\mathbf{u}_{l\tau}$  from the equilibrium position  $\mathbf{x}_{l\tau}$  by the relation<sup>12, 18</sup>

# Sec. C

$$u_{\ell\tau} = \sum_Q (\hbar/2 N m_\tau \omega_Q)^{1/2} e^{i\mathbf{q} \cdot \mathbf{x}_{\ell\tau}} A_Q w_{\tau Q}, \quad (2.16)$$

with  $\tau$  denoting the ion type. For the fundamental mode,

$$U_\gamma(f) = \hat{x}_\gamma \cdot \hat{w}_f (m_</m_r)^{1/2}, \quad (2.17)$$

with  $m_r = (m_<^{-1} + m_>^{-1})^{-1}$ . From Eq. (2.11), we obtain the  $m^{\text{th}}$  derivative

$$\phi^{(m)}(a) = 3Ba^3 \rho^2 / \left\{ (1-2\rho)(-\rho a)^m \right\}. \quad (2.18)$$

Substituting the approximate expression (2.14) for the anharmonic coefficient into Eq. (2.3) for  $\Gamma_n$ , we obtain, by using Eq. (2.2), the contribution of the  $n$ -phonon summation process to the optical absorption in the form

$$\beta_n = (\pi/2)^{1/2} K \omega_{mx}^5 D_\rho (1 - e^{-\omega/\omega_T}) (\omega^4 n!)^{-1} (\omega_{mx} D_e)^n \Lambda_n^2 \Sigma_n. \quad (2.19)$$

We have used the approximation for high frequency ( $\omega^2 \gg \omega_f^2 + \Gamma^2$ ) and introduced the following groups of constants:

$$\begin{aligned} K &= B^2 e^{*2} a \omega_f / \hbar c m_r^2 n_r \omega_{mx}^5, \\ D_\rho &= (2\pi)^{-1/2} [6\pi\rho/(1-2\rho)]^2, \\ D_e &= \hbar/2 \rho^2 a^2 m_< \omega_{mx}. \end{aligned} \quad (2.20)$$

The frequency  $\omega_{mx}$ , introduced for later use, cancels out in Eq. (2.19).

## Sec. C

The factor  $\Sigma_n$  contains the dynamical information of the n-phonon absorption, and is given by

$$\Sigma_n = \sum_{\gamma=1}^6 \sum_{\gamma'=1}^6 (\hat{x}_{\gamma} \cdot \hat{w}_f) (\hat{x}_{\gamma'} \cdot \hat{w}_f) N^{-n} \sum_{Q_1 \dots Q_n} N \Delta \left( \sum_{j=1}^n q_j \right) \delta \left( \omega - \sum_{j=1}^n \omega_{Q_j} \right) \prod_{j=1}^n U_{\gamma}(Q_j) U_{\gamma'}(Q_j)^* \left[ n(\omega_{Q_j}) + 1 \right] / \omega_{Q_j} \quad (2.21)$$

For crystal of NaCl structure, symmetry<sup>19a</sup> ensures that  $\Sigma_n$  and, therefore,  $\beta_n$  are independent of the direction of  $\hat{w}_f$ . Let us choose  $\hat{w}_f$  to be along the positive x-axis. Then, Eq. (2.21) becomes

$$\Sigma_n = 2 \Sigma_{n+} + 2(-1)^{n+1} \Sigma_{n-} \quad (2.22)$$

where

$$\Sigma_{n\pm} = N^{-n} \sum_{Q_1 \dots Q_n} N \Delta \left( \sum_{j=1}^n q_j \right) \delta \left( \omega - \sum_{j=1}^n \omega_{Q_j} \right) \prod_{j=1}^n W_{\pm}(Q_j) (n_{Q_j} + 1) / \omega_{Q_j} \quad (2.23)$$

and, with Re and Im denoting real and imaginary parts, respectively,

$$W_{\pm}(Q) = [ \text{Re } U_x(Q) ]^2 \pm [ \text{Im } U_x(Q) ]^2 \quad (2.24)$$

In passing, notice that the evaluation of the sums in (2.23) is trivial if the density of states  $g(\omega)$  is approximated by the Einstein model

$$g(\omega) = \delta(\omega - \omega_E)$$

and the angle dependence of  $W_{\pm}(Q)$  is neglected:  $W_{\pm}(Q) = W_{\pm}$ . It will be shown later than  $W_+^n \gg W_-^n$ . Then (2.23) and (2.19) give directly

$$\beta = \sum_{n=1}^{\infty} \frac{E \Lambda_n^2}{4^n n!} \left( 1 - e^{-n \omega_E / \omega_T} \right) \left\{ \frac{6 \omega_{mx} D_e W_+[n(\omega_E)+1]}{\omega_E} \right\}^n \delta(\omega - n \omega_E), \quad (2.25)$$

where  $E \equiv (2\pi)^{1/2} K \omega_{mx} D_\rho$ . According to (2.25), the spectrum is approximated by a series of delta functions, which is, of course, not realistic. Even though such a model is not of significant practical value, it does crudely approximate some of the features of the more realistic model discussed below. For example, plotting the coefficients of the delta functions in (2.25), or formally replacing the delta functions by line-shape functions of finite width, gives a nearly exponential decrease with increasing frequency. In Ref. 19b, the result (2.25) was rederived using the simpler model of a one-dimensional lattice with the Einstein approximation and a simpler interaction potential that neglects the angle dependence [our factor  $W_\pm(Q)$ ] from the outset, and an independent-molecule model was considered. Use of this simpler interaction potential gives unreasonably large values of  $\Lambda_n^2$ , which causes noticeable deviation from an exponential frequency dependence.<sup>19b</sup>

Mills and Maradudin<sup>19c</sup> independently used a single-frequency anharmonic-molecule type lattice to study various types of interaction potentials, effects of impurities, and high-temperature effects. Bendow, Ying, and Yukon<sup>19d</sup> have used a different mathematical method that starts with partially summed terms. The method is potentially powerful, but to date they have recovered only our terms without the vertex correction. Since the validity of the perturbation expansion is justified by showing that all diagrams not included in the result are negligible, it is expected that new methods of calculation should give equivalent results. For example, the factor  $\exp(-\gamma T)$  resulting from vertices with phonon loops [ $A_Q A_Q S$ ,  $A_Q A_Q A_Q A_Q S$ , etc., where  $S$  is the simple vertex and the  $A_Q$  are defined in (2.9)] is well approximated by 1 since the phonon-loop terms are negligible with respect to simple vertices. See Sec. V.

### III. ASYMPTOTIC APPROXIMATION FOR ABSORPTION BY A LARGE NUMBER OF PHONONS

Eq. (2.19) gives the contribution to the absorption coefficient by the  $n$ -phonon summation process. It contains the factor  $\Sigma_n$  given by Eqs. (2.22) to (2.24) which involves  $n$ -fold Brillouin-zone sums. Although these are not beyond the means of modern computing capabilities for  $n$  in the experimental range of 2 to 8, we are still interested in analytical approximations that will give us general properties of  $\beta$  which appear to be shared by a rather large number of crystals. The method of evaluation used in this section is correct in the large- $n$  limit.

For  $n \gtrsim 2$  we can neglect the quasi-momentum conservation restriction in the sums given by Eq. (2.23). We shall justify this later in the section. First notice that if the angle dependence of  $W_{\pm}(Q_j)$  is neglected, the summand in (2.23) is a function of phonon frequencies  $\omega_{Q_j}$  only. Then, replacing the sums over  $Q_j$  by integrals over  $d\omega_{Q_j} g(\omega_{Q_j})$ , where  $g(\omega_{Q_j})$  is the phonon density of states, reduces (2.23) to the form

$$\Sigma_{n\pm} = \int d\omega_{Q_1} f(\omega_{Q_1}) \cdots \int d\omega_{Q_n} f(\omega_{Q_n}) \delta(\omega - \sum_{j=1}^n \omega_{Q_j})$$

to which the central-limit theorem applies directly. Here  $f(\omega_{Q_j}) = 6N^{-1} W_{\pm}(Q_j) (n_{Q_j} + 1) g(\omega_{Q_j}) / \omega_{Q_j}$ , where the normalization constant  $6N^{-1}$  arises since  $g$  is normalized to unity.

Eq. (2.23) can be cast into this central-limit-theorem form without neglecting the angle dependence of  $W_{\pm}(Q_j)$  as follows: We introduce two functions which are kindred to the phonon propagators

$$\sigma_{\pm}(\xi) = \left\{ \omega_{\text{mx}} / N \alpha_{0\pm} \right\} \sum_Q W_{\pm}(Q) \left\{ (n_Q + 1) / \omega_Q \right\} \delta(\xi - \omega_Q), \quad (3.1)$$

where

$$\alpha_{0\pm} = \omega_{\text{mx}} N^{-1} \sum_Q W_{\pm}(Q) (n_Q + 1) / \omega_Q \quad (3.2)$$

are constants for normalizing the integrals of  $\sigma_{\pm}(\xi)$  over  $\xi$  to unity.

The  $n$ -fold sums in Eq. (2.23) can be written as  $n$ -dimensional integrals,

$$\Sigma_{n\pm} = (\alpha_{0\pm} / \omega_{\text{mx}})^n \int_{-\infty}^{\infty} d\xi_1 \sigma_{\pm}(\xi_1) \cdots \int_{-\infty}^{\infty} d\xi_n \sigma_{\pm}(\xi_n) \delta(\omega - \sum_{j=1}^n \xi_j). \quad (3.3)$$

These convolution integrals are well known in statistics. For  $n \rightarrow \infty$ , the integral tends to a Gaussian (the central-limit theorem),

$$\Sigma_{n\pm} = \left[ \alpha_{0\pm}^n / (2\pi n)^{1/2} \alpha_{2\pm} \omega_{\text{mx}}^{n+1} \right] \exp \left[ -(\omega - n \alpha_{1\pm} \omega_{\text{mx}})^2 / 2 n \alpha_{2\pm}^2 \omega_{\text{mx}}^2 \right] \quad (3.4)$$

where  $\alpha_{0\pm}$  are defined in Eq. (3.2), and

$$\alpha_{1\pm} = \omega_{\text{mx}}^{-1} \int_{-\infty}^{\infty} d\xi \sigma_{\pm}(\xi) \xi, \quad (3.5)$$

$$(\alpha_{2\pm} \omega_{\text{mx}})^2 = \int_{-\infty}^{\infty} d\xi \sigma_{\pm}(\xi) \xi^2 - (\alpha_{1\pm} \omega_{\text{mx}})^2. \quad (3.6)$$

For small  $n$ , it is possible to improve Eq. (3.4) with an asymptotic series.<sup>20</sup>

A particular series in terms of Hermite polynomials has been used by Sjolander<sup>21</sup> to evaluate the multiphonon background in neutron scatterings in a harmonic crystal.

It is obvious from Eq. (2.24) that  $\alpha_{0-}$ , as defined by Eq. (3.2), is less than  $\alpha_{0+}$ . The estimates discussed in Sec. VI show that  $\alpha_{0-}$  is about one third to one half of  $\alpha_{0+}$ , at most. Since  $\Sigma_{0\pm} \sim (\alpha_{0\pm})^n$  according to (3.4),  $\Sigma_{n-}$  becomes negligible compared with  $\Sigma_{n+}$  for large  $n$ . Therefore, from Eqs. (3.4), (2.22), and (2.19), the absorption coefficient has the explicit form

$$\beta_n = \frac{D_p K}{\alpha_{2+} (n\omega + 1)} \left( \frac{\omega_{mx}}{\omega} \right)^4 \frac{1}{n^{\frac{1}{2}} n!} (\alpha_{0+} D_e)^n \Lambda_n^2 \exp \left[ -(\omega - n\alpha_{1+} \omega_{mx})^2 / 2n (\alpha_{2+} \omega_{mx})^2 \right]. \quad (3.7)$$

By virtue of the central-limit theorem, the multiple sum over  $Q_1, \dots, Q_n$  has been reduced to sums over a single phonon coordinate  $Q_1$ , as given by Eqs. (3.2), (3.5), and (3.6).

The neglect of momentum conservation appears to be physically reasonable since, for larger and larger  $n$ , the restriction on phase space becomes less and less important. However, if we wish not to neglect the momentum conservation in Eq. (2.2), we can extend the foregoing procedure by treating the summations over  $q_j$  in the same manner as the integrals over  $\zeta_j$ . Thus, we introduce the functions  $\sigma_+(q, \zeta)$  similar to Eq. (3.1), except omitting the sum over  $q$ . Eq. (3.3) becomes not only multiple integrals over  $\zeta_j$  but also over  $q_j$  with four  $\delta$  functions, one for the frequency and three for the wavevectors. The convolution integral is evaluated in the same way by means of the central-limit theorem. The integrals over  $q_j$  contribute a factor which is a lattice sum of Gaussians of the form  $\exp(-n\alpha x_\ell^2)$  and is, therefore, approximately unity for large  $n$ . We arrive at the same answer as Eq. (3.4), thereby justifying the neglect of momentum conservation.

## IV. THE CONFLUENCE PROCESSES

In the preceding calculation of the multiphonon absorption of light, only a particular type of phonon processes, called the  $n$ -phonon summation processes and illustrated in Fig. 2a, was considered. We have neglected the confluence processes, illustrated in Fig. 2c. Instead of creating  $n$  phonons after the annihilation of the fundamental phonon,  $m$  phonons are absorbed, and  $n-m$  phonons are created.

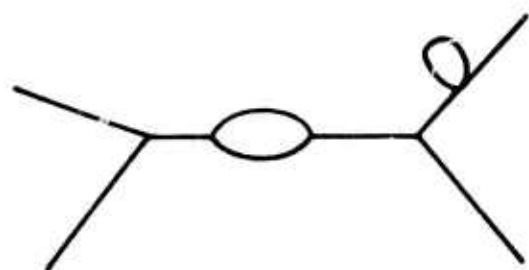
A confluence process involving  $n$  phonons (some of which are created and some annihilated) is governed by the same vertex as the  $n$ -phonon summation process. The contribution to the absorption coefficient of all confluence processes and the summation process is easily obtained by replacing  $\delta(\xi - \omega_Q)$  by  $\delta(\xi - \omega_Q) - \delta(\xi + \omega_Q)$  and  $n(-\omega_Q)$  by  $-[n(\omega_Q) + 1]$  in (3.1). The cross-product terms in (3.3) containing  $m$  factors of  $-\delta(\xi + \omega_Q)$  and  $n-m$  factors of  $\delta(\xi - \omega_Q)$  correspond to the confluence process with  $m$  thermally excited phonons absorbed, as shown in Fig. 2c. Applying the central-limit theorem to this term yields a Gaussian peaked at  $(n-m)\alpha_{1+}\omega_{mx} - m\beta_{1+}\omega_{mx}$  instead of  $n\alpha_{1+}\omega_{mx}$ , where  $\beta_{1+}$  is defined by Eq. (3.5) with the new  $\sigma_+(\xi)$ . This contribution will be masked by the summation process of  $n-2m$  phonons which peaks at about the same frequency but has greater strength, being an anharmonic process of lower order.

## V. VERTEX CORRECTIONS

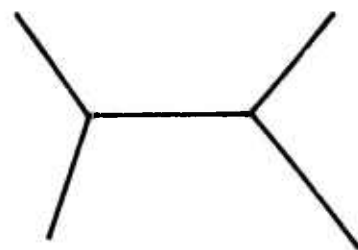
Now we consider all possible processes that contribute to the  $(n+1)^{\text{th}}$ -order vertex  $\Lambda(fQ_1 \cdots Q_n)$  and estimate the vertex correction factor  $\Lambda_n$ , defined by Eq. (2.10). Standard perturbation theory can be applied in a straightforward way to all the higher-order terms. For example, for  $n = 3$ , the diagram in Fig. 4b below has one intermediate state. The contribution from this diagram is easily calculated, but it must be remembered that this diagram represents four diagrams when the arrow is added to the intermediate-state phonon. (There are two time orderings of the two vertices, and the arrow can go in either direction, corresponding to  $a^\dagger$  and  $a^\dagger a$ , in each time ordering.) This procedure has been carried out for a number of low-order diagrams,<sup>10</sup> and the results agree with those presented below.

Since the number of diagrams increases rapidly as  $n$  increases, this method becomes tedious and time consuming when applied to larger values of  $n$ . The following method is more convenient. First, all the self-energy corrections, such as those illustrated in Fig. 3a, are taken to be accounted for by using the measured phonon frequencies, i.e., they are included in the corresponding "skeleton" diagram (Fig. 3b). The lifetime of the intermediate- and final-state phonons is taken to be infinite.

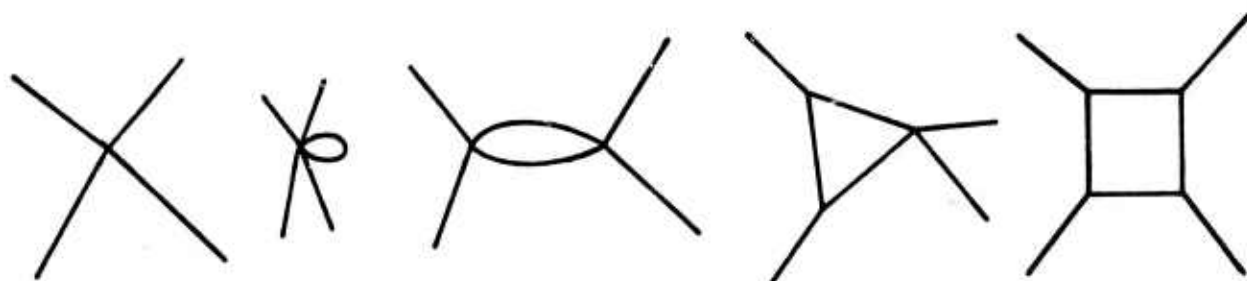
There are two types of vertices: (1) the irreducible ones that cannot be rent asunder by cutting a single phonon line, such as those in Fig. 3c, and (2) the reducible ones that can be separated by cutting a single line, such as those in Fig. 3d.



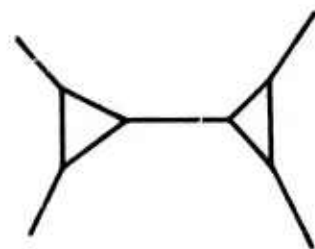
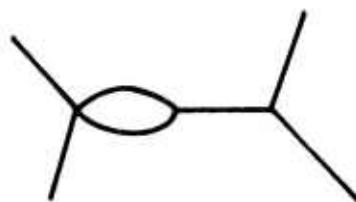
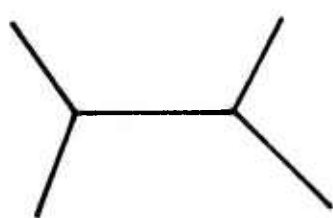
(a)



(b)

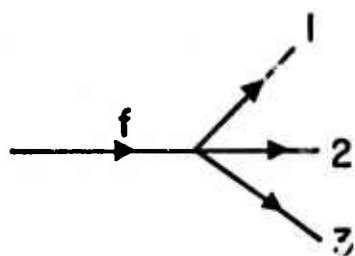


(c)

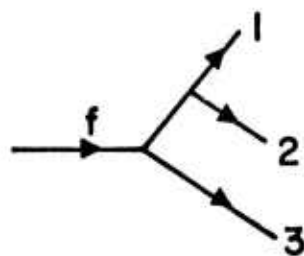


(d)

Figure 3. Various kinds of vertices.



(a)



(b)



(c)

Figure 4. Three-phonon summation processes.

## Sec. C

In the sum of all irreducible vertices of the same number of external phonon lines, the simple vertex dominates. We follow Van Hove<sup>22</sup> in ordering the anharmonic terms in the Hamiltonian,  $V(Q_1 \cdots Q_n)$ , with  $\epsilon^{n-2}$  where  $\epsilon$  is the small parameter given by the ratio of the root-mean-square displacement of the ions to the nearest-neighbor distance. The value of  $\epsilon$  is less than 0.05 in alkali halides. A complex irreducible vertex must be of higher order in  $\epsilon$  than the simple vertex with the same number of external lines, since cutting a phonon line will produce one vertex with a larger number of external lines. For example, the simple vertex in Fig. 3c is  $O(\epsilon^2)$ , but all the other irreducible vertices in Fig. 3c are  $O(\epsilon^4)$ .

On the other hand, a reducible vertex composed of simple irreducible vertices is of the same order in  $\epsilon$  as the simple vertex with the same number of external lines. For example, the first diagram in Fig. 3d is  $O(\epsilon^2)$ . A reducible vertex that contains one or more complex irreducible vertices is again negligible. Therefore, for the total vertex contribution, we need only sum the simple vertex and the reducible vertices which are composed of simple vertices only.

To illustrate the procedure of obtaining the vertex renormalization to the  $n$ -phonon summation process, the simplest non-trivial vertex correction, namely  $\Lambda_3$ , is first calculated. The two vertex terms that contribute to the three-phonon absorption are given in Fig. 4a and 4b. The ratio of the latter to the simple vertex is

$$\frac{(3!)^2}{2!} \sum_{Q_4} V(fQ_3 Q_4) D(Q_4, \zeta_4) V(Q_4 Q_1 Q_2) / \frac{4!}{3!} V(fQ_1 Q_2 Q_3) . \quad (5.1)$$

## Sec. C

The two factors of  $3!$  represent the number of ways<sup>23, 13</sup> the phonon states are attached to the limbs of each vertex in Fig. 4b. The divisor  $2!$  represents the fact that interchanging the labels on phonon lines 1 and 2 again produces the same term. The factor  $4!$  is the number of ways the four-phonon vertex in Fig. 4a can be labelled, and the divisor  $3!$  is the overcounting factor generated by rearranging the labels among lines 1, 2 and 3 in Fig. 4a. The factor  $D(Q_4, \zeta_4)$  represents the Green's function for the intermediate phonon line<sup>23, 13</sup> in Fig. 4b.

By using the form (2.14) for the anharmonic coefficient and keeping only one term in the sum over nearest neighbors for both the numerator and the denominator of the ratio (5.1), we obtain the ratio as

$$\frac{3!}{2!} \phi^{(2)} \sum_{b_4} \frac{\hbar}{2m\omega_{Q_4}} |U_x(Q_4)|^2 D(Q_4, \zeta_4) . \quad (5.2)$$

The factorial that represents the number of ways the states in each vertex are labelled cancels neatly the factorial in the anharmonic coefficient (2.14), leaving the counting factor in front of (5.2). This factor is just the ratio of the number of ways of rearranging the labels on the equivalent outgoing phonon lines of Fig. 4a to the corresponding number for Fig. 4b.

The factor  $\phi^{(2)}$  comes from the fact that

$$\left\{ \phi^{(3)} \right\}^2 / \phi^{(4)} = \phi^{(2)} \quad (5.3)$$

by virtue of Eq. (2.18). The momentum and frequency of the intermediate-phonon Green's function are given by

$$Q_4 = Q_1 + Q_2 \quad (5.4)$$

### Sec. C

and

$$\zeta_4 = \omega_f - \omega_3 = \omega_1 + \omega_2 \approx 2\omega_{mx} \quad (5.5)$$

for the frequencies of interest. Let

$$\omega_{Q_4} = \nu \omega_{mx} \quad (5.6)$$

$$d_\ell = \hbar \omega_{mx}^2 D(Q_4, \ell \omega_{mx}) / 2 \omega_{Q_4} = (\ell^2 - \nu^2)^{-1} \quad (5.7)$$

and

$$\xi = \phi^{(2)} \sum_{b_4} |U_x(Q_4)|^2 D(Q_4, \ell \omega_{mx}) (\hbar / 2 m \omega_{Q_4}) / d_\ell . \quad (5.8)$$

Then, the ratio of the two vertices, (5.2), becomes  $3 d_2 \xi$ , and the vertex renormalization factor is

$$\Lambda_3 = 1 + 3 d_2 \xi . \quad (5.9)$$

Estimates of  $d_2$  and  $\xi$  are provided in the next section. It is easy to verify that (5.9) correctly accounts for all the three-phonon absorption processes shown in Fig. 4c.

The reasoning used in this simple example can be applied to the general case to deduce the rules for writing down the renormalization factor for  $n$ -phonon absorption. The simplest term in the total vertex is the simple  $n+1$  phonon vertex with one of the phonons being the fundamental mode driven at the optical frequency, as depicted by Fig. 5a. A typical reducible vertex is formed by joining a number of irreducible vertices of lower order such that there is only one phonon line connecting any pair of irreducible vertices. Some examples are shown in Fig. 5b-5d.

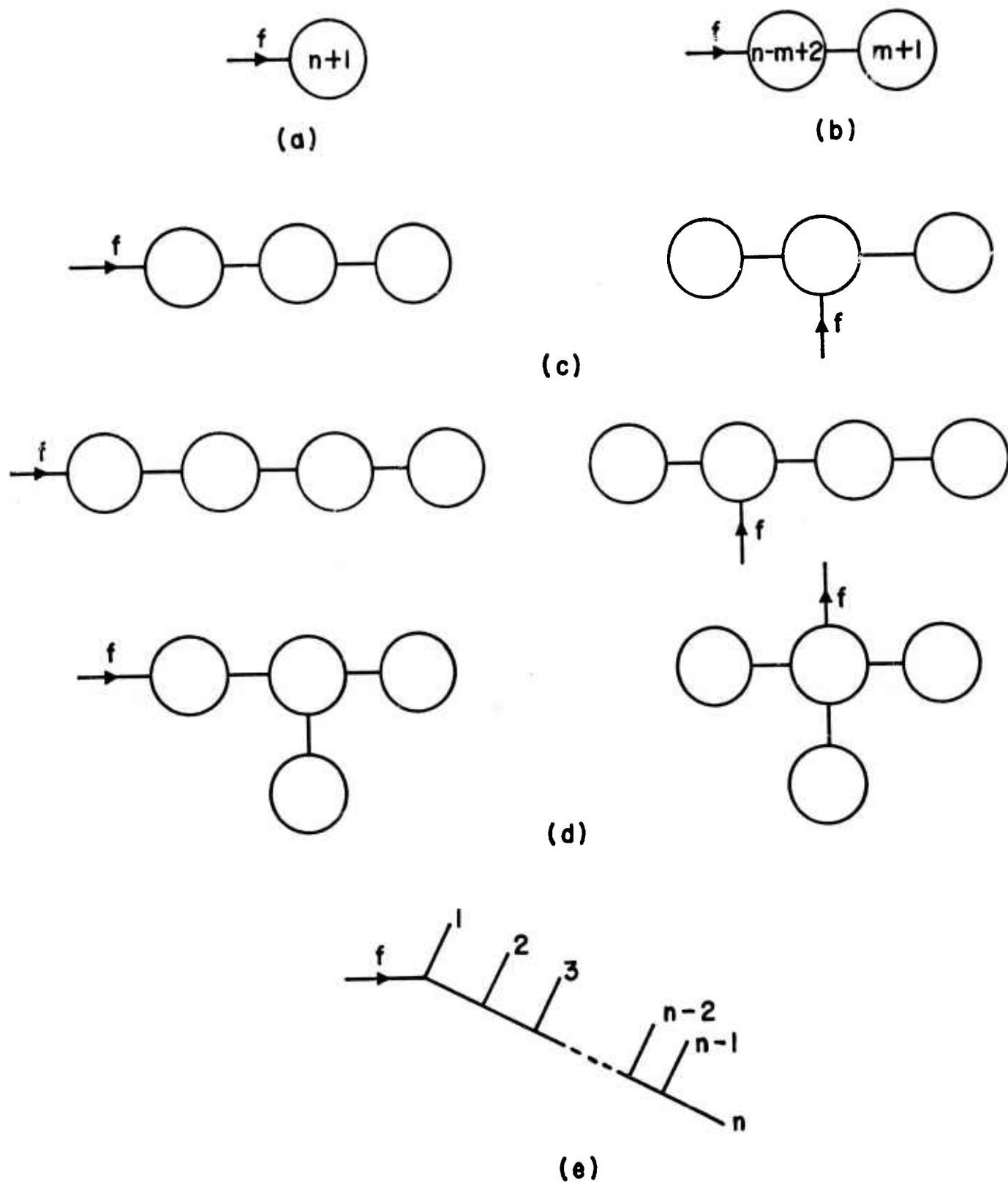


Figure 5. The  $n$ -phonon absorption vertices. The number  $n$  in a circle denotes a simple vertex with  $n$  external lines.

### Sec. C

If a vertex contains  $m$  internal lines, then its ratio to the simple vertex (Fig. 5 a) contains a factor  $\xi^m$ , with  $\xi$  defined by Eq. (5.8). Thus,

$$\Lambda_n = \sum_{m=0}^{n-2} S_n^{(m)} \xi^m, \quad (5.10)$$

with the coefficient  $S_n^{(m)}$  obtained as follows. Draw all topologically distinct reducible vertices with  $m$  internal lines and  $n+1$  external lines, one of which is the fundamental phonon driven at frequency  $n\omega_{mx}$ . Each diagram contributes to  $S_n^{(m)}$  a term of the form

$$C_n^{(m)} d_{\ell_1} d_{\ell_2} \cdots d_{\ell_m}, \quad (5.11)$$

where  $C_n^{(m)}$  is the ratio of  $n!$  to the number of ways of rearranging the states of the  $n$  outgoing phonon lines that do not change the reducible vertex. The factors of  $d_{\ell}$  come from the intermediate phonon lines,  $\ell$  being determined by energy conservation, assuming that all outgoing phonon lines have frequency  $\omega_{mx}$ .

For example, the vertices with one internal line, as in Fig. 5 b, give

$$S_n^{(1)} = \sum_{m=2}^{n-1} \binom{n}{m} d_m, \quad (5.12)$$

and Fig. 5 e contributes to  $S_n^{(n-2)}$  the term

$$(n!/2!) d_2 d_3 \cdots d_{n-1}. \quad (5.13)$$

## Sec. C

Armed with the general rules, we can calculate the contribution of any vertex. Figs. 6 - 8 show the relevant vertices for four- to six-phonon absorption, respectively, and the corresponding contributions to  $S_n^{(m)}$ .

From the considerations in the next section, the factor  $\nu$  in Eq. (5.6) is 0.5 or less; thus (5.7) gives

$$d_\ell \approx \ell^{-2} . \quad (5.14)$$

Therefore, the vertex correction factors are

$$\begin{aligned} \Lambda_2 &= 1 , & \Lambda_3 &= 1 + 0.75 \xi , & \Lambda_4 &= 1 + 1.9444 \xi + 0.5208 \xi^2 , \\ \Lambda_5 &= 1 + 3.9236 \xi + 2.6563 \xi^2 + 0.3711 \xi^3 , \\ \Lambda_6 &= 1 + 7.1497 \xi + 9.2682 \xi^2 + 3.2511 \xi^3 + 0.2806 \xi^4 . \end{aligned} \quad (5.15)$$

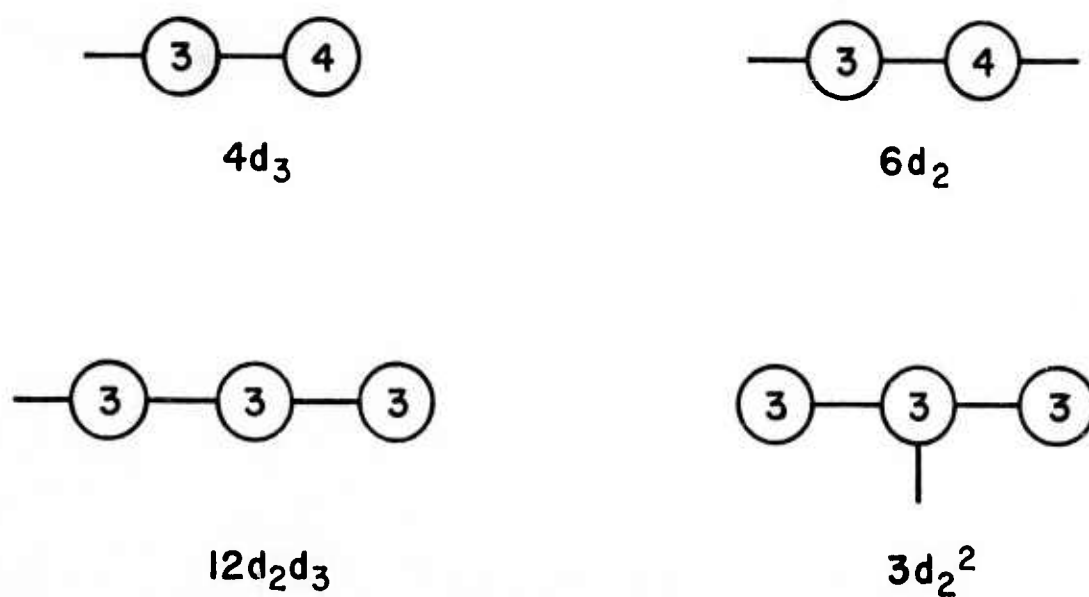


Figure 6. The 4-phonon absorption vertices. The only external line shown is the fundamental mode.

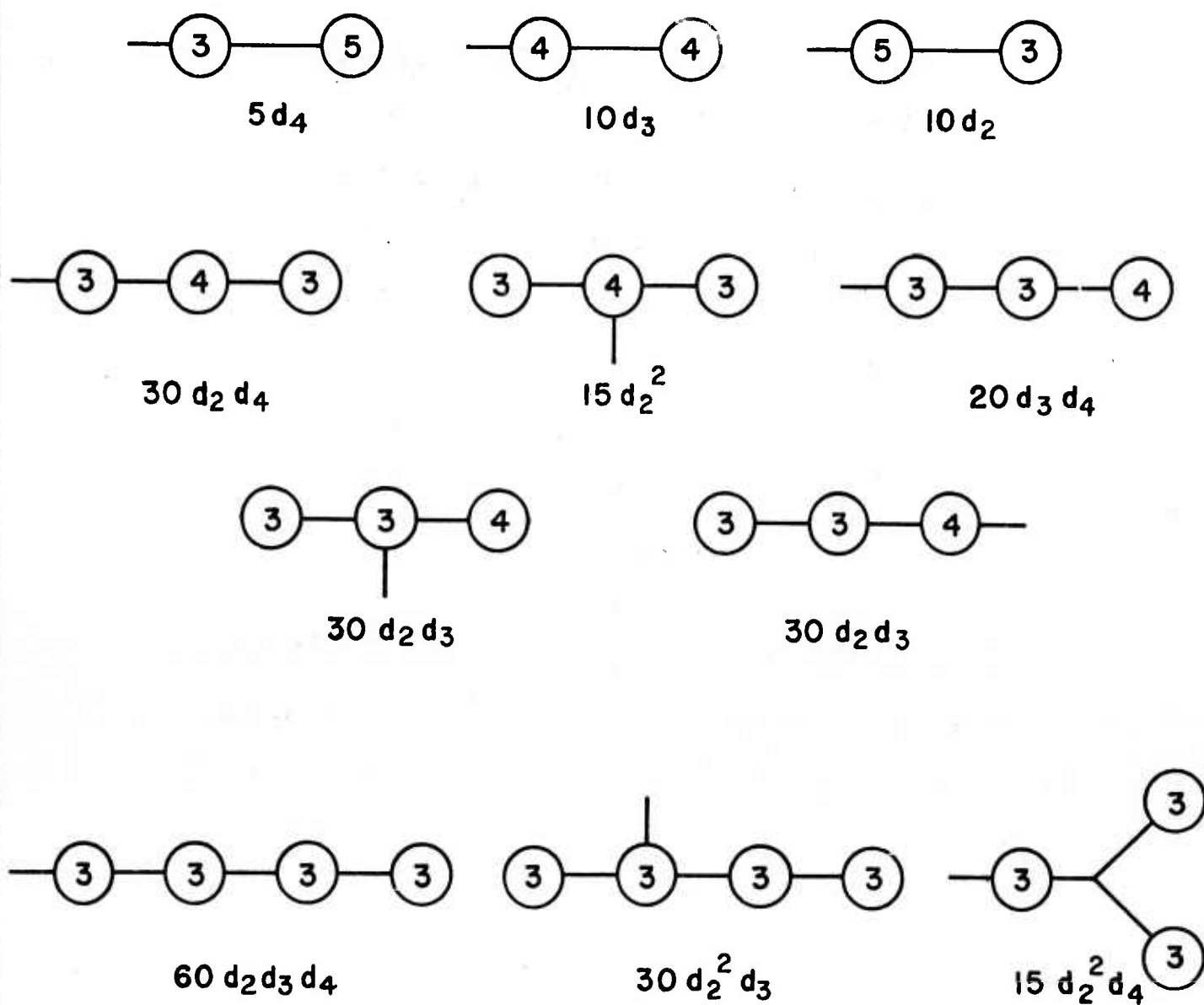


Figure 7. The 5-phonon absorption vertices.

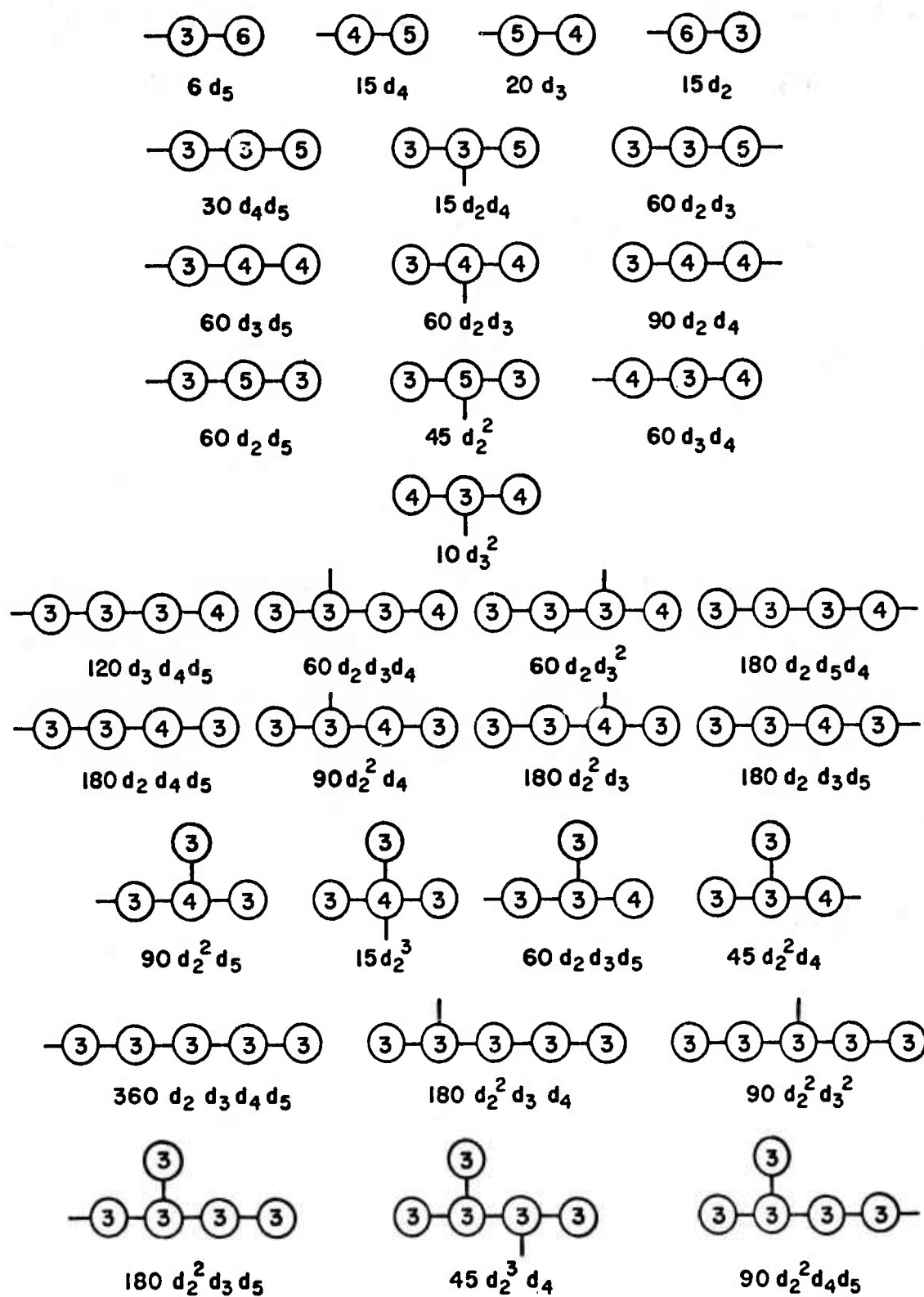


Figure 8. The 6-phonon absorption vertices.

## VI. FREQUENCY AND TEMPERATURE DEPENDENCE OF THE ABSORPTION COEFFICIENT

It is straightforward to evaluate  $\beta_n$  given by Eq. (3.7) with the  $\alpha$ 's given by the Brillouin-zone sums. We shall confine ourselves to two rough estimates of the  $\alpha$ 's.

For a linear-chain model with two atoms per unit cell, all with equal masses, it is possible to evaluate explicitly the  $\alpha$ 's in the low- and high-temperature limits. Table I shows the results for the  $\alpha$ 's with  $\omega_{mx}$  chosen to be the top of the phonon spectrum. This simple model illustrates nicely all the important features that follow from Eq. (3.7). As a function of frequency, the absorption coefficient  $\beta_n$  due to the  $n$ -phonon summation process peaks near  $n\alpha_{1+} \omega_{mx}$ , which is about  $(3/4)n\omega_{mx}$ . Thus, the total absorption coefficient, which is the sum of all  $\beta_n$  with  $n \geq 2$ , is dominated at a particular frequency by the nearest  $n$ -phonon summation process. The frequency dependence of  $\beta$  in the range  $2\omega_{mx} - 8\omega_{mx}$  is, therefore, approximately exponential since the strength of the peak in  $\beta_n$  as a function of  $n$  is approximately exponential. The small values of  $\alpha_{0-}$  confirm the validity of neglecting  $\Sigma_{n-}$  in Eq. (3.7). As the temperature is raised, the strength of the peak in  $\beta_n$  increases, the position of the peak is shifted toward the lower frequency, and the width is either narrowed or broadened, depending on the temperature dependence of the phonon frequencies. Thus,  $\beta$  increases with temperature, but less rapidly than  $T^{n-1}$  at high temperatures.

Now we give a more realistic estimate for NaCl-structure crystals. There are several wavevectors for which the explicit expression of  $|U_x(Q)|^2$  can be

Table I. Values of parameters from the diatomic-chain model with equal masses

|        | $\alpha_{0+}$           | $\alpha_{1+}$ | $\alpha_{2+}$                                  | $\alpha_{0-}$ |
|--------|-------------------------|---------------|--|---------------|
| Low T  | $8/\pi$                 | $\pi/4$       | 0.223  | $8/3\pi$      |
| High T | $4\omega_T/\omega_{mx}$ | $2/\pi$       | $[(\pi\omega_T/4\omega_{mx}) - 4/\pi^2]^{1/2}$ | 0             |

written down. For the acoustic branch at the zone boundary in the (1,1,1) direction, the light-mass ions stand still, and the heavy ions move in the direction  $\hat{w}_{>Q}$ , say. Then,

$$|U_x(Q)|^2 = (\hat{x} \cdot \hat{w}_{>Q})^2 m_{<}/m_{>}. \quad (6.1)$$

Similarly, for the optical branch at the same wavevector,

$$|U_x(Q)|^2 = (\hat{x} \cdot \hat{w}_{<Q})^2. \quad (6.2)$$

For the optical modes near the zone center,  $U_x(Q)$  is given by Eq. (2.17). For the acoustical modes near the zone center,  $|U_x(Q)|^2$  is nearly zero.

As a rough approximation,  $|U_x(Q)|^2$  will be set equal to zero for  $\omega < f\omega_{mx}$  where  $f < 1$ , and where it is not negligible,  $|U_x(Q)|^2$  will be approximated by an average of the three known expressions (6.1), (6.2), and (2.17); thus,

$$|U_x(Q)|^2 \approx \frac{2}{9} (1 + m_{<}/m_{>}) \theta(\omega_Q - f\omega_{mx}), \quad (6.3)$$

where  $\theta$  is the unit step function. In the average, we have replaced  $(\hat{x} \cdot \hat{w}_{<Q})^2$  by  $1/3$ , which is the value for the (1,1,1) zone-boundary mode and is also the angular average of  $\cos^2 \theta$ . The remaining factor is the average of  $1$ ,  $m_{<}/m_{>}$  and  $m_{<}/m_r$ .

The estimates of the  $\alpha$ 's are then, from (3.1), (3.2), (3.5), (3.6), and (6.3), with the usual approximation of the sum over  $Q$  by  $6 \int_0^\infty d\omega g(\omega)$ :

$$\alpha_{0+} = \frac{4}{3} (1 + m_{<}/m_{>}) \langle (n+1) \theta/\omega \rangle \omega_{mx}, \quad (6.4)$$

$$\alpha_{1+} = \langle (n+1) \theta \rangle / \langle (n+1) \theta / \omega \rangle \omega_{mx} , \quad (6.5)$$

$$\alpha_{2+}^2 = [ \langle (n+1) \theta \omega \rangle / \langle (n+1) \theta / \omega \rangle \omega_{mx}^2 ] - \alpha_{1+}^2 , \quad (6.6)$$

where  $n$  is the Bose-Einstein distribution factor ,

$$\langle A \theta \rangle = \int_0^{\infty} d\omega g(\omega) A(\omega) \theta(\omega - f\omega_{mx}) , \quad (6.7)$$

and  $g(\omega)$  is the phonon density of states normalized to unity. Similar estimates give

$$\alpha_{0-} < \alpha_{0+} / (1 + m_{<} / m_{>}) . \quad (6.8)$$

The density of states, shown as the solid curve in Fig. 9, is approximated by the Debye model,

$$g(\omega) = (3\omega^2 / \omega_{mx}^3) \theta(\omega_{mx} - \omega) , \quad (6.9)$$

sketched as the dashed curve in Fig. 9. The value of  $\omega_{mx}$  is taken as the Debye cut-off frequency in (6.9). In the high-temperature limit,

$$n(\omega) + 1 \approx \omega_T / \omega + \frac{1}{2} . \quad (6.10)$$

Then, the averages in Eqs. (6.4) to (6.6) are easily evaluated.

The value of  $f$  will be chosen as  $f = \frac{1}{2}$ , corresponding to the assumption that, for 1/8 of the modes (1/4 of the acoustical modes),  $W_+(Q)$  is negligible. In Table II, we list the data of NaCl along with the values of the  $\alpha$ 's at room temperature corresponding to  $\omega_T / \omega_{mx} = 1.03$  for NaCl.

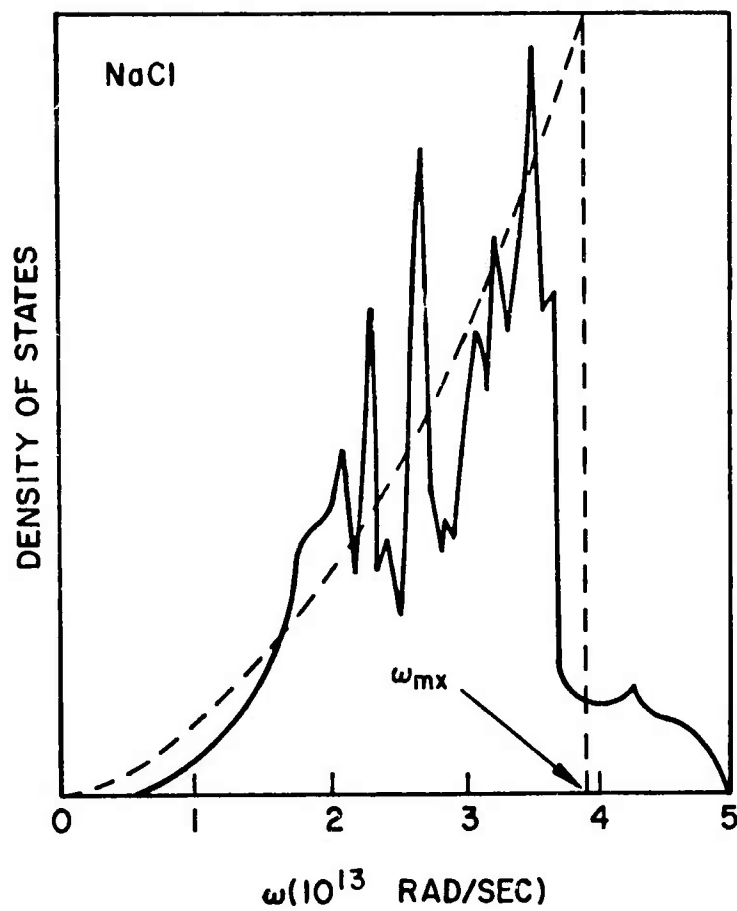


Figure 9. Phonon density of states in NaCl and the Debye approximation.

To estimate the magnitude of the vertex correction, we need to know the contribution of the intermediate phonon in the form of  $\xi$  given by Eq. (5.8). In the process depicted by Fig. 4b, the intermediate phonon splits into two phonons  $Q_1$  and  $Q_2$ , which were taken at frequency  $\omega_{mx}$ , i.e., in the optical branches. This is reasonable since the high-frequency side of the Gaussian  $\beta_n(\omega)$  curves contribute to  $\beta = \sum \beta_n$ , as seen in Fig. 10. By a quasi-selection rule,<sup>10</sup>  $Q_4$  must be an acoustic mode, the largest contribution of which will be at the edge of the Brillouin zone. Thus, we take

$$|U_x(Q_4)|^2 \approx \frac{1}{3} \frac{m_{<}}{m_{>}} \left( \frac{\omega_{Q_4}}{\eta \omega_{mx}} \right)^2 \theta(\eta \omega_{mx} - \omega_{Q_4}) , \quad (6.11)$$

using Eq. (6.1). The frequency of the highest acoustic mode is taken to be  $\eta \omega_{mx}$  with  $\eta^3 = 0.5$ , and the factor  $(\omega_{Q_4} / \eta \omega_{mx})^2$  approximately simulates the effect of the polarization for the long-wavelength acoustic modes. Substituting Eq. (6.11) into Eq. (5.8), averaging over the possible modes of  $Q_4$ , and summing over three branches, we obtain an estimate of  $\xi$ :

$$\xi \approx 3 \phi^{(2)} / 5 m_{>} \omega_{mx}^2 \approx 0.18 . \quad (6.12)$$

Substituting this value into Eq. (5.15) yields the following estimates for the vertex-renormalization factors:

$$\begin{aligned} \Lambda_2^2 &= 1 ; & \Lambda_3^2 &= (1 + 0.142)^2 = 1.30 ; \\ \Lambda_4^2 &= (1 + 0.388)^2 = 1.93 ; & \Lambda_5^2 &= (1 + 0.844)^2 = 3.40 ; \\ \Lambda_6^2 &= (1 + 1.72)^2 = 7.38 . \end{aligned} \quad (6.13)$$

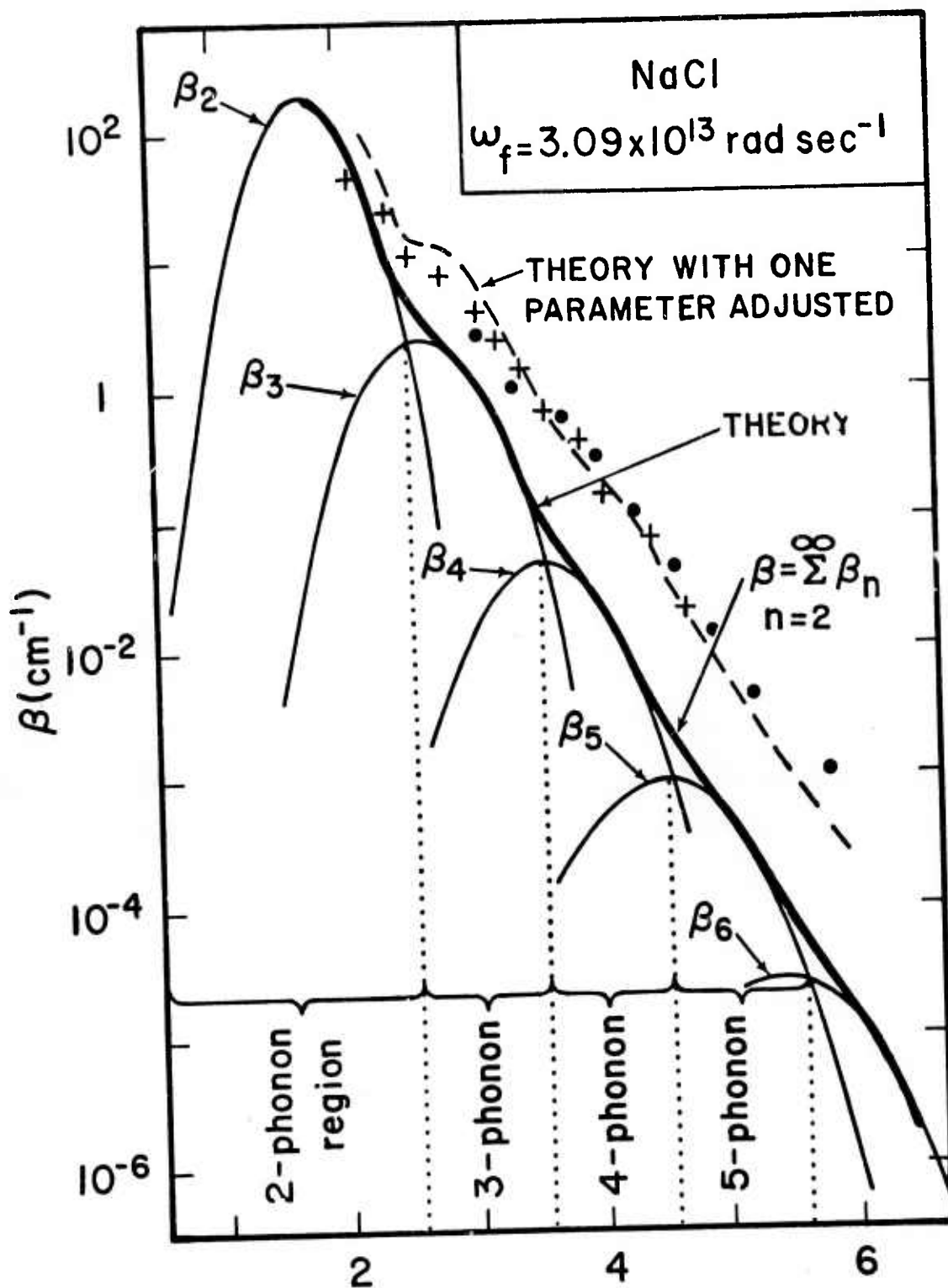


Figure 10. Theoretical estimates of  $\beta_n$  at room temperature for NaCl. Experimental points from Fig. 1 are shown for comparison.

We note that, from Eqs. (5.1) and (5.2), the vertex ratio can be shown to be equal to the ratio of the real parts of the self-energy terms given by Figs. 11b and 11a at zero temperature and frequency  $2\omega_{mx}$ . From R. A. Cowley's calculation<sup>13</sup> for KBr, our estimate of  $\xi$  appears to be somewhat too large.

The multiphonon absorption calculated from (3.7) using the values of parameters from Eq. (6.13) and Table II is shown in Fig. 10, where the individual  $\beta_n$  are plotted as light curves and the sum of the  $\beta_n$  is plotted as the heavy curve. The agreement is rather good in view of the crude approximations used to estimate the  $\alpha$ 's. It should be noted that no parameters have been adjusted in the theoretical result.

By adjusting two parameters in Eq. (3.7), such as  $K$  and  $D_e$  (keeping the  $\alpha$ 's at  $f = \frac{1}{2}$ ), the experimental data can be fitted to within the scatter of the data. In fact, by changing only the value of the single interaction strength parameter  $1/\rho$  from 9.0 to 12, the dashed curve in Fig. 10 is obtained. This larger value could be partly explained by the fact that the higher-order anharmonic coefficients are much more sensitive to the shape of the potential curve than the quadratic terms from which the value of  $\rho$  is determined. Errors introduced by the approximations and uncertainties in the values of the parameters used also could account for the difference, of course.

The near-exponential frequency dependence is evident in Fig. 10. The vertex correction, which is included in Fig. 10, slightly improves the agreement with the experimental result. Without this correction, the  $\beta_2$ - $\beta_5$  curves would be shifted down by factors of 1, 1.3, 1.9, and 3.4, respectively.

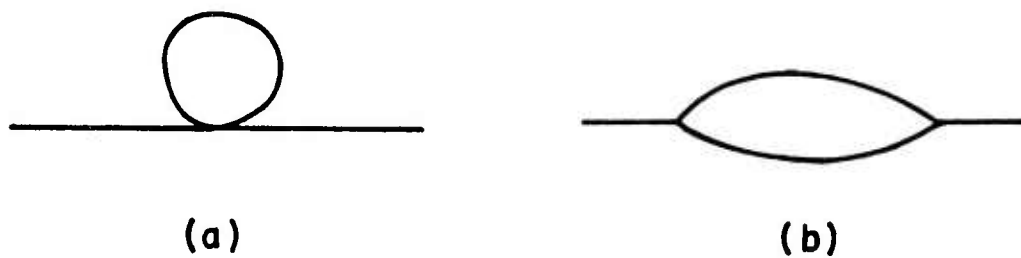


Figure 11. Phonon self-energy terms of order  $\epsilon^2$ .

Table II. Values of parameters for NaCl at room temperature

| $\alpha_{0+}$ | $\alpha_{1+}$ | $\alpha_{2+}$ |
|---------------|---------------|---------------|
| 4.639         | 0.757         | 0.145         |

$$\rho = 1/9.05, \quad a = 2.82 \text{ \AA}, \quad B = 2.44 \times 10^{11} \text{ dynes/cm}^2,$$

$$\omega_f = 3.09 \times 10^{13} \text{ sec}^{-1}, \quad \omega_{mx} = 3.85 \times 10^{13} \text{ sec}^{-1},$$

$$n_r = 1.50 \text{ (formally for all } \omega), \quad m_{<} = 3.82 \times 10^{-23} \text{ gm},$$

$$m_{>} = 5.89 \times 10^{-23} \text{ gm}.$$

The  $n$ -phonon regions, marked on Fig. 10, do not correspond to  $n\omega_f < \omega < (n+1)\omega_f$ , to  $n\omega_{mx} < \omega < (n+1)\omega_{mx}$ , or to  $n\omega_{LO} < \omega < (n+1)\omega_{LO}$ , as is often assumed in the literature. In fact, the  $n$ -phonon regions shift as the temperature changes, as discussed below.

The  $n = 2$  central-limit curve is included in Fig. 10 even though its accuracy is not expected to be good. The two-phonon structure is lost, of course, in approximating  $\beta_2$  by a Gaussian, and the peak does not occur at  $\omega = \omega_f$ .

The temperature dependence of  $\beta$  at a given frequency in the nearly exponential region is considerably weaker<sup>25</sup> than that of the simple expression

$$\beta_n(T)/\beta_n(0) = \left(1 - e^{-\omega/\omega_T}\right) \left(1 - e^{-\omega/n\omega_T}\right)^{-n} \sim T^{n-1} \quad (6.14)$$

obtained formally from the occupation-number factor (2.4) by setting all  $\omega_Q = \omega/n$ . The approximation  $\beta_n \sim T^{n-1}$  in (6.14) is valid in the high-temperature limit, and  $n$  has been assumed to be independent of temperature in the past. The  $T$  dependence of  $\beta$  results from the temperature dependence of the parameters  $a$ ,  $e^*$ , and, particularly, the phonon frequencies  $\omega_Q$  and from the explicit temperature dependence of  $\alpha_{0+}$ ,  $\alpha_{1+}$ , and  $\alpha_{2+}$ .

The following example of NaCl at 300 K and  $10.6 \mu\text{m}$  illustrates the strong deviation from the frequently quoted result  $\beta \sim T^{n-1}$ . The value of the slope  $(T/\beta)d\beta/dT$  of  $\beta$  as a function  $T$  on a log-log plot can be estimated from Eq. (3.7). Using  $n = 5.5$  from Fig. 10 and the following approximate expressions for the temperature dependence of the parameters,<sup>26,27</sup>

$$\omega_Q = \omega_{Q0}(1 - 3.8 \times 10^{-4}T), \quad a = a_0(1 - 4.4 \times 10^{-5}T), \quad \text{and} \quad e^* = e_0^*(1 - 1.06 \times 10^{-4}T),$$

we find

$$(T/\beta) d\beta/dT = 2.5 \quad (6.15)$$

which is considerably smaller than  $n - 1 = 4.5$ . The Born-Mayer-potential parameters  $C$  and  $\rho_K \equiv \rho a$  in (2.11) are essentially temperature independent, being electronic in nature. In particular, (2.12) should not be used to ascribe a temperature dependence to  $\rho_K$  from measured values of  $B(T)$  and  $a(T)$ . The temperature dependence of  $B$  arises from anharmonic and volume effects, not from a  $T$  dependence of  $\rho_K$ .

A weakening of the temperature dependence such as that in (6.15) is apparent in the data of Harrington and Hass,<sup>25</sup> Barker,<sup>8</sup> of Kaiser and co-workers,<sup>8</sup> and of Denham and coworkers.<sup>8</sup> Finally, it is mentioned that in a material, possibly a zinc-blende-structure crystal, in which the position of a given multiphonon peak can be traced as a function of temperature, the temperature dependence should be quite different from that of  $\beta$  at a given frequency. A detailed presentation of the temperature dependence of  $\beta$  will be given elsewhere.

The  $\beta - \omega$  curves of the alkali halides and alkaline earths show less structure than those of the semiconductor materials. It is plausible that the greater anharmonicity of the NaCl-structure crystals could give rise to such short lifetimes of the zone-boundary phonons that the fine structure in the density of states is essentially eliminated.

The lifetime of the fundamental phonon is short,<sup>13,28</sup> and the lifetimes of the zone-boundary phonons should be even shorter since the selection rules

and quasi-selection rules do not apply to the zone-boundary modes (with nonzero wavevectors). A value of relative linewidth  $2\Gamma/\omega$  of the order of 0.3 for the zone-boundary phonons at resonance should be sufficient, and this value is reasonable in view of the value<sup>28</sup> of  $2\Gamma/\omega = 0.07$  for the fundamental mode in NaCl and the fact that  $2\Gamma/\omega$  is expected to be larger at the zone boundaries. Furthermore, as  $n$  becomes larger, more convolutions are involved [ see Eq. (3.3) ], and each convolution tends to smooth out any fine structure in the density of states.

This explanation is consistent with the experimental results which show that the two-phonon peaks are wider in the alkali halides than in the semiconductor materials, that  $\Gamma \sim T^2$  at the fundamental resonance in NaCl (implying that the two-phonon contribution is small at resonance), and that the two-phonon peaks have been observed in NaCl even though  $\Gamma \sim T^2$  at resonance. A careful study of the temperature dependence of the two-phonon summation peaks could show an increase in the widths of the peaks as  $T$  is raised from 77 K to the highest practical temperature of the solid. Such increases are apparent in the small amount of existing data.<sup>29</sup> As the temperature is reduced below room temperature, additional multiphonon peaks could appear in higher- $n$  regions where  $\beta(\omega)$  is relatively smooth at room temperature. Of the three existing known cases (for  $\text{CaF}_2$ ,  $\text{BaF}_2$ , and  $\text{SrF}_2$  at 77 and 300 K),<sup>29</sup> two show a small additional peak at 77 K that is absent at 300 K.

It should be emphasized that the two-phonon peaks are associated with peaks in the appropriate density of states and are not resonance lines. Thus, an extrapolation of  $\beta(\omega)$  from the reststrahl region should not be subtracted from  $\beta$  at higher frequencies to obtain the multiphonon contribution, as is sometimes done in the literature. An alternate, though unlikely, explanation of the lack of structure is that the raw-phonon density of states shows little structure.

## VII. ASSUMPTIONS AND APPROXIMATIONS

The assumptions and approximations made in the previous sections are now summarized: (1) The photon-phonon coupling is given by the leading dipole term, and the Lax-Burstein-Born mechanism<sup>9</sup> is neglected. (2) For the anharmonic forces, only the nearest-neighbor Born-Mayer repulsion term is included and is further approximated. (3) The lifetimes of the intermediate and final-state phonons are assumed to be infinite. (4) The central-limit theorem is used to reduce the  $n$ -fold multiple sum in (2.3) to a Gaussian whose parameters  $\alpha$  are given by single sums, although it is possible to improve the asymptotic approximation.<sup>20</sup> (5) Rough estimates were given for the various Brillouin-zone sums over the phonon coordinates for the coefficients,  $\alpha$ 's. All of these approximations except (1) were shown to be reasonable. The perturbation approach used is justified by showing that all diagrams not included in the results are negligible. Concerning (1), the long-standing question of the importance of the Lax-Burstein-Born mechanism in NaCl-structure materials remains unanswered. The mechanism is quite simple to include formally; estimating the strengths of vertices has been the problem.

Our calculation gives good agreement with experimental results for the frequency dependence of the optical absorption and demonstrates the general nature of this dependence for crystals with tetrahedral symmetry. The estimates listed in (5) above enable us to see explicitly the nature of our results. Some of the estimates must be regarded as tentative. However, these approximations are not essential to our theory. We plan to perform both the multiple sums in (2.21) for  $n = 2 - 6$  and the single-phonon sums in Eqs. (3.2), (3.5), (3.6), and (5.8) by computer. This will enable us to examine more rigorously the validity of the other

## Sec. C

approximations, especially (4). The computer results for the multiple sums in (2.21) should provide greater accuracy in the small- $n$  regions, say  $n = 2$  and  $3$ , where the central-limit results are less accurate, and should afford a good test of the approximations in the region of  $n = 4 - 6$ . The temperature and frequency dependence of  $\beta$  for a number of crystals will be included in the computer program, which is being performed in collaboration with A. Karo of the Lawrence Livermore Laboratory.

REFERENCES

\*This research was supported by the Advanced Research Projects Agency of the Department of Defense and was monitored by the Defense Supply Service - Washington, D.C. under Contract No. DAHC15-73-C-0127.

1. E. Burstein, Lattice Dynamics, Ed. R. F. Wallis (Pergamon Press, Oxford, 1965) p. 315.
2. D. H. Martin, Adv. in Phys. 14, 39 (1965).
3. H. Bilz, Phonons in Perfect Lattices, Ed. R. W. H. Stevenson (Oliver and Boyd, Edinburgh and London, 1966) p. 208; R. A. Cowley, *ibid.*, p. 192.
4. W. G. Spitzer, Semiconductors and Semimetals, Vol. 3, Ed. R. K. Wilkinson and A. C. Beer (Academic Press, New York, 1967) p. 17.
5. L. Van Hove, Phys. Rev. 89, 1189 (1953); J. C. Phillips, Phys. Rev. 104, 1263 (1956).
6. G. Rupprecht, Phys. Rev. Letters 12, 580 (1964).
- 7a. F. A. Horrigan and T. F. Deutsch, "Research in Optical Materials and Structures for High-Power Lasers," Raytheon Research Division, Quarterly Technical Reports No. 1 and 2, ARPA, January and April (1972).
- 7b. American Institute of Physics Handbook, 3rd ed., Ed. D. E. Gray (McGraw-Hill, New York, 1972).
8. W. Kaiser, W. G. Spitzer, R. H. Kaiser, and L. E. Howarth, Phys. Rev. 127, 1950 (1962); P. Denham, G. R. Field, P. L. R. Morse, and G. R. Wilkinson, Proc. Roy. Soc. (London) A 317, 55 (1970); A. J. Barker, J. Phys. C 5, 2276 (1972).
9. M. Lax and E. Burstein, Phys. Rev. 97, 39 (1955).

## Sec. C

10. M. Sparks and L. J. Sham, *Solid State Commun.* 11, 1451 (1972); M. Sparks and L. J. Sham, "Theory of Multiphonon Infrared Absorption," Conference on High Power Infrared Laser Window Materials, Hyannis, Massachusetts, Oct. 30-Nov. 1, 1972 (proceedings to be published by Air Force Cambridge Research Laboratories, Cambridge, Massachusetts); M. Sparks, "Recent Developments in High-Power Infrared Window Research," 4th ASTM Damage in Laser Materials Symposium, Boulder, Colorado, June 14-15, 1972; M. Sparks, "Theoretical Studies of High-Power Infrared Window Materials," Xonics Technical Progress Reports, March and June (1972), and Final Report, December (1972), Contract DAHC15-72-C-0129.
11. R. F. Wallis and A. A. Maradudin, *Phys. Rev.* 125, 1277 (1962).
12. M. Born and K. Huang, *Dynamical Theory of Crystal Lattices* (Oxford University Press, Oxford, 1954).
13. R. A. Cowley, *Adv. in Phys.* 12, 421 (1963); E. R. Cowley and R. A. Cowley, *Proc. Roy. Soc. (London) A* 287, 259 (1965); E. R. Cowley, *J. Phys. C* 5, 1345 (1970).
14. P. N. Keating and G. Rupprecht, *Phys. Rev.* 138, A 866 (1965).
15. B. Szigeti, *Lattice Dynamics*, Ed. R. F. Wallis (Pergamon Press, Oxford, 1965) p. 405.
16. M. Sparks, *Ferromagnetic Relaxation Theory* (McGraw-Hill, New York, 1964).
17. C. Kittel, *Introduction to Solid State Physics* (J. Wiley, New York, 1971), 4th ed.
18. A. A. Maradudin, E. W. Montroll, G. H. Weiss, and I. P. Ipatova, *Theory of Lattice Dynamics in the Harmonic Approximation* (Academic Press, New York, 1971), 2nd ed.
- 19a. A. A. Maradudin and S. H. Vosko, *Rev. Mod. Phys.* 40, 1 (1958).
- 19b. T. McGill, R. Hellwarth, M. Mangir, and H. Winston, private communication.
- 19c. D. L. Mills and A. A. Maradudin, private communication.
- 19d. B. Bendow, S. C. Ying, and S. P. Yukon, private communication.

Sec. C

20. H. Cramer, Methods of Statistics (Princeton University Press, 1946), Chap. 17, and Random Variables and Probability Distribution (Cambridge University Press, 1961), 2nd ed., p. 87.
21. A. Sjolander, Arkiv for Fysik 14, 315 (1958).
22. L. Van Hove, Problems in Quantum Theory of Many-Particle Systems (W. A. Benjamin, New York, 1961).
23. A. A. Maradudin and A. E. Fein, Phys. Rev. 128, 2589 (1962).
24. G. Raunio and S. Rolandson, Phys. Rev. B 2, 2098 (1970).
25. J. Harrington and M. Hass, private communication.
26. R. T. Harley and C. T. Walker, Phys. Rev. B 2, 2030 (1970).
27. A. M. Karo, private communication.
28. R. B. Barnes and M. Czerney, Z. Physik 72, 477 (1931).
29. See Figs. 5 (for  $\text{CaF}_2$ ) and 8 (for  $\text{SrF}_2$ ) of Ref. 8, Denham, et al. for results at 100 and 300 K.

# D. TEMPERATURE DEPENDENCE OF MULTIPHONON INFRARED ABSORPTION\*

M. Sparks

Xonics, Incorporated, Van Nuys, California 91406

and

L. J. Sham

University of California, San Diego, La Jolla, California 92037, and

Xonics, Incorporated, Van Nuys, California 91406

Measurements of Harrington and Hass and of Barker indicate that the temperature dependence of the infrared absorption coefficient  $\beta$  in the n-phonon region is considerably weaker than  $\beta \sim T^{n-1}$ , which had been predicted for the high-temperature limit of multiphonon absorption. This discrepancy is resolved by taking into account the temperature dependence of the phonon frequencies and the lattice constant. The agreement between the experimental and theoretical results with no adjustable parameters is good. A new evaluation of the multiphonon sums yields  $\beta \sim \exp(-\omega \tau)$  directly, rather than as a sum on n.

The nearly exponential frequency dependence<sup>1</sup> of infrared absorption in the region of low absorption has been explained recently by a simple multiphonon-absorption theory<sup>2-5</sup> and by independent-molecule models.<sup>6</sup> The frequency and temperature dependence of the optical absorption coefficient  $\beta$  are of fundamental interest, and both should be useful in identifying intrinsic absorption and in distinguishing between intrinsic and extrinsic absorption.<sup>7, 3, 4</sup> Harrington and Hass<sup>8</sup> have shown that the temperature dependence of  $\beta$  is considerably weaker than the expected dependence<sup>2-4</sup>  $\beta \sim [1 - \exp(-\omega/\omega_T)][1 - \exp(-\omega/n\omega_T)]^{-n} \cong T^{n-1}$  for n-phonon absorption.

## Sec. D

The approximate equality is the high-temperature limit,  $\omega$  is the laser frequency, and  $\omega_T \equiv k_B T / \hbar$ . Reexamination of earlier data<sup>9</sup> reveals similar discrepancies, which constitute the most serious problem in the recent developments in the theory of multiphonon absorption.

These discrepancies are explained by including the temperature dependence of the phonon frequencies  $\omega_Q$  and lattice constant in our previous theory. A simple estimate indicated previously that the resulting deviations would be quite large.<sup>10</sup> The previous expression<sup>2-4, 10</sup> for  $\beta$  is

$$\beta = f(\omega) \omega^{-4} \sum_{n=2}^{\infty} (\Lambda_n^2 v^n / n!) \sum_{Q_1} \cdots \sum_{Q_n} \delta \left( \omega - \sum_{j=1}^n \omega_{Q_j} \right) \prod_{\ell=1}^n \sigma_{Q_\ell} \quad (1)$$

where  $f(\omega) = \text{con.} [1 - \exp(-\omega/\omega_T)]$ ,  $v = \hbar / 2 \rho_K^2 m$ ,  $\sigma_{Q_\ell} = W_{Q_\ell} (n_{Q_\ell} + 1) / N \omega_{Q_\ell}$ ,  $W_{Q_\ell}$  is of order unity for large  $\omega_{Q_\ell}$  and is very small for small  $\omega_{Q_\ell}$ ,  $n_{Q_\ell}$  are phonon occupation numbers, the  $Q$ 's denote wavevectors and branches,  $m$  is the reduced mass,  $\rho_K$  is the Born-Mayer repulsive-potential parameter (con),  $2N$  is the number of ions in the crystal, and the higher-order terms in the perturbation expansion give rise to the vertex-correction factors<sup>4, 10</sup>  $\Lambda_n = 1 + A_n \xi + \gamma (\xi^2)$ , where  $A_4 = 1.94$ ,  $A_5 = 3.92$ ,  $A_6 = 7.15$ , and  $\xi = 9B_0 a_0 / 5 (1 - 2\rho_0) m \omega_m^2$ . Here  $B$  is the bulk modulus,  $\rho \equiv \rho_K / a$ , the subscript 0 denotes  $T = 0$ , and  $\omega_m$  is a frequency near the top of the phonon spectrum. Eq. (1) can be written down immediately from the well known expression<sup>11, 10, 2-4</sup> for  $\beta$  with  $\omega^2 \gg (\text{reststrahl frequency, } \omega_f)^2$  and standard perturbation-theory results,<sup>12</sup> apart from the details<sup>2-4, 10</sup> of  $\Lambda_n$  and  $\omega_{Q_\ell}$  which are not needed here.

It is simple to show<sup>10,2-4</sup> that for  $n \geq 2$  the central-limit approximation to the multiple sums on  $Q_1 \cdots Q_n$  is satisfied, thus reducing (1) to  $\beta = \sum \beta_n$  with

$$\beta_n = f(\omega) \omega_f (uvC)^n \exp(-a/\rho_K) G/a^3, \quad u \equiv [(n_Q + 1)/\omega_Q]_{av}, \quad (2)$$

where  $av$  denotes the weighted (with  $W_Q$ ) average over phonons,  $a$  is the near neighbor distance, and  $G/\sqrt{n}$  is the Gaussian from the central-limit approximation.<sup>2-4, 10</sup>

The small temperature dependence of the effective charge was neglected, and  $\Lambda_n^2/n! \sqrt{n}$  was approximated by  $C^n$ , which is accurate over the range of  $n$ 's used here (typically  $n = 3-6$ ), as seen by the straight line obtained by plotting  $\ln[\Lambda_n^2/n! \sqrt{n}]$  vs  $n$ . The two parameters in the Born-Mayer potential are essentially independent of temperature, being electronic in nature. The standard relation  $B = \text{con. } a^2 \rho_K^{-1} - 2$ , with experimental values for the temperature dependence of  $B$  and  $a$ , should not be used to determine the  $T$  dependence  $\rho_K$  since the  $T$  dependence of  $B$  and  $a$  arises from anharmonic and volume effects, not from the temperature dependence of  $\rho_K$ .

The average in (2) is easily evaluated by using the Taylor's expansion  $n_Q + 1 \cong (\omega_T/\omega_Q) + \frac{1}{2} + (\omega_Q/12 \omega_T)$ , which is well satisfied for all cases considered, and a Debye spectrum (with cut-off frequency  $\omega_{mx}$ ) truncated at  $\frac{1}{2} \omega_{mx}$  to account for the angle factor in the vertex [see  $W_{Q_\ell}$  in (1)].<sup>2-4, 10</sup> This gives  $u = 9 \hbar(n_x + 1)/16 \rho_K^2 x m$ , with  $x = 3\omega_{mx}/4$ . The factor of  $\frac{3}{4}$  is obtained when the three terms in the expansion are recombined after integration.

A simple, accurate expression for the slope  $(T/\beta) d\beta/dT$  of  $\ln \beta$  vs  $\ln T$ , which is a convenient and sensitive measure of the  $T$  dependence of  $\beta$ , is obtained by approximating  $\beta$  by the locus of the inflection points on the high- $\omega$  sides of the peaks of the Gaussians. The analysis leading to (4) below or inspection of the

curves  $\beta_n$  and their sum<sup>2-4, 10</sup> show the validity of this approximation. In the absence of detailed information on the temperature dependence of the  $\omega_Q$ , it is assumed that  $(T/\omega_{mx}) d\omega_{mx}/dT = (T/\omega_f) d\omega_f/dT$ . Then (1) gives

$$\begin{aligned} \frac{T}{\beta} \frac{d\beta}{dT} &= D_T + D_\omega + D_a, & D_T &= \left( n \frac{3\omega_{mx}}{4\omega_T} n \frac{3}{4} \omega_{mx} - \frac{\omega}{\omega_T} n_\omega \right), \\ D_\omega &= - \left[ n \left( \ln C v u + \frac{3\omega_{mx}}{4\omega_T} n \frac{3}{4} \omega_{mx} + 1 \right) + \frac{\Lambda_n \xi - 1}{1 + \Lambda_n \xi} \right] \frac{T}{\omega_f} \frac{d\omega_1}{dT}, \\ D_a &= - \left( 3 + \frac{2}{\rho_0} \right) \frac{T}{a} \frac{da}{dT}. \end{aligned} \quad (3)$$

The results from (3) for NaF, LiF, NaCl, and KBr, for which experimental values are available, are listed in Table I along with the values of input parameters and experimental values of Harrington and Hass<sup>8</sup> and Barker.<sup>9</sup> The agreement is surprisingly good, probably fortuitously so, in view of the uncertainties in the experimental values and the fact that the  $\omega_Q(T)$  are not well known. Note that there are no adjustable parameters in the theoretical result, and that the value of  $D_\omega$  is sensitive to small errors in the values of the input parameters. Fig. 1 shows the excellent agreement between theoretical curves and the experimental points of Harrington and Hass and of Barker and illustrates the greater sensitivity of the parameter  $(T/\beta)d\beta/dT$  than of such a plotted comparison, the 10 percent difference between experiment and theory for KBr at 1000 K appearing smaller than the corresponding 40 percent difference in the values of  $(T/\beta)d\beta/dT$ .

In order to obtain the experimental intrinsic value of  $(T/\beta)d\beta/dT$  for NaCl at  $943 \text{ cm}^{-1}$ , which is obscured by the extrinsic contribution, the extrinsic contribution was assumed to be independent of temperature, and the

Table Caption

Table I. Theoretical and experimental values of  $(T/\beta)d\beta/dT$ . Experimental values marked  $\sim$  and  $\approx$  are uncertain ( $\sim 50\%$ ) and highly uncertain (factor of  $\sim 3$ ).

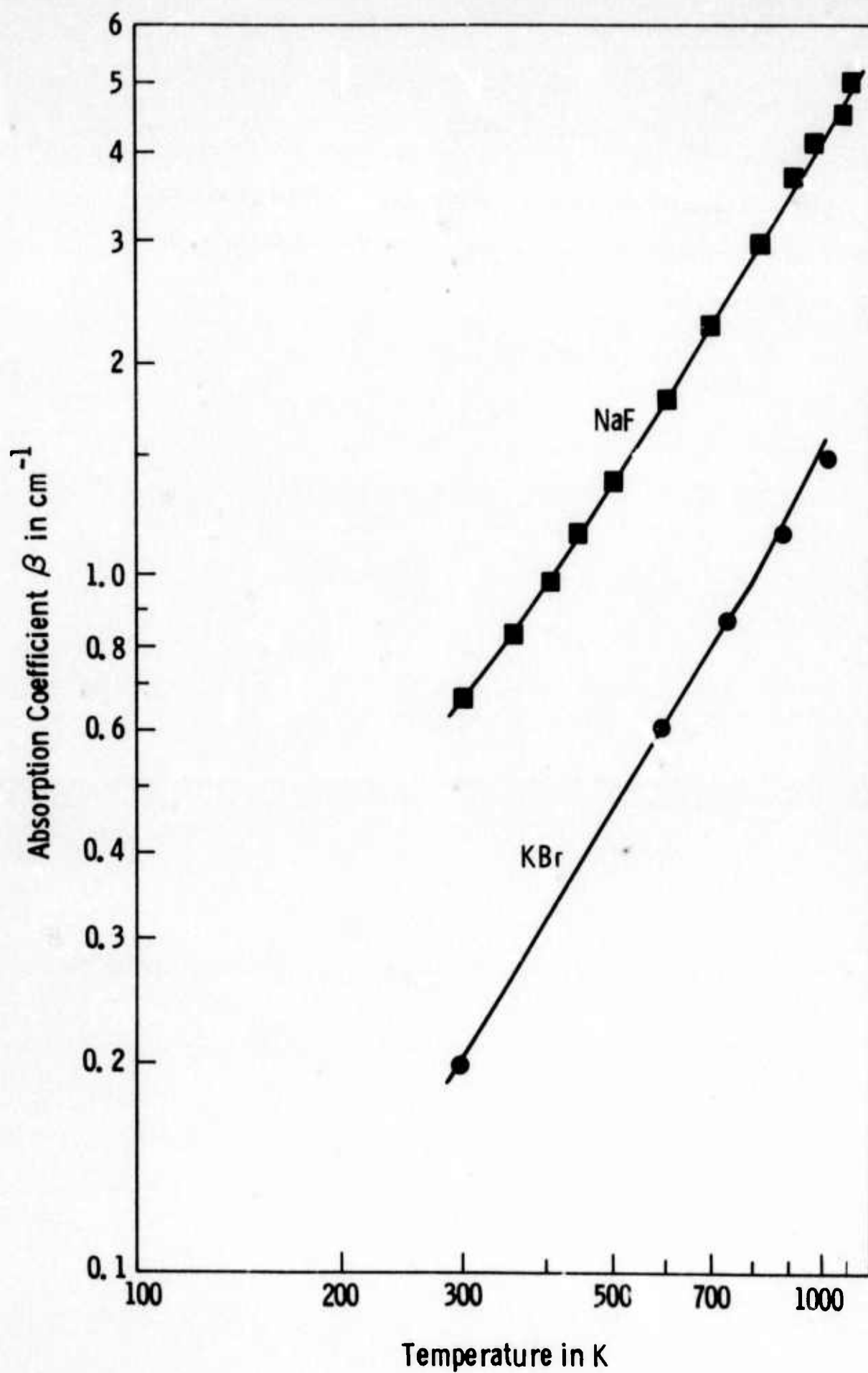
- a. A. M. Karo and J. R. Hardy, Lawrence Radiation Laboratory Report UCRL-14822, April (1966).
- b. American Institute of Physics Handbook, 2nd Ed.
- c. J. P. Jasperse, A. Kahan, J. N. Plendl, and S. S. Mitra, Phys. Rev. 146, 526 (1966).
- d. I. F. Chang and S. S. Mitra, Phys. Rev. B 5, 4094 (1972).
- e. J. E. Mooij, W. B. Van De Bunt, and J. E. Schrijvers, Phys. Letters 28 A, 573 (1969).

Table I. Theoretical and experimental values of  $(1/\beta)d\beta/dT$ . Experimental values marked ~ and ~ are uncertain (~50%) and highly uncertain (factor of ~3).

| Material    | T (K) | $D_T$ | $D_3$ | $D_2$ | $\left(\frac{1}{\beta} \frac{d\beta}{dT}\right)_{\text{theo.}}$ | $\left(\frac{1}{\beta} \frac{d\beta}{dT}\right)_{\text{exp.}}$ | $n-1$ | $10^2 \frac{d}{dT} \left(\frac{1}{\beta} \frac{d\beta}{dT}\right) (\text{cm K})^{-1}$ (b) | $10^2 \frac{d}{dT} \left(\frac{1}{\beta} \frac{d\beta}{dT}\right) (\text{cm K})^{-1}$ (c) | $10^9 \rho_K (\text{cm})$ (a) | $10^{-11} B_0 (\text{dynes/cm}^2)$ |
|-------------|-------|-------|-------|-------|---|--|-------|---|---|-------------------------------|------------------------------------|
| LiF<br>1800 | 300   | 1.4   | -0.6  | -0.1  | 0.7   | ~1.3 <sup>(9)</sup>  | 4.9   | 3.3   | -4.64 <sup>(c)</sup>  | 2.858                         | 6.99                               |
|             | 700   | 3.6   | -1.0  | -0.6  | 2.0   | 2.2  | 5.2   | 5.1   | -4.64   | 2.858                         | 6.99                               |
|             | 1000  | 4.5   | -1.0  | -1.1  | 2.4   | 2.5  | 5.6   | 6.8   | -4.64   | 2.858                         | 6.99                               |
| NaF<br>943  | 300   | 1.6   | -0.3  | -0.2  | 1.1   | 1.2 <sup>(8)</sup>   | 2.8   | 3.2   | -3.80 <sup>(d)</sup>  | 2.786                         | 5.025                              |
|             | 700   | 2.8   | -0.5  | -0.6  | 1.7   | 1.7  | 3.2   | 4.1   | -3.80   | 2.786                         | 5.025                              |
|             | 1000  | 3.3   | -0.6  | -0.9  | 1.7   | 1.7  | 3.5   | 4.8   | -9.21   | 2.786                         | 5.025                              |
| NaCl<br>700 | 300   | 2.4   | -0.6  | -0.2  | 1.6   | ~1.5 <sup>(9)</sup>  | 3.3   | 4.0   | -4.11 <sup>(e)</sup>  | 0.3107                        | 2.57                               |
|             | 700   | 3.5   | -0.5  | -0.8  | 2.2   | 2.3  | 3.7   | 5.2   | -4.11   | 0.3107                        | 2.57                               |
|             | 1000  | 4.0   | 0.1   | -1.4  | 2.7   | 2.4  | 4.1   | 6.8   | -4.11   | 0.3107                        | 2.57                               |
| NaCl<br>943 | 300   | 3.4   | -0.7  | -0.2  | 2.5   | ~6 <sup>(8)</sup>  | 4.8   | 4.0   | -4.11 <sup>(e)</sup>  | 0.3107                        | 2.57                               |
|             | 700   | 4.9   | -0.5  | -0.8  | 3.6   | ~2.5   | 5.4   | 5.2   | -4.11   | 0.3107                        | 2.57                               |
|             | 1000  | 5.7   | 0.2   | -1.4  | 4.4   | ~2.4   | 5.9   | 6.8   | -4.11   | 0.3107                        | 2.57                               |
| KBr<br>418  | 300   | 2.3   | -0.5  | -0.3  | 1.6   | 1.6 <sup>(8)</sup>   | 2.6   | 3.9   | 3.28 <sup>(e)</sup>   | 0.3192                        | 1.62                               |
|             | 700   | 3.0   | -0.4  | -0.9  | 1.7   | 1.6  | 3.1   | 5.3   | 3.28  | 0.3192                        | 1.62                               |
|             | 1000  | 3.5   | 0.2   | -1.7  | 2.0   | 1.6  | 3.6   | 7.5   | 3.28  | 0.3192                        | 1.62                               |

Figure Caption

Figure 1. Comparison of experimental points of Harrington and Hass (NaF,  $943\text{ cm}^{-1}$ ) and Barker (KBr,  $418\text{ cm}^{-1}$ ) with theoretical curves fit to the data at 300 K.



intrinsic value of  $\beta$  at 300 K was assumed to be equal to  $7 \times 10^{-4} \text{ cm}^{-1}$ .<sup>1</sup> These questionable assumptions surely introduce considerable errors. Indeed, the large experimental value of  $(T/\beta) d\beta/dT = 6$  at 300 K and the equal values of 2.4 at 700 and  $943 \text{ cm}^{-1}$  appear to be unreasonable.

In the classical, high-temperature limit of  $\omega_T \gg \omega$ , all occupation numbers  $n_{\omega_Q}$  are replaced by  $\omega_T/\omega_Q$ . For LiF at  $1800 \text{ cm}^{-1}$  and 300 K the classical approximation to  $(T/\beta)(d\beta/dT)$  from (3) is approximately three times greater than the unapproximated value. Even at 1000 K, the classical limit gives 3.5, compared with 2.4 from theory and 2.5 for experiment. Thus, considerable care must be exercised in applying classical theories to practical cases, as already discussed by Maradudin and Mills in the accompanying Letter.

In a material, such as AlSb for example, in which the position of a given multiphonon peak can be traced as a function of temperature,<sup>13</sup> the temperature dependence should be quite different from that of  $\beta$  at a given frequency, since following the peak eliminates the contribution from  $dn/dT$ .

The exponential frequency dependence of  $\beta$  can be obtained directly, rather than as a sum over  $n$ , as follows: Representing the delta function by an integral over  $t$  reduces (1) to  $\beta = f(\omega) \omega^{-4} \int (dt/2\pi) \exp(i\omega t) \sum_n n^4 [g(t)]^n$ , where  $g(t) = D \sum_Q \sigma_Q \exp(-i\omega_Q t)$ . Here  $\Lambda_n^2 v^n/n^4 n!$  was approximated by  $D^n$ , which is quite accurate for  $n = 3-8$ . The sum on  $n$  can be written as a linear combination of  $(1-g)^{-1} = \sum g^n$  and its first four derivatives. The contour integrals, which have poles at  $t = i\tau$ , are easily evaluated by residues, giving

$$\beta = \beta_0 e^{-\omega\tau} \quad (4)$$

where<sup>14</sup>  $\beta_0 \cong f(\omega) [dg(i\tau)/d\tau]^{-5}$  and  $\tau$  is the solution to  $1 - g(i\tau) = 0$ , i.e.,  
 $1 - DN^{-1} \sum_Q W_Q (n_Q + 1) \omega_Q^{-1} \exp(\omega_Q \tau) = 0$ , which is easily solved numerically.<sup>15</sup>  
 The following approximation illustrates the general dependence of  $\tau$  on  $T, \Lambda_n$ , etc.,  
 although it is too crude to afford accurate values of  $\tau$ . Neglecting the angle dependence of  $W_Q$  and approximating the density of states by  $\delta(\omega - \omega_b)$  gives  
 $\tau = -\omega_b^{-1} \ln[6CW_b(n_b + 1)/\omega_b]$  and  $dg(i\tau)/d\tau = \omega_b$ .

The temperature dependence of  $\beta$  from (4) is formally the same as that from (3).<sup>15</sup> The numerical values will differ slightly, corresponding to the slight numerical difference between  $\tau$  in (4) and the effective  $\tau$  from (2).

We would like to thank Dr. J. A. Harrington and Dr. M. Hass for sending their data prior to publication. Discussions with Dr. A. A. Maradudin and Dr. D. L. Mills are gratefully acknowledged. Dr. C. J. Duthler kindly assisted with the calculations.

## REFERENCES

\*This research was supported by the Advanced Research Projects Agency of the Department of Defense and was monitored by the Defense Supply Service - Washington, D. C. under Contract DAHC15-73-C-0127.

1. G. Rupprecht, Phys. Rev. Letters 12, 580 (1964); T. Deutsch, to be published; F. A. Horrigan and T. F. Deutsch, "Research in Optical Materials and Structures for High-Power Lasers," Raytheon Research Division, Final Technical Report, Contract DA-AH01-70-C-1251, September 1971.
2. M. Sparks and L. J. Sham, Solid State Commun. 11, 1451 (1972); M. Sparks and L. J. Sham, "Theory of Multiphonon Infrared Absorption," Conference on High Power Infrared Laser Window Materials, Hyannis, Massachusetts, Oct. 30-Nov. 1, 1972 (proceedings published by Air Force Cambridge Research Laboratories, Bedford, Massachusetts).
3. M. Sparks, "Recent Developments in High-Power Infrared Window Research," 4<sup>th</sup> ASTM Damage in Laser Materials Symposium, Boulder, Colorado, June 14-15, 1972.
4. M. Sparks, "Theoretical Studies of High-Power Infrared Window Research," Xonics, Inc. Technical Progress Reports, March and June (1972), and Final Report, December (1972), Contract DAHC15-72-C-0129.
5. B. Bendow, S. C. Ying, and S. P. Yukon, private communication.
6. D. L. Mills and A. A. Maradudin, Phys. Rev., in press; T. C. McGill, R. W. Hellwarth, M. Mangir, and H. V. Winston, private communication.
7. M. Sparks, "Immediate Needs of the High-Power Infrared Window Program," The Rand Corporation Report WN-7243-PR, June 1971.

Sec. D

8. J. Harrington and M. Hass, to be published.
9. A. J. Barker, J. Phys. C, 5, 2276 (1972); W. Kaiser, W. G. Spitzer, R. H. Kaiser, and L. E. Howarth, Phys. Rev. 127, 1950 (1962).
10. M. Sparks and L. J. Sham, Phys. Rev., in press.
11. R. A. Cowley, Phonons in Perfect Lattices, Ed. R. W. H. Stevenson (Oliver and Boyd, Edinburgh and London, 1966).
12. M. Sparks, Ferromagnetic Relaxation Theory (McGraw-Hill, New York, 1964).
13. W. J. Turner and W. E. Reese, Phys. Rev. 127, 126 (1962).
14. This expression for  $\beta_0$  is exact in the limit of the single frequency approximation discussed below or when  $\omega/n$  is approximated by a constant. The small corrections for the general case are given elsewhere in terms of the cumulant moments.
15. A. Kare, M. Sparks, and L. J. Sham, to be published.

E. THEORY OF INFRARED ABSORPTION BY CRYSTALS IN THE  
HIGH FREQUENCY WING OF THEIR FUNDAMENTAL  
LATTICE ABSORPTION\*

D. L. Mills and A. A. Maradudin

Department of Physics  
University of California  
Irvine, California 92664

and

Xonics Corporation  
Van Nuys, California 91406

\*This research supported by The Advanced Research  
Projects Agency of The Department of Defense and  
was monitored by The Defense Supply Service, Wash-  
ington, D.C. under Contract No. DAHC15-73-C-0127.

Technical Report #73-7

Abstract

We have calculated the frequency dependence of infrared absorption in the classical limit for an exactly soluble model of a lattice of noninteracting diatomic molecules, each bound internally by a potential for which the classical equation of motion can be solved in closed form. Four potentials have been used: a Morse potential, a potential of the form  $V(x) = (a/x^2) + bx^2$ , an infinite square well potential, and a triangular well potential. The analytic results we obtain show that the absorption coefficient for large frequencies associated with potentials which admit an harmonic approximation decreases nearly exponentially over the frequency region covered by recent experiments, with significant deviations from exponential behavior at higher frequencies. For the square and triangular well potentials, the absorption decreases as  $\omega^{-2}$  for frequencies large compared to a characteristic frequency.

## I. Introduction

The absorption of electromagnetic radiation by the lattice vibrations in anharmonic crystals has received considerable attention from both theorists and experimentalists for many years. However, most studies have focused attention on frequencies either in the near vicinity of the fundamental reststrahl absorption bands, or at frequencies sufficiently low that the dominant portion of the absorption may be accounted for by processes which involve at most two phonons.<sup>(1)</sup>

Recently, interest has been aroused in the behavior of the absorption coefficient at frequencies several times (say 2 to 10 times) the maximum vibrational frequency of the crystal, but still small compared to the electronic band gap. In this frequency region, the principal contribution to the absorption coefficient in a pure crystal presumably comes from multiphonon processes, where the number of phonons involved may be quite large. The behavior of the absorption coefficient in this frequency regime is clearly important to understand for fundamental physical reasons. There is also a great deal of practical interest in this region, since high power CO<sub>2</sub> lasers produce intense beams of radiation at 10.6 $\mu$ . This corresponds to a frequency several times that of the maximum vibrational frequency of many materials that may prove useful for the fabrication of windows and lenses for use with these devices. Because the radiation from these lasers is very intense, even a small amount of absorption can lead to appreciable heating of any window through which the beam passes. It is therefore of interest to understand the nature of

the intrinsic absorption processes, as well as impurity and surface induced absorption at frequencies high compared to the characteristic vibrational frequencies of the crystal.

One may readily come to appreciate the difficulty of carrying out a first principles calculation of the frequency dependence of the absorption coefficient in the multiphonon regime, for a realistic model of an anharmonic crystal lattice. What is quite intriguing is that experimental studies of the frequency dependence of the absorption coefficient in several alkali halide crystals<sup>(2)</sup> have revealed that in all the cases studied, for frequencies in the region of  $200\text{ cm}^{-1}$  to  $800\text{ cm}^{-1}$  the absorption coefficient at room temperature may be fitted quite accurately by the empirical formula

$$\beta(\omega) = A \exp(-B\omega) , \quad (\text{I-1})$$

where  $\beta(\omega)$  is the absorption coefficient at frequency  $\omega$ , and  $A$  and  $B$  are constants characteristic of the particular crystal. It is extremely important to know whether Eq.(1) can be derived from a theoretical model of some generality, and, if so, it is important to know if it holds to frequencies as high as  $10.6\mu$  (which lies outside the range accessible to the experimental studies), and also if it holds at temperatures higher than room temperature.

In this paper, we wish to address ourselves to these questions. Because of the difficulty of carrying out calculations of the absorption coefficient in the multiphonon regime that are both realistic and that lead to conclusions of a general nature, we have chosen to explore the properties of a model of a solid

that is highly schematic, but which allows simple analytic expressions to be obtained for the absorption coefficient for a variety of interatomic potentials. We replace a diatomic solid which consists of  $N$  unit cells by an array of  $N$  electric dipole active, but anharmonic oscillators. While such a model is rather oversimplified if we choose to represent a real solid by it, by an examination of the model we can gain insight into the question of whether the form in Eq.(I-1) is valid quite generally. If it is valid quite generally, it should also be valid for our model. If a realistic potential is chosen for the anharmonic oscillator, we feel the model also provides a reliable semi-quantitative estimate for the magnitude of the absorption in the multi-phonon regime. On the basis of our model, we will also be led to the conjecture that at high frequencies, the magnitude of the absorption coefficient might be quite sensitive to the presence of certain impurities.

Since the region of experimental interest to date is room temperature and above, we have used the methods of classical physics to compute the absorption coefficient. We obtain a general expression for the absorption coefficient for the model described above, and then apply the expression to the study of the frequency dependence of the absorption coefficient for four potential functions. We consider absorption by anharmonic oscillators described by the Morse potential, a second potential which possesses a hard core and admits a harmonic approximation ( $V(x) = b x^2 + a/x^2$ ), the square well, and a potential of triangular shape.

## Sec. E

The outline of the paper is as follows. In section II, we obtain a general expression for the absorption coefficient of the oscillator array by the use of the methods of classical statistical mechanics. In section III, we apply this expression to the four examples mentioned in the preceding paragraph. In section IV, we present a discussion of some implications of the results obtained in section III.

Quite recently, McGill, Hellwarth, Mangir and Winston<sup>(3)</sup> have also presented a theoretical discussion of multiphonon absorption by an array of uncoupled oscillators. In the body of this paper, these authors present a diagrammatic calculation of the absorption coefficient which they argue leads to an exponential form identical to that displayed in our Eq.(I-1), for a specific model of the interatomic potential. Their model presumes that in the crystal Hamiltonian the term proportional to the  $n^{\text{th}}$  power of the atomic displacements is proportional to only the quantity  $g^{n-2}/n!$ , where  $g$  is independent of  $n$ , and the factor  $n!$  apparently comes from the Taylor series expansion of the crystal potential. This model is quite special, since one may find a large variety of realistic potentials which admit an harmonic approximation, and for which their factor  $g^n$  will be replaced by a quantity that exhibits a fundamentally different dependence on  $n$ . (Consider the Lennard-Jones 6-12 potential, or any potential which contains a term which varies inversely with a power of the interatomic separation.) Their conclusion that the absorption coefficient varies exponentially with frequency follows upon counting the number of important diagrams in the first few

orders of perturbation theory. In view of the discussion in the following paragraph of the present paper and also that in our section IV, we are led to question the conclusion that for a potential of general form, the theory produces an analytic expression for the absorption coefficient exponential in character in the multi-phonon regime.

In Appendix A of their paper, McGill et al.<sup>(3)</sup> consider an array of non-interacting oscillators, each of which is described by a Morse potential. They insert the expression exhibited by Heaps and Herzberg<sup>(4)</sup> for the appropriate electric dipole moment matrix element into the quantum mechanical form for the absorption coefficient. A simple analytic expression for the absorption coefficient of the model follows from this procedure. If  $\omega_0$  is the maximum vibration frequency of the crystal, then when  $k_B T > \hbar \omega_0$  the correspondence principle applies, and their expression may be compared with the result we obtain below. The two results agree in this regime. However, while both results provide a rather good fit to the room temperature data in the regime of frequencies explored by Deutsch, and they thus appear qualitatively consistent with the form in Eq.(1-1), at higher frequencies significant deviations are predicted by both expressions. As the temperature is increased, these deviations are expected to set in at progressively lower frequencies. Neither our calculation nor that presented in the Appendix of the paper of McGill et al., produces an analytic expression for the absorption coefficient of an array of independent oscillators which exhibits the exponential behavior suggested by Eq.(1-1), although as remarked above, the quantitative differences are small in the frequency regime

## Sec. E

explored by the experiments so far. Thus, while one may construct a particular potential that leads to something close in form to an exponential law, we feel that quite generally, the exponential law is not valid, and one may fit the data quite well by the forms we obtain below.

## II. General Theory

Since we consider the crystal to be an array of non-interacting molecules, infrared absorption by the collection of oscillators will be  $N$  times that of a single molecule, where  $N$  is the number of molecules in the crystal. Thus, in what follows, we consider only the absorption by a single molecule. For this the motion of the center of mass of the molecule is irrelevant, since it makes no contribution to its dipole moment. Consequently, the equation of motion which provides the starting point for our treatment is

$$m\ddot{x} = \dot{p} = - \frac{dV(x)}{dx} + \frac{dM(x)}{dx} E(t) , \quad (II-1)$$

where  $m$  is the reduced mass of the molecule,  $x$  is the relative coordinate of the two atoms comprising the molecule with  $p$  the momentum canonically conjugate to  $x$ ,  $V(x)$  is the interaction potential energy between these two atoms,  $M(x)$  is the dipole moment of the molecule and  $E(t)$  is the electric field of the incident infrared radiation.

To obtain the rate at which energy is absorbed by the molecule from the electromagnetic field, we multiply both sides of Eq.(II-1) by  $\dot{x}$  and rewrite the result in the form

$$\frac{d}{dt} \left[ \frac{1}{2} m\dot{x}^2 + V(x) \right] = E(t) \frac{dM(x)}{dt} . \quad (II-2)$$

The left hand side of this equation is the instantaneous time rate of change of the energy of the molecule; we will denote it by  $d\mathcal{E}/dt$ . It is not the instantaneous time rate of change of the energy in the molecule we require, but rather its average with respect to the canonical ensemble described by the Hamiltonian for the system

$$\begin{aligned}
 H &= \frac{p^2}{2m} + V(x) - M(x)E(t) \\
 &= H_0 - M(x)E(t) ,
 \end{aligned}
 \tag{II-3}$$

and the time average of the resulting expression.

The average with respect to the canonical ensemble can be expressed in the form

$$\begin{aligned}
 \left\langle \frac{d\mathcal{E}}{dt} \right\rangle &= \int_{-\infty}^{+\infty} dp \int_{-\infty}^{+\infty} dx \, \rho(x, p, t) \frac{d\mathcal{E}}{dt} \\
 &= \int_{-\infty}^{+\infty} dp \int_{-\infty}^{+\infty} dx \, \rho(x, p, t) E(t) \frac{dM}{dt}(x) ,
 \end{aligned}
 \tag{II-4}$$

where  $\rho(x, p, t)$  is the canonical distribution function which obeys the Liouville equation

$$\frac{\partial \rho}{\partial t} + \frac{\partial \rho}{\partial x} \frac{\partial H}{\partial p} - \frac{\partial \rho}{\partial p} \frac{\partial H}{\partial x} = 0 .
 \tag{II-5}$$

In view of Eq.(II-3), this equation can be rewritten as

$$\frac{\partial \rho}{\partial t} + \frac{\partial \rho}{\partial x} \frac{\partial H_0}{\partial p} - \frac{\partial \rho}{\partial p} \frac{\partial H_0}{\partial x} = - \frac{\partial \rho}{\partial p} \frac{dM(x)}{dx} E(t) .
 \tag{II-6}$$

We now expand  $\rho$  in powers of the driving electric field of the infrared radiation,

$$\rho = \rho_0 + \rho_1 + \dots ,
 \tag{II-7}$$

where the subscript denotes the order of the corresponding term in  $E(t)$ . When we substitute the expansion of Eq.(II-7) into Eq.(II-6), and equate terms of like order in  $E(t)$  on both sides of the equation, we obtain the system of equations

$$\frac{\partial \rho_0}{\partial t} + \frac{\partial \rho_0}{\partial x} \frac{\partial H_0}{\partial p} - \frac{\partial \rho_0}{\partial p} \frac{\partial H_0}{\partial x} = 0 \quad (\text{II-8})$$

$$\frac{\partial \rho_1}{\partial t} + \frac{\partial \rho_1}{\partial x} \frac{\partial H_0}{\partial p} - \frac{\partial \rho_1}{\partial p} \frac{\partial H_0}{\partial x} = - \frac{\partial \rho_0}{\partial p} \frac{dM}{dx} E(t) \quad (\text{II-9})$$

.....

We now use the results that

$$\frac{\partial H_0}{\partial p} = \frac{p}{m} = \dot{x} \quad (\text{II-10a})$$

$$\frac{\partial H_0}{\partial x} = \frac{d^2x}{dx^2} = -\dot{p} \quad (\text{II-10b})$$

Equation (II-8) and Eq.(II-9) can then be rewritten as

$$\frac{d}{dt} \rho_0 = 0 \quad (\text{II-11})$$

$$\frac{d}{dt} \rho_1 = - \frac{\partial \rho_0}{\partial p} \frac{dM}{dx} E(t) \quad , \quad (\text{II-12})$$

where  $d\rho_0/dt$  and  $d\rho_1/dt$  are the total time derivatives of  $\rho_0$  and  $\rho_1$ , respectively. From a physical point of view,  $d\rho/dt$  is the change in the distribution function seen by an observer moving with a particle that traverses the orbit generated by the Hamiltonian  $H$ , and which passes through the point  $(x,p)$  in phase space at time  $t$ .

For the equilibrium distribution function  $\rho_0$  we assume the canonical form

$$\rho_0 = \frac{\exp(-\beta H_0)}{Z} \quad , \quad \beta = \frac{1}{k_B T} \quad , \quad (\text{II-13})$$

where the partition function  $Z$  is defined by

$$Z = \int_{-\infty}^{+\infty} dp \int_{-\infty}^{+\infty} dx \exp(-\beta H_0) \quad . \quad (\text{II-14})$$

If we now use the fact that

$$\frac{\partial \rho_0}{\partial p} = \frac{d\rho_0}{dH_0} \frac{\partial H_0}{\partial p} = -\beta \rho_0 \frac{p}{m} = -\beta \rho_0 \dot{x}, \quad (\text{II-15})$$

Eq.(II-12) for  $\rho_1$  becomes

$$\frac{d\rho_1}{dt} = \beta \rho_0 \dot{x} \frac{dM}{dx} E(t). \quad (\text{II-16})$$

We now assume that the perturbing electric field was switched on adiabatically in the infinitely distant past, so that

$$\rho_1(-\infty) = 0 \quad (\text{II-17})$$

The solution of Eq.(II-16) which obeys the initial condition Eq.(II-17) is

$$\rho_1(t) = \beta \int_{-\infty}^t \rho_0 \dot{x}(t') \left[ \frac{dM}{dx} \right]_{x(t')} E(t') dt'. \quad (\text{II-18})$$

With the results given by Eqs. (II-7), (II-13) and (II-14), we can rewrite Eq.(II-4) in the form

$$\begin{aligned} \left\langle \frac{d\mathcal{E}}{dt} \right\rangle &= \int_{-\infty}^{+\infty} dp \int_{-\infty}^{+\infty} dx \rho_0 \dot{x} \frac{dM(x)}{dx} E(t) \\ &+ \beta \int_{-\infty}^{+\infty} dp \int_{-\infty}^{+\infty} dx \int_{-\infty}^t \rho_0 \dot{x}(t') \left[ \frac{dM}{dx} \right]_t \frac{dM}{dt} E(t') E(t) dt' + \dots \end{aligned} \quad (\text{II-19})$$

If we use Eqs. (II-3) and (II-13), and rewrite the first term on the right hand side of Eq. (II-19) in the form

$$E(t) \int_{-\infty}^{+\infty} dp e^{-\frac{p^2}{2m}} \frac{p}{m} \int_{-\infty}^{+\infty} dx e^{-\beta V(x)} \frac{dM}{dx}, \quad (\text{II-20})$$

we see that it vanishes due to the vanishing of the integral over  $p$ . Thus, the first non-vanishing contribution to  $\langle \frac{d\mathcal{E}}{dt} \rangle$  comes from the second term. This term may be arranged to read

$$\langle \frac{d\mathcal{E}}{dt} \rangle = \beta \int_{-\infty}^t \langle \dot{M}(t') \dot{M}(t) \rangle_0 E(t') E(t) dt' , \quad (\text{II-21})$$

where we have introduced the notation

$$M(x(t)) = M(t) , \quad (\text{II-22})$$

and where for any function  $A(x, p, t)$  ,

$$\langle A \rangle_0 = \int_{-\infty}^{+\infty} dp \int_{-\infty}^{+\infty} dx \rho_0(x, p) A(x, p, t) . \quad (\text{II-23})$$

For  $E(t)$ , we now assume the form

$$E(t) = E_0 \cos \omega t e^{\eta t} , \quad (\text{II-24})$$

where  $e^{\eta t}$  is an adiabatic switching factor ( $\eta$  is a positive infinitesimal). With this choice, Eq.(II-21) becomes

$$\langle \frac{d\mathcal{E}}{dt} \rangle = \beta E_0^2 \int_{-\infty}^t \langle \dot{M}(t') \dot{M}(t) \rangle_0 \cos \omega t' \cos \omega t e^{\eta(t+t')} dt' . \quad (\text{II-25})$$

Let  $t' = t - \tau$  , and integrate over  $\tau$  rather than  $t'$ . Then

$$\langle \frac{d\mathcal{E}}{dt} \rangle = \beta E_0^2 e^{2\eta t} \cos \omega t \int_0^{\infty} \langle \dot{M}(t-\tau) \dot{M}(t) \rangle_0 \cos \omega(t-\tau) e^{-\eta\tau} d\tau . \quad (\text{II-26})$$

Because  $H_0$  is time independent, our system possesses time translation invariance, which in the context of the present problem is expressed by

$$\langle \dot{M}(t - \tau) \dot{M}(t) \rangle_0 = \langle \dot{M}(0) \dot{M}(\tau) \rangle_0 \quad . \quad (\text{II-27})$$

The time average of Eq.(II-26) thus becomes (in the limit  $\eta \rightarrow 0$ )

$$\langle \langle \frac{d\mathcal{E}}{dt} \rangle \rangle = \frac{\beta E_0^2}{2} \int_0^\infty d\tau \cos(\omega\tau) e^{-\eta\tau} \langle \dot{M}(0) \dot{M}(\tau) \rangle_0 \quad . \quad (\text{II-28})$$

In Eq.(II-28), we can replace  $\tau$  by  $-\tau$  as an integration variable, and use time reversal symmetry, which leads to the identity

$$\langle \dot{M}(0) \dot{M}(-\tau) \rangle_0 = \langle \dot{M}(0) \dot{M}(\tau) \rangle_0 \quad . \quad (\text{II-29})$$

We then obtain an alternative expression for  $\langle \langle \frac{d\mathcal{E}}{dt} \rangle \rangle$ :

$$\langle \langle \frac{d\mathcal{E}}{dt} \rangle \rangle = \frac{\beta E_0^2}{2} \int_{-\infty}^0 d\tau \cos(\omega\tau) e^{+\eta\tau} \langle \dot{M}(0) \dot{M}(\tau) \rangle_0 \quad (\text{II-30})$$

Upon adding half of Eq.(II-28) to Eq.(II-30), we obtain

$$\langle \langle \frac{d\mathcal{E}}{dt} \rangle \rangle = \frac{\beta E_0^2}{4} \int_{-\infty}^{+\infty} \langle \dot{M}(0) \dot{M}(\tau) \rangle \cos \omega\tau e^{-\eta|\tau|} d\tau \quad . \quad (\text{II-31})$$

for the time and thermodynamically averaged rate at which energy is absorbed by a diatomic molecule acted on by an external a c electric field.

The result in Eq.(II-31) may be recognized as a classical version of the well known Kubo formula for the absorption coefficient.

In what follows, we shall confine our attention to the case of infrared absorption by a first order dipole moment. That is, if we expand  $M(x)$  in a Maclaurin series

$$M(x) = M'(0)x + \frac{1}{2} M''(0)x^2 + \dots \quad , \quad (\text{II-32})$$

where the primes denote differentiation with respect to  $x$  (we assume the equilibrium configuration of the molecule has no dipole moment), we retain only the contribution from the leading term in the expansion. McGill et al., have examined the effect of the second term on the absorption coefficient and find its effect quantitatively small.<sup>(3)</sup> The coefficient  $M'(0)$  has the dimensions of a charge, and we replace it by  $q$  in what follows. Thus, the starting point for the investigations in this paper is the following expression for the average rate of energy absorption by a diatomic molecule:

$$\langle \langle \frac{d\mathcal{E}}{dt} \rangle \rangle = \frac{\beta q^2 E_0^2}{4m^2} \int_{-\infty}^{+\infty} \langle p(0)p(\tau) \rangle_0 \cos(\omega\tau) e^{-\eta|\tau|} d\tau . \quad (\text{II-33})$$

We next turn to the problem of casting the momentum autocorrelation function  $\langle p(0)p(\tau) \rangle_0$  into a form convenient for computational purposes. This autocorrelation function can be written explicitly in the form

$$\langle p(0)p(t) \rangle_0 = \frac{1}{Z} \int_{-\infty}^{+\infty} dp \int_{-\infty}^{+\infty} dx e^{-\beta \left[ \frac{p^2}{2m} + V(x) \right]} p p(t) . \quad (\text{II-34})$$

Because the Hamiltonian is time independent, we have expressed it in terms of the values of  $p$  and  $x$  at time  $t = 0$  in Eq.(II-34). Thus, here and in what follows  $p$  and  $x$  denote  $p(0)$  and  $x(0)$ , respectively. In addition, as integration of the equations of motion shows, the value of the momentum at time  $t$  is a function of the initial values  $x$  and  $p$ , and we indicate this explicitly by writing  $p(t)$  as  $p(x,p,t)$ .

We now rewrite Eq.(II-34) in the form

$$\begin{aligned}
\langle p(o)p(t) \rangle_o &= \frac{1}{Z} \int_{-\infty}^{+\infty} dE e^{-\beta E} \int_{-\infty}^{+\infty} dp \int_{-\infty}^{+\infty} dx \delta\left(E - V(x) - \frac{p^2}{2m}\right) pp(x, p, t) \\
&= \frac{m}{Z} \int_{E_{\min}}^{\infty} dE e^{-\beta E} \int_{x_1(E)}^{x_2(E)} dx \int_{-\infty}^{+\infty} dp \frac{\delta(p-p_E) + \delta(p+p_E)}{p_E} pp(x, p, t)
\end{aligned}
\tag{II-35}$$

where

$$p_E = \sqrt{2m(E - V(x))} \tag{II-36}$$

and  $x_1(E)$  and  $x_2(E)$  (chosen so  $x_1(E) \leq x_2(E)$ ) are the classical turning points for motion in the potential  $V(x)$ , i.e., they are the solutions of

$$E = V(x) \quad . \tag{II-37}$$

We assume the potential  $V(x)$  is such that there are two classical turning points for energies  $E \geq E_{\min}$ , where  $E_{\min}$  is the minimum value of  $V(x)$ . The physical significance of  $p_E$  is that it is the momentum at  $t = 0$  in a motion corresponding to the total energy  $E$ .

Upon carrying out the integration over  $p$  in Eq.(II-35), we obtain the result that

$$\begin{aligned}
\langle p(o)p(t) \rangle_o &= \frac{m}{Z} \int_{E_{\min}}^{\infty} dE e^{-\beta E} \left\{ \int_{x_1(E)}^{x_2(E)} dx p(x, p_E, t) + \right. \\
&\quad \left. + \int_{x_2(E)}^{x_1(E)} dx p(x, -p_E, t) \right\} .
\end{aligned}
\tag{II-38}$$

Since the momentum at  $t = 0$  for  $x$  in the interval  $(x_2(E), x_1(E))$

is the negative of that at the same point in the interval  $(x_1(E), x_2(E))$ , because the motion reverses itself at each turning point, the expression in brackets is the integral over one period of the motion beginning at  $x_1(E)$ , and returning to  $x_1(E)$  after one period. Thus, we may write Eq.(II-38) in the form

$$\langle p(o)p(t) \rangle_o = \frac{m}{Z} \int_{E_{\min}}^{\infty} dE e^{-\beta E} \oint dx p(x, p_E, t) . \quad (II-39)$$

The one-dimensional motion of a particle in a region bounded by two turning points is a periodic function of time with a period  $T(E)$  given by<sup>(5)</sup>

$$T(E) = \sqrt{2m} \int_{x_1(E)}^{x_2(E)} \frac{dx}{\sqrt{E - V(x)}} . \quad (II-40)$$

This result holds for any initial position  $x$  and momentum  $p_E$  in a motion corresponding to total energy  $E$ . Thus, the integral over a period in Eq.(II-39) is a periodic function of time with the same period  $T(E)$ , and we expand it in a Fourier series:

$$\oint dx p(x, p_E, t) = \sum_{n=-\infty}^{+\infty} p_n(E) e^{-in\omega(E)t} \quad (II-41)$$

where

$$p_n(E) = \frac{1}{T(E)} \int_0^{T(E)} dt \oint dx p(x, p_E, t) e^{+in\omega(E)t} , \quad (II-42)$$

and we have defined

$$\omega(E) = \frac{2\pi}{T(E)} . \quad (II-43)$$

To obtain a simple expression for  $p_n(E)$ , note that the

solution of the equation of motion for a particle moving in a one dimensional potential is given explicitly by<sup>(5)</sup>

$$t - t_0 = \left(\frac{m}{2}\right)^{\frac{1}{2}} \int_{x_1(E)}^x \frac{dx'}{\sqrt{E - V(x')}} , \quad x_1(E) \leq x \leq x_2(E) . \quad (\text{II-44})$$

In writing this expression, we are measuring time with respect to an instant  $t_0$  at which the particle is at the left hand turning point  $x_1(E)$ . It is necessary to know  $x$  as a function of  $t$  only for  $x_1(E) \leq x \leq x_2(E)$  because as  $t$  increases past  $t_0 + T(E)/2$ , where  $x = x_2(E)$ , the motion reverses itself (i.e.,  $x(t)$  is symmetric about  $t = t_0 + T(E)/2$ ) until the time  $t_0 + T(E)$  is reached, at which point the particle has returned to  $x_1(E)$ , and the motion begins to repeat again.

The solution of Eq.(II-44) can be written

$$x(t) = x_1(E) + f_E(t - t_0) \quad (\text{II-45})$$

where the function  $f_E(t)$  is an even function of  $t$ , is periodic in  $t$  with period  $T(E)$ , is even about  $t = T(E)/2$ , and vanishes as  $t \rightarrow 0$ . The momentum  $p_E(t)$  for the orbit of energy  $E$  is

$$p_E(t) = m \frac{df_E(t - t_0)}{dt} = m g_E(t - t_0) , \quad (\text{II-46})$$

where  $g_E(t)$  is an odd function of  $t$ , is periodic in  $t$  with period  $T(E)$ , and is odd about  $t = T(E)/2$ .

With these results, Eq.(II-42) becomes

$$P_n(E) = \frac{1}{T(E)} \oint dx e^{in\omega(E)t_0} \int_0^{T(E)} dt m g_E(t - t_0) e^{in\omega(E)(t - t_0)} , \quad (\text{II-47})$$

# Sec. E

where the integrations over  $x$  and  $t$  have been interchanged.

Since  $g_E(t)$  is periodic with period  $T(E)$ , and we integrate over a complete period, this result becomes

$$p_n(E) = \frac{i}{T(E)} \oint dx e^{in\omega(E)t_0} \int_0^{T(E)} dt m g_E(t) \sin(n\omega(E)t), \quad (II-48)$$

where we have used the fact that  $g_E(t)$  is odd about  $t = T(E)/2$ .

We now convert the first integral from an integral over  $x$  into an integral over  $t_0$ :

$$p_n(E) = \frac{i}{T(E)} \int_0^{-T(E)} dt_0 \frac{dx}{dt_0} e^{in\omega(E)t_0} \int_0^{T(E)} dt m g_E(t) \sin(n\omega(E)t). \quad (II-49)$$

The coordinate  $x$  is obtained as a function of  $t_0$  by setting  $t = 0$  in Eq.(II-44). The limits on the first integral follow from the fact that the original integral on  $x$  around a period of the motion corresponds to  $t - t_0$  increasing from 0 to  $T(E)$  as  $x$  goes from  $x_1(E)$  to  $x_2(E)$ , and back to  $x_1(E)$ . Setting  $t = 0$ , we see that  $t_0$  goes from 0 to  $-T(E)$  as  $x$  makes the same circuit. Making the change of variable  $t_0 = -t'$ , and using the fact that  $f_E(t)$  in Eq.(II-45) is an even function of  $t$ , we obtain for  $p_n(E)$

$$p_n(E) = \frac{i}{T(E)} \int_0^{T(E)} dt' g_E(t') e^{-in\omega(E)t'} \int_0^{T(E)} dt m g_E(t) \sin(n\omega(E)t) \quad (II-50)$$

or, using the oddness of  $g_E(t')$  about  $t' = T(E)/2$ , we find finally

$$m p_n(E) = \frac{1}{T(E)} p_n^2(E). \quad (II-51)$$

where

$$\rho_n(E) = \int_0^{T(E)} dt p_E(t) \sin n\omega(E)t, \quad (\text{II-52})$$

where the momentum  $p_E(t) = m g_E(t)$  appearing in Eq.(II-52) must be understood to be obtained from Eq.(II-44) with  $t_0 = 0$  (since that is how  $g(t)$  is defined).

Upon combining Eqs. (II-39), (II-41), (II-43) and (II-51), we obtain for the momentum auto-correlation function

$$\langle p(0)p(t) \rangle_0 = \sum_{n=-\infty}^{+\infty} \int_{E_{\min}}^{\infty} \frac{dE e^{-\beta E}}{2\pi Z} \omega(E) \rho_n^2(E) e^{-in\omega(E)t}. \quad (\text{II-53})$$

When this result is substituted into Eq.(II-33), and the integration over time is carried out, we obtain (as  $\eta \rightarrow 0+$ )

$$\begin{aligned} \langle \langle \frac{d\mathcal{E}}{dt} \rangle \rangle = & \frac{\beta q^2 E_0^2}{8m^2 Z} \sum_{n=-\infty}^{+\infty} \int_{E_{\min}}^{\infty} dE e^{-\beta E} \omega(E) \rho_n^2(E) \times \\ & \times \left[ \delta(\omega - n\omega(E)) + \delta(\omega + n\omega(E)) \right]. \end{aligned} \quad (\text{II-54})$$

If we note that  $\rho_n^2(E)$  vanishes for  $n = 0$ , and is an even function of  $n$  for  $n \neq 0$ , we finally obtain for the average rate of energy absorption by a diatomic molecule

$$\langle \langle \frac{d\mathcal{E}}{dt} \rangle \rangle = \frac{\omega \beta q^2 E_0^2}{4m^2 Z} \sum_{n=1}^{\infty} \frac{1}{n} \int_{E_{\min}}^{\infty} dE e^{-\beta E} \rho_n^2(E) \delta(\omega - n\omega(E)), \quad (\text{II-55})$$

where we have assumed  $\omega > 0$ .

The dynamics of the problem are seen to enter simply through

## Sec. E

the necessity of knowing  $p_E(t)$  for the evaluation of  $\rho_n(E)$ , and  $\omega(E)$ . Moreover, if  $\omega(E)$  is a sufficiently simple function of  $E$  so that the equation  $\omega = n\omega(E)$  can be inverted, the integration over  $E$  can be carried out using properties of the delta function.

We briefly summarize in words the procedure for computing the quantities which enter Eq.(II-55). Given a potential function  $V(x)$ , one requires the period  $T(E)$  as a function of energy. This function may be obtained from Eq.(II-40), and  $\omega(E)$  is defined by Eq.(II-43). By solving the equations of motion, one finds the momentum as a function of time  $p_E(t)$  for an orbit of energy  $E$ , with the origin of time chosen so the parameter  $t_0$  in Eq.(II-44) is set equal to zero. The quantity  $\rho_n(E)$  is a measure of the amplitude of the  $n^{\text{th}}$  harmonic in the function  $p_E(t)$ , and is obtained from Eq.(II-52). Finally,  $Z$  is the partition function.

We conclude the present section by displaying a remarkably simple relation between the partition function of the oscillator, and the function  $T(E)$ , that gives the period as a function of energy.

$$\begin{aligned}
 \text{We have} \\
 Z &= \int_{-\infty}^{+\infty} dp \int_{-\infty}^{+\infty} dx e^{-\beta \left\{ \frac{p^2}{2m} + V(x) \right\}} \\
 &= \int_{-\infty}^{+\infty} dE e^{-\beta E} \int_{-\infty}^{+\infty} dp \int_{-\infty}^{+\infty} dx \delta \left( E - V(x) - \frac{p^2}{2m} \right) \\
 &= \int_{E_{\min}}^{\infty} dE e^{-\beta E} \int_{x_1(E)}^{x_2(E)} dx \frac{m}{p_E} \int_{-\infty}^{+\infty} dp \left[ \delta(p - p_E) + \delta(p + p_E) \right] \\
 &= \int_{E_{\min}}^{\infty} dE e^{-\beta E} \sqrt{2m} \int_{x_1(E)}^{x_2(E)} \frac{dx}{\sqrt{E - V(x)}} ,
 \end{aligned}$$

Sec. E

or finally

$$Z = \int_{E_{\min}}^{\infty} dE e^{-\beta E} T(E) \quad . \quad (11-56)$$

We next proceed to apply the results of the present section to the examples mentioned in section I.

### III. Applications of the Formalism to the Study of Multiphonon Absorption for Some Specific Potentials

In this section, we study the behavior of the absorption coefficient as a function of frequency for four specific forms of the interatomic potential  $V(x)$ . We first derive the form of the absorption coefficient for the Morse potential, a form used frequently in molecular physics. We then consider the potential  $V(x) = ax^2 + b/x^2$ , the square well, and the potential  $V(x) = \gamma x$  for  $x \geq 0$ ,  $V(x) = \infty$  for  $x < 0$ . The last two potentials are interesting examples to consider, since one cannot construct a discussion of a perturbative nature, because an harmonic approximation does not exist for either case.

#### a) The Morse Potential

The Morse potential may be written in the form

$$V(x) = D[1 - \exp(-a[x - x_0])]^2 \quad . \quad (III-1)$$

The minimum value of  $V(x)$  is zero and the minimum occurs at  $x = x_0$ . For large values of the interparticle separation  $V(x)$  approaches the constant value  $D$ , the dissociation energy of the molecule. For most cases of interest here,  $D$  assume a value the order of one electron volt, an energy very large compared to  $k_B T$ , as long as we confine our attention to temperatures the order of or lower than the melting temperature of the solids of interest to us. We shall make use of the fact that  $k_B T \ll D$  in the discussion below.

If we consider only motions of small amplitude,  $x$  remains near  $x_0$ , and  $V(x)$  is well approximated by the parabolic form

$$V(x) = Da^2(x - x_0)^2 \quad . \quad (III-2)$$

## Sec. E

Thus, in the limit where the amplitude of the motion is small, the molecule behaves like an harmonic oscillator with frequency  $\omega_0$  given by

$$\omega_0^2 = \frac{2a^2 D}{m} \quad . \quad (\text{III-3})$$

We begin by deriving an expression for the quantity  $p_E(t)$  defined in section II, following the procedure outlined there.

We begin with Eq. (II-44), which with  $t_0$  equal zero becomes

$$t = \left(\frac{m}{2}\right)^{\frac{1}{2}} \int_{x_1(E)}^x dx' \left[ E - D + 2De^{a(x_0 - x)} - De^{2a(x_0 - x)} \right]^{-\frac{1}{2}} \quad . \quad (\text{III-4a})$$

The integral can be evaluated in closed form. This may be done by letting  $\theta = \exp(-ax)$ , and  $\theta_1 = \exp(-ax_1(E))$ . If we then define  $C = D \exp(2ax_0)$ ,  $B = 2D \exp(ax_0)$  and  $A = D - E$ , the integral becomes

$$t = \frac{1}{a} \left(\frac{m}{2}\right)^{\frac{1}{2}} \int_{\theta}^{\theta_1} [B\theta' - A - C\theta'^2]^{-\frac{1}{2}} \frac{d\theta'}{\theta'} \quad (\text{III-4b})$$

For bound motions of the molecule, the only case of interest here,  $B\theta \geq A + C\theta^2$  everywhere. The integral is then readily evaluated<sup>(6)</sup> to give

$$\begin{aligned} \text{at} \left[ \frac{2}{m}(D-E) \right]^{\frac{1}{2}} &= \sin^{-1} \left[ \frac{(D-E) - De^{ax_0\theta'}}{\sqrt{DE} e^{ax_0\theta'}} \right]_{\theta_1}^{\theta} \\ &= \sin^{-1} \left[ \frac{(D-E) - De^{ax_0\theta}}{\sqrt{DE} e^{ax_0\theta}} \right] + \frac{\pi}{2} \end{aligned} \quad (\text{III-5})$$

## Sec. E

If this relation is solved for  $\epsilon$  as a function of  $t$ , and  $x(t)$  is obtained from this result, one finds

$$x(t) = x_0 + \frac{1}{a} \ln \frac{D}{D-E} + \frac{1}{a} \ln \left[ 1 - \left( \frac{E}{D} \right)^{\frac{1}{2}} \cos \alpha(E) t \right] \quad (\text{III-6})$$

where we have introduced the quantity  $\alpha(E)$ , defined by

$$\alpha(E) = \omega_0 \left[ 1 - \frac{E}{D} \right]^{\frac{1}{2}}. \quad (\text{III-7})$$

From Eq. (III-6), it is evident that the period  $T(E)$  of the motion is

$$T(E) = \frac{2\pi}{\alpha(E)}. \quad (\text{III-8})$$

For small energies,  $T(E)$  assumes a value independent of energy and equal to  $2\pi/\omega_0$ , and the period lengthens as  $E$  increases.

The momentum  $p_E(t)$  is found from  $m\dot{x}(t)$ , with  $x(t)$  given by Eq. (III-6). If this differentiation is carried out and the result substituted into the expression for  $\rho_n(E)$  given in Eq. (II-52), one obtains

$$\begin{aligned} \rho_n(E) &= \frac{(2mE)^{\frac{1}{2}}}{\omega_0} \int_0^{T(E)} \frac{\sin n\alpha(E)t \sin \alpha(E)t}{1 - \left( \frac{E}{D} \right)^{\frac{1}{2}} \cos \alpha(E)t} dt \\ &= \frac{2(2mE)^{\frac{1}{2}}}{\omega_0} \int_0^{\pi} \frac{\sin n\varphi \sin \varphi}{1 - \left( \frac{E}{D} \right)^{\frac{1}{2}} \cos \varphi} d\varphi. \end{aligned} \quad (\text{III-9})$$

The integral in Eq. (II-9) may be evaluated exactly, to give<sup>(6)</sup>

$$\rho_n(E) = \frac{2\pi(2mE)^{\frac{1}{2}}}{\omega_0} \left( \frac{D}{E} \right)^{\frac{n+1}{2}} \left[ 1 - \left( 1 - \frac{E}{D} \right)^{\frac{1}{2}} \right]^n. \quad (\text{III-10})$$

The discussion shows that for the Morse potential, exact results for all quantities which enter the expression for the absorption coefficient are readily obtained, for the bound orbits. We shall compute an approximate form for the absorption rate in the limit  $k_B T \ll D$ , where only orbits with energy  $E \ll D$  contribute significantly to the rate of absorption. In this regime, we replace  $\rho_n(E)$  by its leading contribution when  $E \ll D$ :

$$\rho_n(E) = \frac{2\pi (2mD)^{\frac{1}{2}}}{\omega_0} \left( \frac{E}{4D} \right)^{\frac{n}{2}}. \quad (\text{III-11})$$

In this limit, the function  $\omega(E)$  may also be replaced by the approximate form  $\omega_0$  independent of energy, for  $E \ll D$ . From Eq. (II-56), one readily sees that the expression for the partition function becomes

$$Z = \frac{2\pi}{\omega_0 \beta}. \quad (\text{III-12})$$

If these approximations are inserted into the expression for  $\langle \frac{d\mathcal{E}}{dt} \rangle$  displayed in Eq. (II-55), one finds that

$$\langle \frac{d\mathcal{E}}{dt} \rangle = \sum_{n=1}^{\infty} \alpha_n \delta(\omega - n\omega_0) \quad (\text{III-13a})$$

where

$$\alpha_n = \frac{\pi}{4} \frac{q^2 E_0^2}{m} n! \left( \frac{k_B T}{4D} \right)^{n-1} \quad (\text{III-13b})$$

For the case  $n = 1$ , we have

$$\alpha_1 = \frac{\pi}{4} \frac{q^2 E_0^2}{m}, \text{ independent of temperature,} \quad (\text{III-13c})$$

## Sec. E

the well known result for the integrated strength of the fundamental absorption line of a simple harmonic oscillator of mass  $m$ , charge  $q$  and frequency  $\omega_0$ . (Recall that  $E_0$  is the peak value of the field.)

The integrated strength of the absorption peak at the frequency  $\omega = n\omega_0$  (the  $n$  phonon absorption peak for this model) is related to that of the fundamental absorption peak by the simple relation

$$\frac{\alpha_n}{\alpha_1} = n! \left( \frac{k_B T}{4D} \right)^{n-1} \quad (III-14)$$

b) The Potential  $V(x) = (a/x^2) + bx^2$

The second potential function we consider is

$$V(x) = \frac{a}{x^2} + bx^2 \quad x \geq 0. \quad (III-15)$$

Setting  $t_0 = 0$  in Eq. (II-44), we obtain for the equation determining  $x(t)$

$$t = \frac{m}{2} \int_{x_1(E)}^x \frac{xdx}{\sqrt{-a + Ex^2 - bx^4}} \quad (III-16)$$

The turning points  $x_{1,2}(E)$  are the solutions of the equation

$$E = \frac{a}{x^2} + bx^2, \quad (III-17)$$

and are found to be

$$x_1(E) = \left[ \frac{E - [E^2 - 4ab]^{\frac{1}{2}}}{2b} \right]^{\frac{1}{2}} \quad (III-18a)$$

$$x_2(E) = \left[ \frac{E + [E^2 - 4ab]^{\frac{1}{2}}}{2b} \right]^{\frac{1}{2}} \quad (III-18b)$$

# Sec. E

The energy  $E_{\min}$  equals the minimum value of the potential energy (III-15). Equivalently, it is the energy for which  $x_1(E) = x_2(E)$ , and hence is given by

$$E_{\min} = 2\sqrt{ab} \quad . \quad (\text{III-19})$$

The change of variable  $x^2 = y$  transforms Eq. (III-16) into

$$\begin{aligned} t &= \frac{1}{2} \left( \frac{m}{2} \right)^{\frac{1}{2}} \int_{x_1^2(E)}^{x^2} \frac{dy}{\sqrt{-a + Ey - by^2}} \\ &= \frac{1}{2} \left( \frac{m}{2b} \right)^{\frac{1}{2}} \left\{ \frac{\pi}{2} - \sin^{-1} \frac{E - 2bx^2}{\sqrt{E^2 - 4ab}} \right\} \quad . \end{aligned} \quad (\text{III-20})$$

If we evaluate this expression for  $x = x_2(E)$ , the left hand side must be set equal to  $T(E)/2$ , and in this way we obtain

$$T(E) = \pi \sqrt{\frac{m}{2b}} \quad . \quad (\text{III-21})$$

Consequently, the frequency  $\omega(E)$  is given by

$$\omega(E) = \sqrt{\frac{8b}{m}} \equiv \omega_0 \quad . \quad (\text{III-22})$$

It should be noted that the period  $T(E)$  and the corresponding frequency  $\omega(E)$  for the potential (III-15) are independent of the energy  $E$ .

It follows immediately from Eqs. (II-56) and (III-21) that the partition function  $Z$  is given by

$$Z = \frac{2\pi}{\beta\omega_0} e^{-2\beta\sqrt{ab}} \quad . \quad (\text{III-23})$$

# Sec. E

The expression (II-55) for the rate at which energy is absorbed by the molecule described by the potential function (III-15) now becomes

$$\langle \langle \frac{d\mathcal{E}}{dt} \rangle \rangle = \frac{\omega\omega_0}{8\pi} \beta^2 \frac{q^2}{m^2} E_0^2 \sum_{n=1}^{\infty} \frac{1}{n} \left\{ e^{2\beta\sqrt{ab}} \int_{E_{\min}}^{\infty} dE e^{-\beta E} \rho_n^2(E) \right\} \delta(\omega - n\omega_0) . \quad (\text{III-24})$$

If we make the change of variable  $E = 2\sqrt{ab}(z+1)$ , we obtain the convenient form

$$\langle \langle \frac{d\mathcal{E}}{dt} \rangle \rangle = 2\sqrt{ab} \frac{\omega\omega_0}{8\pi} \beta^2 \frac{q^2}{m^2} E_0^2 \sum_{n=1}^{\infty} \frac{1}{n} \left\{ \int_0^{\infty} dz e^{-2\beta\sqrt{ab}z} \rho_n^2(2\sqrt{ab}(z+1)) \right\} \times \delta(\omega - n\omega_0) . \quad (\text{III-25})$$

Since  $2\sqrt{ab} = E_{\min}$ , we see that for temperatures such that  $E_{\min} \gtrsim k_B T$ , only values of  $z \lesssim 1$  contribute significantly to the integral. We now turn to a determination of  $\rho_n(E)$ .

Inverting Eq. (III-20) we obtain for  $x(t)$

$$x(t) = \left\{ \frac{E}{2b} - \frac{\sqrt{E^2 - 4ab}}{2b} \cos \omega_0 t \right\}^{\frac{1}{2}} , \quad (\text{III-26})$$

from which we immediately obtain  $p(t)$ :

$$p(t) = \sqrt{m} \frac{\sqrt{E^2 - 4ab}}{\sqrt{E}} \frac{\sin \omega_0 t}{\sqrt{1 - \frac{\sqrt{E^2 - 4ab}}{E} \cos \omega_0 t}} . \quad (\text{III-27})$$

The integral  $\rho_n$  in this case is given by

$$P_n(E) = 2\sqrt{mE} \frac{\delta}{w_0} \int_0^{\pi} \frac{\sin x \sin nx}{\sqrt{1 - \delta \cos x}} dx \quad (\text{III-28})$$

where we have set

$$\delta = \frac{\sqrt{E^2 - 4ab}}{E} \quad (\text{III-29})$$

The change of variable  $x = \pi - 2\varphi$  yields the following expression for  $P_n(E)$ ,

$$P_n(E) = (-1)^{n-1} \frac{\sqrt{mE}}{w_0} \frac{2\delta}{\sqrt{1+\delta}} \int_0^{\frac{\pi}{2}} \frac{\cos 2(n-1)\varphi - \cos 2(n+1)\varphi}{\sqrt{1 - \frac{2\delta}{1+\delta} \sin^2 \varphi}} d\varphi \quad (\text{III-30})$$

The integral

$$K_n(k) = \int_0^{\frac{\pi}{2}} \frac{\cos 2nx}{\sqrt{1 - k^2 \sin^2 x}} dx \quad \begin{array}{l} 0 \leq k < 1 \\ n = 0, 1, 2, \dots \end{array} \quad (\text{III-31})$$

has the following expansion in powers of  $k^2$  (7)

$$K_n(k) = (-1)^n \frac{\pi}{2} \sum_{\nu=n}^{\infty} \left[ \frac{\Gamma(\nu + \frac{1}{2})}{\Gamma(\frac{1}{2})} \right]^2 \frac{k^{2\nu}}{(\nu-n)! (\nu+n)!} \quad (\text{III-32a})$$

$$= (-1)^n \frac{\pi}{2} \left[ \frac{\Gamma(n + \frac{1}{2})}{\Gamma(\frac{1}{2})} \right]^2 \frac{k^{2n}}{(2n)!} \left\{ 1 + \frac{(2n+1)}{4} k^2 + \frac{(2n+1)(2n+3)}{32(2n+2)} k^4 + \dots \right\} \quad (\text{III-32b})$$

Consequently, since in the present case

$$k^2 = \frac{2\delta}{1+\delta} < 1, \quad (\text{III-33})$$

the first two terms in the expansion of  $\rho_n(E)$  are found to be

$$\rho_n(E) = \frac{\pi}{2} \frac{\sqrt{mE}}{\omega_0} \left[ \frac{\Gamma(n-\frac{1}{2})}{\Gamma(\frac{1}{2})} \right]^2 \frac{1}{(2n-2)!} \frac{(2\delta)^n}{(1+\delta)^{n-\frac{1}{2}}} \times$$

$$\times \left\{ 1 + \frac{(2n-1)}{4} \frac{2\delta}{1+\delta} + O\left(\left(\frac{2\delta}{1+\delta}\right)^2\right) \right\} \quad (III-34)$$

Consequently, we have that

$$\rho_n^2(E) \sim \frac{\pi^2}{4} \frac{mE}{\omega_0^2} \left[ \frac{\Gamma(n-\frac{1}{2})}{\Gamma(\frac{1}{2})} \right]^4 \frac{1}{[(2n-2)!]^2} \frac{(2\delta)^{2n}}{(1+\delta)^{2n-1}} \times$$

$$\times \left\{ 1 + \frac{(2n-1)}{2} \frac{2\delta}{1+\delta} + O\left(\left(\frac{2\delta}{1+\delta}\right)^2\right) \right\} \quad (III-35)$$

Since  $\delta < 1$ , we can simplify this expression to

$$\rho_n^2(E) = \pi^2 \frac{mE}{\omega_0^2} \frac{[(2n-2)!]^2}{2^{6n-6} [(n-1)!]^4} \delta^{2n} [1 + O(\delta^2)] \quad (III-36)$$

If we make the replacement  $E = 2\sqrt{ab}(z+1)$  in Eq.(III-29), we find that as a function of  $z$   $\delta$  is given by

$$\delta = \frac{\sqrt{z^2 + 2z}}{z + 1}$$

$$= \sqrt{2z} \left( 1 - \frac{3}{4} z + \frac{23}{32} z^2 + \dots \right) \quad 0 \leq z < 1 \quad (III-37)$$

Thus, the leading term in the expansion of  $\rho_n^2(2\sqrt{ab}(1+z))$  for small  $z$  is

$$P_n^2 \left( 2\sqrt{ab} (1+z) \right) \sim \pi^2 \frac{m}{\omega_0^2} 2\sqrt{ab} \frac{[(2n-2)!]^2}{2^{5n-6} [(n-1)!]^4} z^n + O(z^{n+1}) . \quad (\text{III-38})$$

When this result is substituted into Eq. (III-25), and the integral over  $z$  is carried out, we obtain finally

$$\langle \langle \frac{d\xi}{dt} \rangle \rangle = \frac{\pi}{4} \frac{q^2}{m} E_0^2 \sum_{n=1}^{\infty} \frac{[(2n-2)!]^2 n!}{2^{5n-5} [(n-1)!]^4} \left( \frac{k_B T}{E_{\min}} \right)^{n-1} \delta(\omega - n\omega_0) . \quad (\text{III-39})$$

We see from this result that the integrated strength of absorption at the frequency  $\omega = \omega_0$ ,  $(\pi q^2/4m)E_0^2$ , is independent of temperature, and has the same value as in the case of the Morse potential. The integrated strength of the absorption at the frequency  $\omega = n\omega_0$  is related to that of the fundamental absorption peak ( $n = 1$ ) by

$$\frac{[(2n-2)!]^2}{2^{5n-5} [(n-1)!]^4} n! \left( \frac{k_B T}{E_{\min}} \right)^{n-1} , \quad (\text{III-40})$$

which is very close in form to the corresponding relation, (III-14), obtained for the Morse potential.

### c) The Square Well

We next apply the method to compute the shape of the absorption spectrum for a particle trapped in a square well potential, with infinitely steep sides. This example is an interesting application of the formalism developed in section II of the present paper, since the potential does not admit an harmonic approximation. In section IV, we shall argue that there are certain impurities in alkali halides that may be regarded as moving in a very steep sided potential that can be approximated by a square well, at least for qualitative purposes.

## Sec. E

We suppose the square well has width  $L$ , with infinitely steep sides. If we consider motion of a particle of mass  $m$  in the well, with energy  $E$ , then the velocity  $v$  of the particle is  $(2E/m)^{1/2}$ .

The period  $T(E)$  is  $2L/v$ , or

$$T(E) = L \left( \frac{2m}{E} \right)^{1/2} = \frac{2\pi}{\omega(E)} \quad (\text{III-41})$$

For the momentum  $p_E(t)$ , one has

$$p_E(t) = \begin{cases} + (2mE)^{1/2} & 0 < t < T(E)/2 \\ - (2mE)^{1/2} & T(E)/2 < t < T(E) \end{cases} \quad (\text{III-42})$$

A short calculation gives for this potential

$$\rho_n(E) = \frac{2mL}{\pi n} [1 - (-1)^n]$$

It is a straightforward matter to insert this expression into Eq. (II-55), and obtain the form of  $\langle \frac{d\rho}{dt} \rangle$ . The computation of the partition function is also quite elementary. The final result is best expressed in terms of a characteristic frequency  $\omega_T$ , given by

$$\omega_T = \pi \left( \frac{2k_B T}{mL^2} \right)^{1/2} \quad (\text{III-43})$$

In terms of  $\omega_T$ , the expression for the rate of energy absorption is

$$\left\langle \frac{d\bar{E}}{dt} \right\rangle = \frac{8}{\pi^{3/2}} \frac{q^2 E_0^2}{m} \frac{\omega}{\omega_T} \sum_{n=0}^{\infty} \frac{\exp \left[ - \frac{\omega^2}{\omega_T^2 (2n+1)^2} \right]}{(2n+1)^5} \quad (\text{III-44})$$

The absorption coefficient is thus a superposition of a sequence of Gaussians. The function on the right hand side of Eq. (III-44) has a prominent peak very near  $\omega = \omega_T$ , with weak subsidiary maxima at higher frequencies. Of particular interest is the behavior of the absorption coefficient for frequencies large compared to  $\omega_T$ . In this region, one may find the asymptotic form of the absorption coefficient by replacing the sum in Eq. (III-44) by an integration. For  $\omega \gg \omega_T$ , by this means one finds

$$\begin{aligned} \langle \langle \frac{d\epsilon}{dt} \rangle \rangle &\approx \frac{4}{\pi^{3/2}} \frac{q^2 E_0^2}{m} \frac{\omega_T^2}{\omega} \int_0^\infty \frac{dS}{S^5} e^{-\frac{\omega^2}{\omega_T^2} \frac{1}{S^2}} \\ &= \frac{2}{\pi^{3/2}} \frac{q^2 E_0^2}{m} \frac{\omega_T}{\omega^2} \end{aligned} \quad (III-45)$$

Thus, for frequencies large compared to the characteristic frequency  $\omega_T$ , the square well potential gives rise to an absorption coefficient which falls off as  $\omega^{-2}$ , a result qualitatively different from the empirical form displayed in Eq. (I-1).

d) The Triangular Well

We next display the form of the absorption coefficient for a potential  $V(x)$  of the form

$$V(x) = \begin{cases} \infty & x < 0 \\ \gamma x & x > 0 \end{cases}, \quad (III-46)$$

## Sec. E

where the constant  $\gamma$  is presumed positive. This is a second example of a potential for which a harmonic approximation fails to exist.

The classical equations of motion for this example are quite elementary. For an orbit with energy  $E$ , the period  $T(E)$  is

$$T(E) = \frac{2}{\gamma} (2mE)^{\frac{1}{2}}, \quad (\text{III-47})$$

and the momentum of the particle as a function of time is

$$\begin{aligned} p_E(t) &= (2mE)^{\frac{1}{2}} \left( 1 - \frac{2t}{T(E)} \right), \quad 0 < t < \frac{T(E)}{2} \\ &= -(2mE)^{\frac{1}{2}} \left( 1 - \frac{2t}{T(E)} \right), \quad \frac{T(E)}{2} < t < T(E). \end{aligned}$$

A short and straightforward calculation then gives

$$\rho_n(E) = \frac{4mE}{\pi\gamma n}, \quad (\text{III-48})$$

and for the partition function

$$Z = \frac{(2\pi m)^{\frac{1}{2}}}{\gamma} (k_B T)^{3/2}. \quad (\text{III-49})$$

When these results are inserted in Eq. (II-55), one finds that the results assume the form

$$\langle \langle \frac{d\mathcal{E}}{dt} \rangle \rangle = \frac{4}{\pi^{5/2}} \frac{q^2 F_o^2}{m} \frac{\Omega_T^5}{\omega^6} \sum_{n=1}^{\infty} n^3 \exp(-n^2 \frac{\Omega_T^2}{\omega^2}) \quad (\text{III-50})$$

where  $\Omega_T$  is a characteristic frequency given by

$$\Omega_T = \pi \gamma (2mk_B T)^{-1/2} \quad (\text{III-51})$$

When  $\omega \gg \Omega_T$ , the form of the absorption coefficient may be deduced by replacing the sum over  $n$  by an integration, as we did in the preceding example. In the high frequency regime, one finds that

$$\langle \langle \frac{d\mathcal{E}}{dt} \rangle \rangle = \frac{2}{\pi^{5/2}} \frac{q^2 E_0^2}{m} \frac{\Omega_T}{\omega^2}, \quad (\text{III-52})$$

a result remarkably similar to that obtained for the square well.

In both examples, for  $\omega$  large compared to a characteristic frequency, the absorption falls off as  $\omega^{-2}$ .

IV. General Discussion

The purpose of this section is to examine some implications of the results in section III.

We first examine the question of the validity of the phenomenological form displayed in Eq.(I-1), which is suggested by the absorption data reported to date. If this form is in fact a general result which holds in the limit of high frequencies, then we should expect it to emerge from our analysis. If we consider the Morse potential, and also the potential  $bx^2 + a/x^2$ , our independent oscillator model predicts a series of absorption peaks at the frequencies  $\omega_n = n\omega_0$ , where  $\omega_0$  is the fundamental vibration frequency of the anharmonic oscillator. If the exponential law is obeyed for these models, then we should expect the integrated strength of the  $n$  phonon peak (the absorption peak at  $n\omega_0$ ) to vary with  $n$  as  $\epsilon^n$ , where  $\epsilon$  is a parameter independent of  $n$  that depends on the details of the interatomic potential and the temperature.

If we examine the results obtained in section III, we see that a relation of this form does not hold for any of the four potentials we have examined. The two potentials most directly applicable to real physical systems are the Morse potential and the potential  $bx^2 + a/x^2$ , since both of these potentials admit an harmonic approximation. If we denote the integrated strength of the  $n$ -phonon peak by  $a_n$ , then for the Morse potential we find that

$$a_n = n! \left( \frac{kT}{h\nu} \right)^{n-1} a_1, \quad (\text{IV-1})$$

## Sec. E

where  $\alpha_1$  is the integrated strength of the fundamental reststrahl band at  $\omega_0$ . A very similar relation obtains for the potential  $bx^2 + a/x^2$ , as we have seen. Because of the factor of  $n!$  that appears in Eq.(IV-1), a plot of  $\alpha_n$  vs.  $n$  does not give an exponential law of the form displayed in Eq.(I-1). It is for this reason that we feel that the proof offered by McGill et al., leads to conclusions that are not correct. Both examples we have investigated lead to results which contradict this conclusion. As we remarked in section I, these authors have also calculated the intensity of the multiphonon absorption peaks for a set of independent oscillators, each of which is described by the Morse potential. Their calculation is carried out by a quantum mechanical means, and yields a result in agreement with ours in the limit  $\hbar\omega_0 < k_B T$ , where the correspondence principle dictates that the classical and quantum mechanical results must concur.

One must then inquire into the reason why the data are so well fitted by the exponential form displayed in Eq.(I-1). Of course, it may be that our independent oscillator model is so highly simplified that conclusions based on it are unreliable. We feel that that the problem does not lie here, but in the fact that the data obtained to date extend only over a rather small range of frequency, from  $2\omega_0$  to  $6\omega_0$  at best. The frequency only varies by a factor of at most three through this range. While the absorption coefficient changes by many decades as one passes through this frequency range, measurements over a wider range of frequencies, or at higher temperatures will be required to determine whether the phenomenological form in Eq.(I-1) is valid.

We illustrate this point in Figure (1), where we present the multiphonon absorption data obtained by Deutsch<sup>(2)</sup>, and compare it with the prediction of Eq.(IV-1) at integral values of  $n\omega_0$ . The solid line in Figure (1) is a straight line, chosen with slope such that it passes through the data obtained by Deutsch. We have omitted the data points simply to avoid cluttering the figure but, as noted by Deutsch, the data fall on the straight line. It will be important for our purposes to note that the data points all lie below the frequency of  $750\text{ cm}^{-1}$ , to the left of the square bracket which has been placed on the straight line. Thus, the portion of the straight line to the right of this bracket represents an extrapolation of the data to higher frequencies, in particular to the frequency of the  $\text{CO}_2$  laser. This extrapolation assumes the phenomenological form given in Eq.(I-1) is valid for all frequencies, since it is a linear extrapolation on a semi log plot.

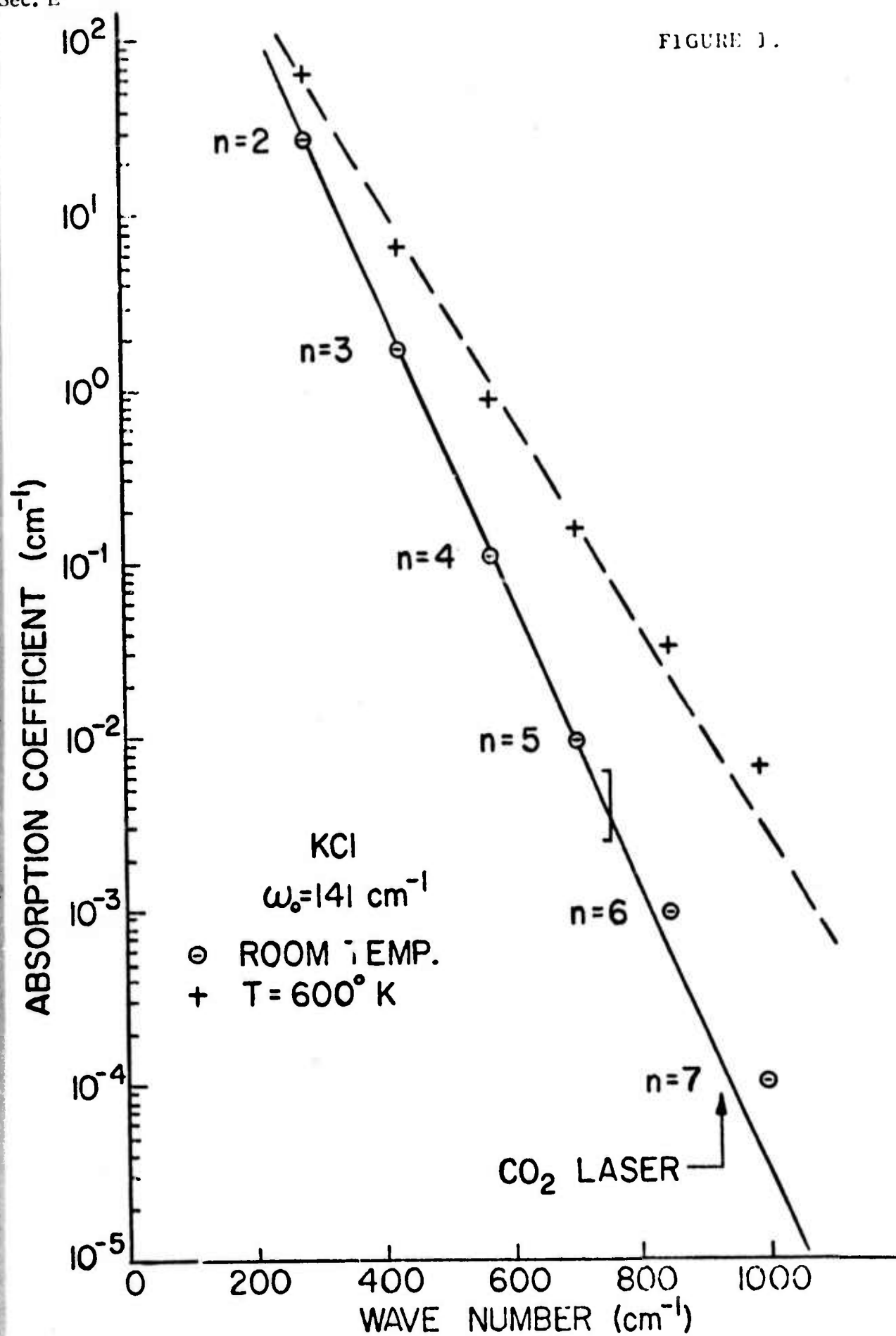
In the figure, the barred circles represent the prediction of Eq.(IV-1). To place the points on the figure, we have adjusted  $\alpha_1$  and  $D$  so that Eq.(IV-1) fits the data at the two points  $n = 2$  and  $n = 5$ . When we then calculate the strength of the absorption at  $n = 3$  and  $n = 4$ , we obtain results that agree very well with the data, to within the accuracy of the graph. Thus, we can also fit the function in Eq.(IV-1) to the data, and it is clear that the measurements do not extend over a range of frequencies large enough to warrant the conclusion that the exponential law provides a unique description of the results.

It is not hard to see why we obtain a good fit to the data. The ratio  $k_B T/4D$  is quite small, of the order of  $10^{-2}$  typically, as we

Figure Caption

Figure (1) Comparison between the multiphonon data in  $KCl$ , and the non-interacting oscillator model, for the case where the motion of the oscillator is governed by the Morse potential. The solid line passes through the room temperature data points of Deutsch, and all the data lie below the square bracket placed on the curve near  $750\text{ cm}^{-1}$ . The barred circles are computed from the theoretical model, with parameters adjusted to fit the data at  $n = 2$  and  $n = 5$ . The crosses give the theoretical prediction when  $T = 600^\circ K$ , and the dashed line is a straight line drawn as an aid to the eye.

FIGURE 1.



## Sec. E

shall see shortly. If we plot the data on a semi-log plot, then we are concerned with the behavior of  $\log \alpha_n$  as a function of  $n$ . Eq.(IV-1) then gives

$$\ln \alpha_n = - n \left[ \ln \frac{4D}{k_B T} - \frac{1}{n} \ln n! \right] + \ln \left[ \frac{4D \alpha_1}{k_B T} \right].$$

If  $n$  is large enough for Stirling's approximation to be used,  $\log n! \approx n \log n - n$ , and

$$\ln \alpha_n = - n \left[ 1 + \ln \frac{4D}{k_B T} - \ln n \right] + \ln \left[ \frac{4D \alpha_1}{k_B T} \right].$$

Since  $4D/k_B T \gg 1$ , the  $\ln (4D/k_B T)$  contribution to the quantity in square brackets is quite large. Furthermore, if we plot  $\log \alpha_n$  as a function of  $n$ , deviations from a straight line arise only because of the  $\log n$  term. Since  $\log n$  is a slowly varying function of  $n$ , a plot of  $\ln \alpha_n$  vs.  $n$  can give a result approximated very well by a straight line, if only a small range of  $n$  is examined.

If we accept the results of our independent oscillator model as realistic for the moment, then from Figure (1) one can see that extrapolation of the exponential law of Eq.(I-1) to higher frequencies can lead to serious errors in estimates of the absorption coefficient. For example, by the time  $n = 7$ , the expression in Eq.(IV-1) gives a value of the absorption coefficient larger by a factor of 5 than that obtained from extrapolation of the exponential law. This example suggests that to estimate the absorption coefficient at  $10.6\mu$  by the use of Eq.(I-1) to extrapolate data from lower frequencies may lead to a serious underestimate of the absorption coefficient at  $10.6\mu$ .

## Sec. E

If the temperature of the crystal is raised, the discussion above suggests that deviations from the near exponential behavior should be expected to be more severe, and to set in at lower values of  $n$ . To illustrate this point, on Figure (1) we have placed a series of crosses to represent the prediction of Eq.(IV-1) at  $T = 600^\circ\text{K}$ , once  $\alpha_1$  and  $D$  have been adjusted to fit the room temperature data at  $n = 2$  and  $n = 5$ , as described above. The dashed line is a straight line placed on the graph as an aid to the eye. The deviations are indeed more pronounced, although on the semi-log plot they do not look large if one adjusts the slope of the straight line to give the best fit.

In order to see if the independent oscillator model provides a fit to the data with realistic parameters, we have done the following, for the case where the molecular potential is assumed to be the Morse potential. We have determined the parameters of the Morse potential by the use of the value of the TO frequency, and the multiphonon data on the four alkali halide crystals studied by Deutsch<sup>(2)</sup>. When this information is combined with the tabulated value of the interatomic spacing, the coefficient of (linear) thermal expansion may be calculated for the model. We shall describe the details of the analysis below. The results of the investigation are summarized in Table 1. For  $\text{NaCl}$ ,  $\text{KCl}$  and  $\text{KBr}$ , this procedure gives results in remarkable accord with measured values of the thermal expansion coefficient. For  $\text{LiF}$ , the agreement is poorer, but the estimated and measured value of the thermal expansion coefficient still differs by little more than a factor of 2. On the basis of this analysis, we conclude

Table I. The Morse potential parameters D and a required to fit the TO phonon frequency and multiphonon absorption data of Deutsch, for a series of alkali halides. Included in the table is the (linear) thermal expansion coefficient computed from the model for these crystals, along with measured values of the thermal expansion coefficient, at room temperature.

| Crystal | D(Units of $10^{-12}$ ergs) | a(in units of $10^8 \text{ cm}^{-1}$ ) | Calculated Thermal Expansion Coefficient (Units of $10^{-6} \text{ }^\circ\text{K}$ ) | Measured Thermal Expansion Coefficient (Units of $10^{-6} \text{ }^\circ\text{K}$ ) |
|---------|-----------------------------|--|---|---|
| NaCl    | 0.73                        | 1.2                                    | 40  | 40  |
| KCl     | 0.60                        | 1.4                                    | 40  | 37  |
| KBr     | 0.77                        | 0.9                                    | 46  | 39  |
| LiF     | 0.32                        | 2.2                                    | 75  | 33  |

that multiphonon absorption processes of an intrinsic character are indeed responsible for the absorption measured by Deutsch.

To obtain the numbers displayed in Table 1, we have employed the following procedure. From Eq.(III-14), one sees that the slope of a plot of  $\log \alpha_n$  vs.  $n$  is controlled only by the parameter  $D$ , for the Morse potential. We have obtained the value of  $D$  given in Table 1 by fitting the ratio  $\alpha_5/\alpha_2$  to the data of Deutsch. The value of  $a$  is obtained by identifying the frequency  $\omega_0$  (Eq.(III-3)) with the TO phonon frequency of the crystal. The parameter  $x_0$  in the Morse potential is chosen to be equal to the nearest neighbor interatomic spacing in the crystal.

In the quasi-harmonic region, where  $k_B T \ll D$ , it is an elementary matter to calculate the mean value  $\langle x \rangle$  of the interatomic separation of the two atoms in the molecule. One finds

$$\langle x \rangle = x_0 + \frac{3k_B T}{4aD} ,$$

where the second term is small compared to  $x_0$ . We identify the coefficient of (linear) thermal expansions with the ratio  $\frac{\delta \langle x \rangle}{x_0 \delta T}$ , where  $\delta \langle x \rangle$  is the change in the mean separation of the atoms produced by the temperature change  $\delta T$ . If we call  $\beta_T$  the expansion coefficient, then

$$\beta_T = \frac{3k_B}{4aDx_0} . \quad (IV-2)$$

The figures in the third column of Table 1 have been obtained from Eq.(IV-2), and in the right hand column we give the experimental data<sup>(8)</sup>.

One intriguing feature of the results of section III is that

## Sec. E

the strength of the  $n$ -phonon absorption peak for the Morse potential, and for the potential  $bx^2 + a/x^2$  exhibits nearly the same functional dependence on  $n$ . This leads one to expect that the result in Eq.(IV-1) may be rather general in the limit of large  $n$ , valid in the classical regime for any potential which admits an harmonic approximation, as long as the anharmonic corrections to the particle motion are small. At this time, we have not succeeded in providing a general proof of this result, however.

We conclude this section with some comments about the possible role impurities may play in affecting the behavior of the absorption coefficient at high frequencies. If the impurities are coupled to the ions of the host lattice by means of an interaction that may be crudely represented by either the Morse potential or the potential  $bx^2 + a/x^2$ , then within the framework of our model, the impurities will not affect the qualitative behavior of the absorption coefficient, although they will affect it in a quantitative sense, since a certain fraction of the lattice oscillators will then be described by parameters which differ from the oscillators which describe the host lattice.

However, there are certain impurity ions which behave in an anomalous manner when present as substitutional impurities in alkali halides. An example is the  $\text{Li}^+$  ion, which frequently gives rise to a very low frequency resonance phonon mode, even though it is a very light ion which produces a high frequency local phonon mode if it is coupled to the host ions by interactions characterized by harmonic force constants comparable to those in the host matrix. Evidently in the case of  $\text{Li}$ , in the

harmonic approximation the force constants are very much smaller than those which characterize the host, small enough to offset the tendency of the light mass to create a high frequency local mode. In fact, in  $KCl$ , the  $Li^+$  ion sits off the substitutional lattice site, in the (111) direction while it sits on site in  $KBr$ . These facts suggest that the  $Li^+$  ion moves in a potential well with a rather flat bottom, while terms higher order than quadratic in the displacement of the  $Li^+$  ion from the substitutional site play an important role in the lattice potential energy. This notion is supported by theoretical studies<sup>(9)</sup>, and by experimental observations which show very large electric field induced shifts in the frequency of the resonance mode<sup>(10)</sup>. It is also true that a number of other ions have been observed to produce resonance modes with frequencies very much lower than the frequency expected on the basis of mass defect considerations alone<sup>(10)</sup>.

The remarks of the preceding paragraph indicate that there are a certain number of impurities which when placed in alkali halides may be crudely described as moving in the cage formed by their nearest neighbors, with the floor of the cage quite flat in character. The calculation presented in section III of the contribution to the absorption coefficient from the particle in the square well suggests that these impurities may give a contribution to the absorption coefficient which falls off as  $\omega^{-2}$  for frequencies large compared to the resonance frequency  $\omega_T$  at which the peak in the impurity-induced absorption occurs. Thus, the presence of a significant number of impurities which give rise to very low frequency resonances may have a significant qualitative

## Sec. E

effect on the behavior of the high frequency absorption coefficient.

Before we proceed to an estimate of the quantitative effect of these impurities on the absorption coefficient near  $10.6\mu$ , we first note that for typical values of parameters, the characteristic frequency  $\omega_T$  in the discussion of section III(c) indeed lies in the proper spectral region. For example, if  $L = 3 \times 10^{-8}$  cm, and if  $m$  is chosen to be fifty atomic units, then  $\omega_T \approx 15 \text{ cm}^{-1}$ , a frequency in the spectral region where the low lying impurity induced lattice resonances are observed. Also, the resonance mode frequency in some cases is observed to increase significantly with temperatures. Of course, we cannot expect our very crude model to account for the features of these resonance modes in a systematic and complete manner, but the overall qualitative features seem to be reasonable.

It is a straightforward matter to find an expression for the contribution of  $N_I$  impurities to the absorption coefficient, in the limit  $\omega \gg \omega_T$ . This may be done by multiplying Eq.(III-45) by  $N_I$ , the number of impurities in the sample, dividing the result by the (time averaged) energy stored in the electromagnetic field ( $\epsilon_\omega V E_0^2 / 8\pi$ , where  $\epsilon_\omega$  is the optical dielectric constant and  $V$  the crystal volume), then multiplying this by  $\epsilon_\omega^{1/2}/c$ , to obtain  $1/L$ , where  $L$  is the distance required for the energy density of the wave to decay to  $1/e$  of its initial value. One finds

$$\frac{1}{L} = 16 \pi^{1/2} f \frac{nq^2}{m} \frac{1}{c \epsilon_\omega^{1/2}} \frac{\omega_T}{\omega^2}, \quad (\text{IV-3})$$

## Sec. E

where  $n = N/V$  is the number of unit cells/unit volume of the host crystal and  $f$  is the impurity concentration. In Eq.(IV-3),  $q$  and  $m$  are the effective charge and mass of the impurity. Let  $q_0$  and  $m_0$  be the effective charge and reduced mass of the unit cell in the host crystal, and let

$$R = \frac{q^2}{q_0^2} \frac{m_0}{m} \quad . \quad (IV-4)$$

Then Eq.(IV-3) may be written

$$\frac{1}{L} = \frac{4}{\pi^2} R \left( \frac{\epsilon_s - \epsilon_\infty}{\epsilon_\infty^{\frac{1}{2}}} \right) f \left( \frac{\omega_0}{\omega} \right)^2 \frac{\omega_T}{c} \quad , \quad (IV-5)$$

where  $\epsilon_s = \epsilon_\infty + 4\pi n q_0^2 / m_0 \omega_0^2$  is the static dielectric constant of the host.

For the purposes of providing a crude estimate of the sensitivity of the absorption coefficient at  $10.6\mu$  to the presence of these anomalous impurities, we set  $R$  and  $(\epsilon_s - \epsilon_\infty)/\epsilon_\infty^{\frac{1}{2}}$  equal to unity, and suppose  $\omega/\omega_0 \sim 7$  and  $\omega_T = 20 \text{ cm}^{-1}$ . We then find

$$\frac{1}{L} \approx 5 f (\text{cm}^{-1}) \quad (IV-6)$$

where  $f$  is the impurity concentration.

The quantitative estimate of  $L$  displayed in Eq.(IV-6) must be regarded as extremely crude, because the model is highly oversimplified. It does suggest that near  $10.6\mu$ , the absorption coefficient of the crystal may be quite sensitive to small concentrations of Li, Ag, Cu or other impurities which give rise to impurity induced resonance modes with frequency very much lower

Sec. E

than expected on mass defect considerations. It would be extremely interesting to measure the effect on the absorption coefficient of doping KCl with Li, with concentrations in the range of 0.1% to test this conjecture.

References

1. For a discussion of the fundamental physical concepts employed in this area, we refer the reader to Dynamical Theory of Crystal Lattices, M. Born and K. Huang, (Oxford University Press, London, 1954).
2. T. F. Deutsch (to be published).
3. T. C. McGill, R. W. Hellwarth, M. Mangir and H. V. Winston, preprint entitled "Infra-red Absorption in Ionic Insulators due to Multiphonon Processes".
4. H. S. Heaps and G. Herzberg, Zeit.fur Physik, 133, 48 (1952).
5. See the discussion in Chapter III of Mechanics, L. D. Landau and E. M. Lifshitz, (Pergamon Press, Oxford, 1969).
6. Table of Integrals, Series and Products, I. S. Gradshteyn and I. M. Rhyzik, (Academic Press, New York, 1965).
7. W. Gröbner and N. Hofreiter, Integraltafel Vol. II (Springer-Verlag, Vienna and Innsbruck, 1950), p. 115.
8. The experimental data have been taken from the tabulations on P. 4-137 and P. 4-138 of American Institute of Physics Handbook, edited by Dwight E. Gray, (McGraw-Hill, New York, 1972).
9. R. J. Quigley and T. P. Das, Phys. Rev. 164, 1185 (1967), 177, 1340 (1969).

Sec. E

(References continued)

10. For a rather complete discussion of the properties of a number of impurities in alkali halides which give rise to low lying lattice resonance modes, see B. P. Clayman, R. D. Kirby and A. J. Sievers, Phys. Rev. B3, 1351 (1971).

F. TEMPERATURE DEPENDENCE OF THE ABSORPTION COEFFICIENT OF  
ALKALI HALIDES IN THE MULTIPHONON REGIME<sup>†</sup>

A. A. Maradudin and D. L. Mills  
Department of Physics  
University of California  
Irvine, California 92664

and

Xonics Corporation  
Van Nuys, California 91406

ABSTRACT

The theory of infrared absorption by an array of independent, anharmonic oscillators is discussed. When the oscillator potential is the Morse potential, the theory provides an excellent description of the temperature dependence of the absorption coefficient at  $10.6\mu$  in NaCl and NaF reported by Harrington and Hass.

<sup>†</sup>This research supported by The Advanced Research Projects Agency of the Department of Defense and was monitored by the Defense Supply Service, Washington, D. C. under Contract No. DAHC15-73-C-0217.

There has recently been interest in the mechanisms for absorption of infrared radiation by insulating crystals at frequencies high compared with the Reststrahl frequency. In the vicinity of the  $\text{CO}_2$  laser line at  $10.6\mu$ , and in alkali halide crystals where the electronic band gap is very large, the principal contribution to the absorption coefficient from the bulk of the crystal comes from multiphonon processes in which five, six or perhaps a larger number of phonons are created in the absorption process.

Quite recently, Deutsch<sup>1</sup> has completed a detailed experimental study of the frequency dependence of the absorption coefficient in several alkali halide crystals at room temperature. Several groups have addressed the theory of the absorption process by models that differ significantly in physical content,<sup>1-3</sup> and there seems to be general agreement that the frequency dependence of the intrinsic contribution to the absorption coefficient may be understood if the absorption has its origin in multiphonon processes. All of the theories which have been applied to the analysis of the data presume that anharmonic effects on the lattice motion may be treated by perturbation methods. One then predicts that for temperatures  $T$  large compared to the Debye temperature  $\theta_D$ , the contribution to the absorption coefficient from processes which involve  $n$  phonons should vary with temperature like  $T^{n-1}$ .

A recent experimental study of the temperature dependence of the absorption coefficient  $\alpha$  at  $10.6\mu$  in several alkali halides has been reported by Harrington and Hass.<sup>4</sup> These authors find that  $\alpha$  varies with  $T$  more slowly than  $T^{n-1}$  in the crystals examined by them. The purpose of this paper is to apply the simple theoretical

model developed in our previous paper<sup>3</sup> to an analysis of this data. We obtain an excellent quantitative description of the observed temperature dependence, and the model also predicts absolute values of  $\alpha$  at high temperatures close to the observed values. We analyze the data on NaCl and NaF in detail. In the case of NaCl, a crystal considered in our previous paper, an excellent description of the data may be obtained without introducing any parameters not found in our earlier work and for NaF, a crystal not examined earlier by us, one parameter is required. The value of this parameter may be checked by comparing the thermal expansion coefficient predicted by our simple model with the experimental result, and the two agree well. Thus, we conclude that our model provides an excellent account of the data reported by Harrington and Hass. Furthermore, the physical content of the model suggests that at high temperatures anharmonic effects have a strong influence on multiphonon excitations in the alkali halides.

In our previous paper, we replaced the crystal by a set of  $N$  classical, non-interacting by anharmonic oscillators, where  $N$  is the number of unit cells in the crystal. Each oscillator has a reduced mass  $m$ , and a transverse effective charge  $q$ . If the crystal is illuminated by radiation with the electric field  $E(t) = E_0 \cos \omega t$ , then the time and ensemble averaged rate at which energy is absorbed by a single oscillator is given by<sup>3</sup>

$$\langle \langle \frac{d\mathcal{E}}{dt} \rangle \rangle = \frac{\omega \beta q^2 E_0^2}{4m^2 Z} \sum_{n=1}^{\infty} \frac{1}{n} \int_0^{\infty} dE e^{-\beta E} \rho_n^2(E) \delta(\omega - n\omega(E)) , \quad (1)$$

where  $\beta = 1/k_B T$ ,  $Z$  is the partition function for a single oscillator, the period  $T(E)$  of the bound orbit of energy  $E$  is written

$T(E) = 2\pi/\omega(E)$ , and  $\rho_n(E)$  is a measure of the amplitude of the  $n^{\text{th}}$  harmonic in the orbit of energy  $E$ . If  $p_E(t)$  gives the time dependence of the momentum in the orbit of energy  $E$ , with the origin of time chosen so that the particle is at a classical turning point at  $t = 0$ , then

$$\rho_n(E) = \frac{2}{T(E)} \int_0^{T(E)} dt p_E(t) \sin n\omega(E)t . \quad (2)$$

The virtue of the model is that exact expressions for  $\alpha$  may be obtained with it, even when the oscillator motion is very anharmonic. For the Morse potential  $V(x) = D[1 - \exp(a[x - x_0])]^2$  we previously obtained exact expressions for  $\omega(E)$  and  $\rho_n(E)$ , although we found  $\alpha$  only when  $k_B T$  was small enough for the oscillator motion to be treated as nearly harmonic. In this paper, we work with the full form of  $\alpha$ , without this last assumption. In our earlier paper, we found

$$\omega(E) = \omega_0 (1 - E/D)^{\frac{1}{2}} \quad (3)$$

$$\rho_n(E) = \frac{2\pi(2mE)^{\frac{1}{2}}}{\omega_0} \left(\frac{D}{E}\right)^{\frac{(n+1)}{2}} \left[1 - \frac{\omega(E)}{\omega_0}\right]^n , \quad (4)$$

where  $\omega_0 = a(2D/m)^{\frac{1}{2}}$  is the frequency of the oscillatory motion, in the harmonic approximation. Equations (3) and (4) may be inserted into Eq. (1), and the integration carried out. We make one simplification in the exact result. For  $k_B T \ll D$ , a limit that applies to our discussions here, the partition function is well approximated by the result  $Z = 2\pi k_B T / \omega_0$  obtained from the harmonic approximation.<sup>5</sup> In the results that follow, we use this form for  $Z$ . Then if we let  $\xi = \omega/\omega_0$ , and  $n_m$  is the first integer larger than  $\xi$ , we find

$$\langle \langle \frac{d\mathcal{E}}{dt} \rangle \rangle = \frac{2\pi q^2 E_o^2}{m\omega_o} \left( \frac{D}{k_B T} \right)^2 \xi^2 \sum_{n=n_m}^{\infty} \left( \frac{n-\xi}{n+\xi} \right)^n \frac{\exp \left[ -\frac{D}{k_B T} \left( 1 - \frac{\xi^2}{n^2} \right) \right]}{n^3} \quad (5)$$

At fixed frequency, the temperature dependence of the absorption coefficient is controlled by the single parameter  $D/k_B T$ , which for the case of NaCl may be obtained from our earlier work.<sup>3</sup>

We first recover from Eq. (5) the result valid in the quasi-harmonic regime, where for the  $n^{\text{th}}$  term, this requires  $nk_B T \ll D$ . In this limit, the  $n^{\text{th}}$  term of Eq. (5) peaks sharply just below  $\xi = n$ . Thus, let  $\xi = n - \epsilon$ , with  $\epsilon$  small. If the  $n^{\text{th}}$  term in Eq. (5) is denoted by  $\langle \langle \frac{d\mathcal{E}}{dt} \rangle \rangle_n$ ,

$$\langle \langle \frac{d\mathcal{E}}{dt} \rangle \rangle_n \cong \frac{2\pi q^2 E_o^2}{m\omega_o} \left( \frac{D}{k_B T} \right)^2 \frac{\epsilon^n \theta(\epsilon)}{2^n n^{n+1}} \exp \left[ -\frac{2D}{nk_B T} \epsilon \right], \quad (6)$$

where  $\theta(\epsilon) = 1$  if  $\epsilon > 0$  and is zero for  $\epsilon < 0$ . The integrated strength of the absorption line in Eq. (6) is

$$\int d\omega \langle \langle \frac{d\mathcal{E}}{dt} \rangle \rangle_n = \frac{\pi q^2 E_o^2}{4m} n! \left( \frac{k_B T}{4D} \right)^{n-1}. \quad (7)$$

Thus, in the limit  $nk_B T \ll D$ , the  $n^{\text{th}}$  term in Eq. (5) contributes to the absorption coefficient a term well approximated by the form

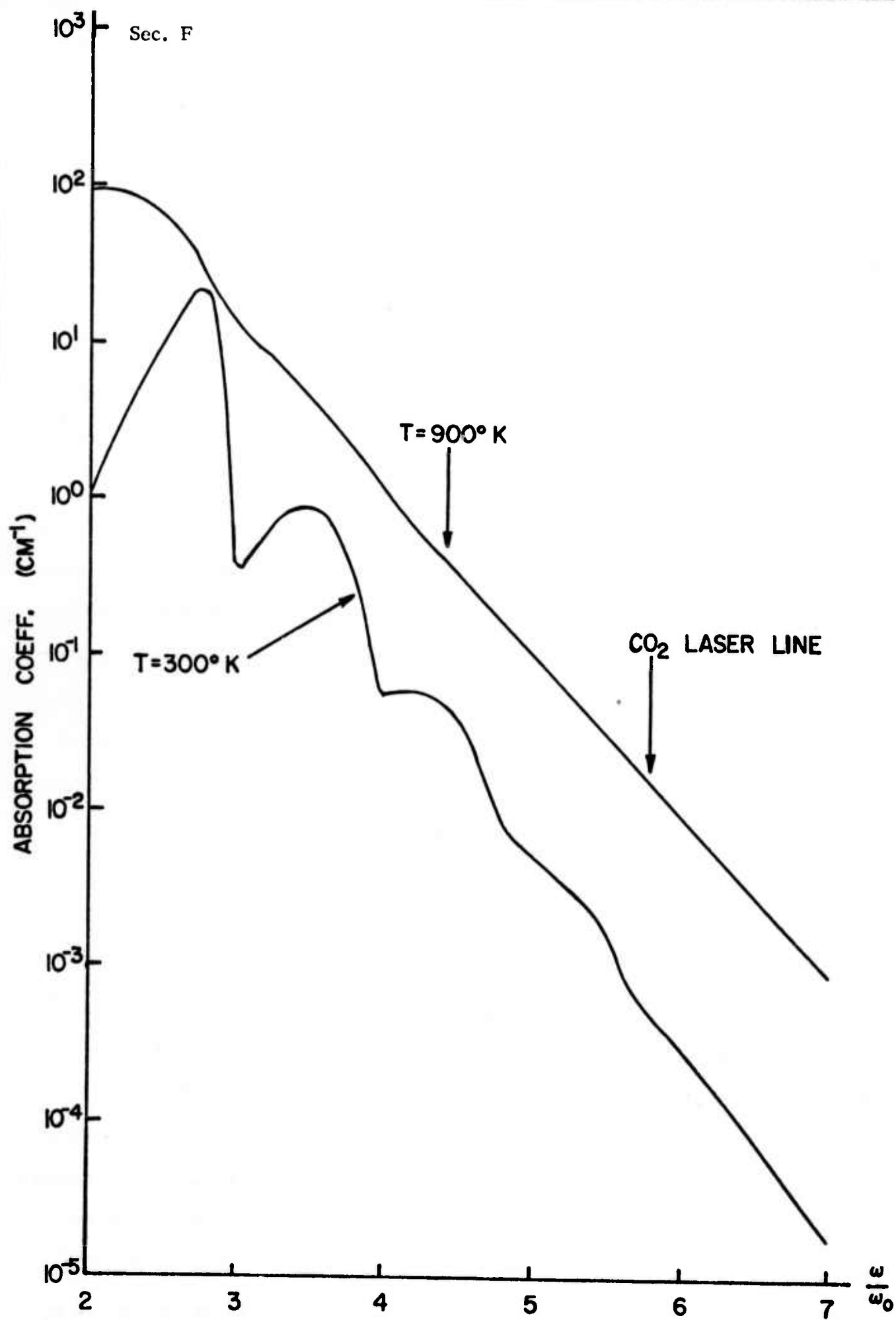
$$\langle \langle \frac{d\mathcal{E}}{dt} \rangle \rangle_n \cong \frac{\pi q^2 E_o^2}{4m} n! \left( \frac{k_B T}{4D} \right)^{n-1} \delta(\omega - n\omega_o). \quad (8)$$

This expression is identical to that produced by the quasi-harmonic approximation utilized earlier by us.<sup>3</sup>

In Figure 1, we present a calculation of the frequency dependence of the absorption coefficient for the model for  $T = 300^\circ \text{K}$  and  $T = 900^\circ \text{K}$ , from Eq. (5). We have used the value of  $D$  obtained for

Figure Caption

Figure 1. Frequency dependence of the absorption coefficient for a Morse potential oscillator at  $T = 300^\circ \text{K}$  and  $900^\circ \text{K}$ , with a  $D$  chosen for NaCl.



NaCl from our earlier work, and with the absolute value of the  $\alpha$  adjusted to fit the 10.6 $\mu$  data of Harrington and Hass at 900° K.

Several features of these results deserve comment. For  $T=300^\circ\text{K}$ , the  $n=3$  term in Eq.(5) produces a very sharp peak centered a bit below  $\xi = 3$ . This peak is quite narrow and well defined, as one would expect in the quasi-harmonic approximation. For  $\xi$  near 5 or 6, the effect of anharmonicity is severe enough that  $\alpha$  varies smoothly with frequency, displaying only gentle shoulders as a reminder of the sharp structure present in the quasi-harmonic approximation. But the time  $T=900^\circ\text{K}$ , the theory produces a very smooth dependence of  $\alpha$  with frequency.

These calculations suggest that for large values of  $\omega/\omega_0$ , even at room temperature, the lattice motion cannot be regarded as nearly harmonic, so the absorption coefficient cannot be calculated by perturbation theoretic methods which treat the anharmonic terms in the crystal Hamiltonian as small. This is also clear from the data of Harrington and Hass, which we shall see is well fitted by our model, since the data show very large departures from the  $T^{n-1}$  behavior cited earlier.

It must be emphasized that at fixed  $T$ , the relative importance of the anharmonicity increases as  $\omega/\omega_0$  increases. If we examine the absorption coefficient for the model near the Reststrahl region (the Reststrahl absorption is described by the term  $n = 1$  in Eq. (5)), then the parameters we employ produce rather modest anharmonic effects. For example, at temperature  $T$ , the Reststrahl peak occurs very close to  $\tilde{\omega}_0 = \omega_0(1 - k_B T/2D)$ , where  $\omega_0$  is the Reststrahl frequency at  $T = 0$ . For our parameters, at room temperature,  $k_B T/2D \cong 0.03$  for NaCl. The half width at half maximum is also close to  $k_B T/2D$  in magnitude, and increases linearly with  $T$ . As the parameter  $\omega/\omega_0$

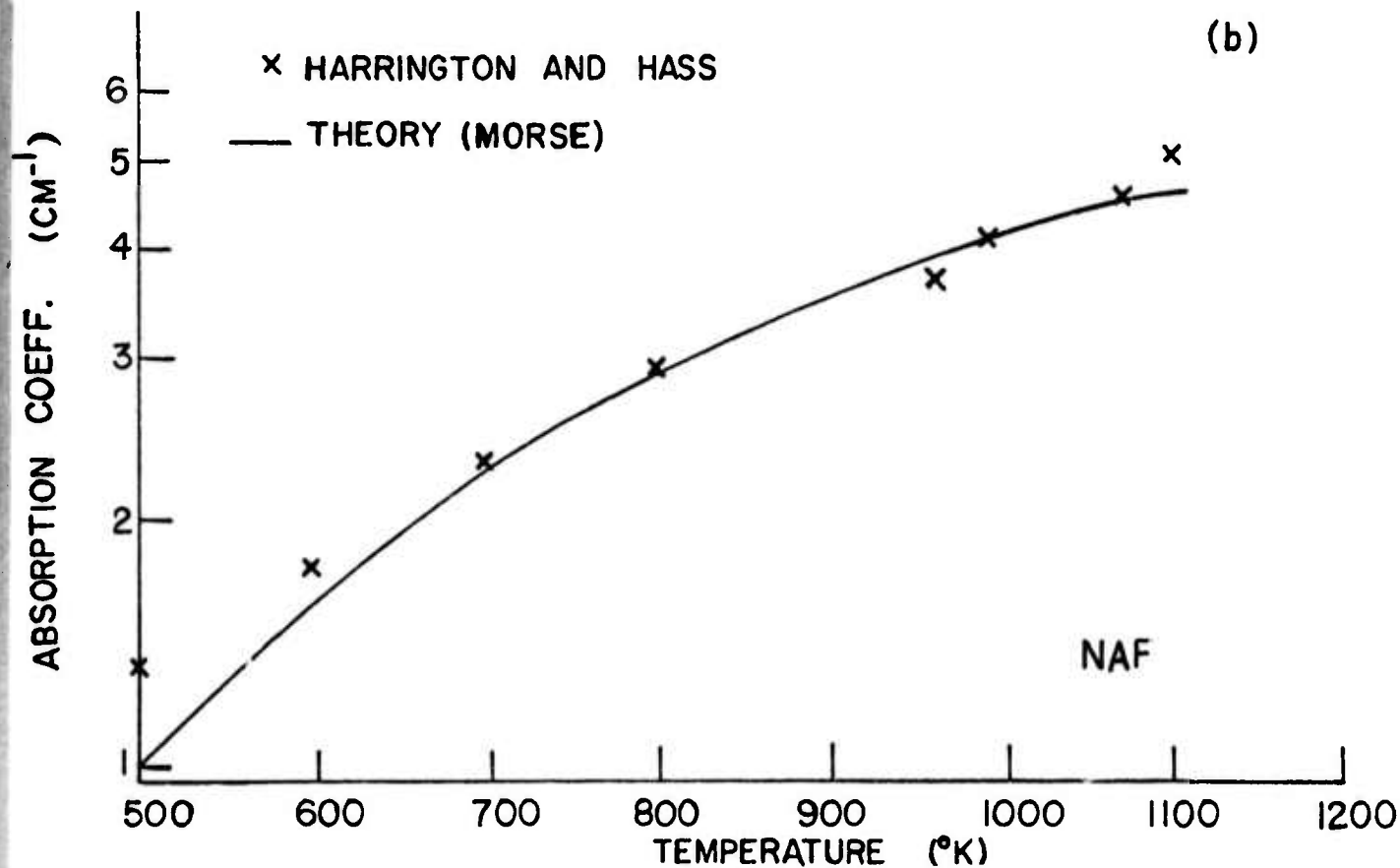
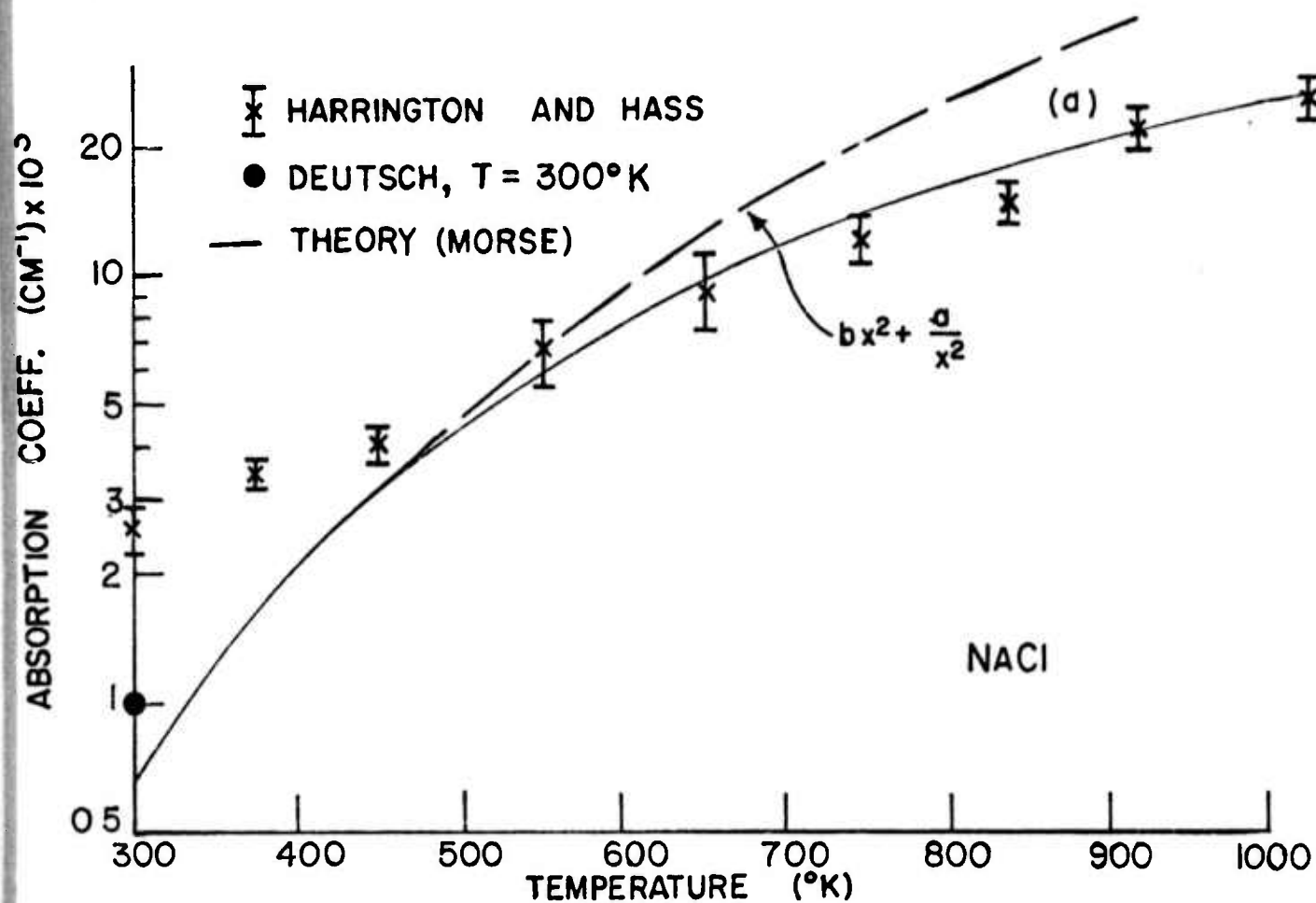
increases, each successive peak shifts to lower frequency by a fractional amount that increases with increasing order, and the width of each feature described by the terms in Eq. (5) increases rapidly enough so that by the time  $\xi = 6$ , the absorption coefficient varies smoothly with frequency at room temperature.

In Figure 2a, we compare the temperature dependence of the absorption coefficient at  $10.6\mu$  obtained from our calculations with the data of Harrington and Hass. The theory has been fitted to the data at  $900^\circ\text{K}$ , and gives a very good account of the observed temperature dependence for all but the lowest temperature. In his previous work, Deutsch has reported a value of  $0.001\text{ cm}^{-1}$  for the absorption coefficient at room temperature, while the value reported by Harrington and Hass is larger by a factor of 2.7. Thus, near room temperature, the absorption coefficient measured by Harrington and Hass presumably contains an extrinsic contribution which is dominated by the intrinsic contribution at higher temperatures. If we accept Deutsch's value as the correct one at room temperature (see the diamond in Fig. 2a), then we may fit  $\alpha$  to within a factor of two over the entire temperature range.

Our model also predicts the absolute magnitude of the absorption coefficient. The rate at which energy is absorbed from the field is found by multiplying Eq. (5) by the number of molecules  $N$  (equal to the number of unit cells) in the crystal. Then upon dividing by the time averaged energy  $V\epsilon_0 E_0^2/8\pi$  stored in the field, where  $\epsilon_0$  is the high frequency dielectric constant, and dividing by the propagation velocity  $c/\epsilon_0^{1/2}$ , one obtains the inverse of the length  $d$  required for the energy density in the beam to decay to  $1/e$  of its

Figure Caption

Figure 2. Temperature dependence of the absorption coefficient at  $10.6\mu$  in (a) NaCl and (b) NaF. The solid curve is calculated from the Morse potential and the dashed curve from  $V(x) = bx^2 + a/x^2$ .



initial value. This quantity is the absorption coefficient  $\alpha$  measured in the experiments. The magnitude of  $\alpha$  may be estimated in the multiphonon regime from dielectric constant data once  $D$  is known, since  $\epsilon_s - \epsilon_0 = 4\pi nq^2/m$  for ionic crystals. For NaCl, the theory predicts that at  $T = 900^\circ\text{K}$ , the absorption length should be  $0.011 \text{ cm}^{-1}$  at  $10.6\mu$ , while the data shows it to be  $0.020 \text{ cm}^{-1}$ . Our model thus gives an absolute value for  $\alpha$  in good accord with the data.

In Figure 2b, we compared the temperature dependence predicted for the absorption coefficient at  $10.6\mu$  with the data on NaF. Again we obtain an excellent fit for  $500^\circ\text{K} < T < 1200^\circ\text{K}$ . The theory does poorly for  $T < 500^\circ\text{K}$ , presumably because  $\theta_D \approx 490^\circ$  in NaF, and our classical model is inapplicable for  $T \leq \theta_D$ . In Figure 2b, we have chosen  $D_{\text{NaF}} = D_{\text{NaCl}}$ , and adjusted the magnitude of the absorption length to fit the data at  $700^\circ\text{K}$ . For NaF,  $\xi \approx 3.96$  at  $10.6\mu$ . The value selected for  $D$  predicts the coefficient of linear thermal expansion for the crystal to be  $38 \times 10^{-6} \text{ }^\circ\text{K}^{-1}$  when  $T > \theta_D$ , if we use our earlier procedure to make this estimate.<sup>3</sup> This value is in excellent accord with the measured value of the thermal expansion coefficient.<sup>7</sup> From the dielectric constant data, the theory predicts the absorption length to be  $1.2 \text{ cm}^{-1}$  at  $900^\circ\text{K}$ , while the measured value is  $3.4 \text{ cm}^{-1}$ . Thus, while the absolute value for  $\alpha$  in NaF agrees less well with the data than in the case of NaCl, the theory gives reasonable semiquantitative agreement.

One can inquire about sensitivity of these results to the details of the potential. To test this, the dashed curve in Fig. (2a) gives the dependence on  $T$  for  $\alpha$  at  $6\omega_0$  for the potential  $bx^2 + a/x^2$  examined previously<sup>(3)</sup>, with the fit to the room

temperature data carried out as in our earlier paper. This potential also provides a reasonable fit to the data, so the detailed form of the potential does not seem to be critical.

Thus our model gives a good account of the dependence of  $\alpha$  on  $T$  in alkali halides through the use of only a single parameter whose value may be checked through use of data on the thermal expansion coefficient. Quite recently, Sparks and Sham<sup>8</sup> have extended their earlier work<sup>2</sup> to provide an account of the dependence of  $\alpha$  on  $T$ . Their theory includes the effect of phonon dispersion in an approximate way. They also treat the problem by quantum mechanical methods while our theory is purely classical. Thus, their theory may be applied to the region  $T < \theta_D$  while ours may not be. The two pieces of work are complementary in a certain sense. While their model is more detailed than ours, they introduce a sequence of approximations, such as the inclusion of terms only through a finite order of perturbation theory, approximate treatment of phonon dispersion, and finally a phenomenological inclusion of certain anharmonic effects by allowing the phonon frequencies to be temperature dependent. Our model is more schematic in nature, but its virtue is the use of only a small number of parameters to characterize a given material, and we obtain exact results for  $\alpha$ . The two theories concur in one important regard. At high temperature, and in the multiphonon regime, in the alkali halides the effect of anharmonicity is very large, so large deviations from the  $T^{n-1}$  law occur.

# ACKNOWLEDGMENTS

We are indebted to Dr. J. A. Harrington for sending us his data in advance of publication, and for useful discussions. We are also grateful to Dr. M. Sparks for many useful conversations.

# REFERENCES

1. T. F. Deutsch (to be published). See also F. A. Horrigan and T. F. Deutsch "Research in Optical Materials and Structures," Quarterly Technical Report No. 2, April 1972, Raytheon Corp., Waltham, Mass.
2. M. Sparks and L. J. Sham, Solid State Communications 11, 1451 (1972); M. Sparks and L. J. Sham (to be published); T. C. McGill, R. W. Hellwarth, M. Mangir and H. V. Winston (to be published); B. Bendow, S. C. Ying and S. P. Yukon (to be published).
3. D. L. Mills and A. A. Maradudin, Phys. Rev. (to be published).
4. J. A. Harrington and M. Hass (to be published).
5. For  $k_B T \ll D$ , one has the asymptotic form  $Z = 2\pi k_B T / \omega_0 (1 + k_B T / 2D + \dots$  where  $k_B T / 2D < 0.1$  for values of  $T$  needed here.
6. See p. 190 of C. Kittel, Introduction to Solid State Physics, Fourth Edition (J. Wiley and Sons, New York, 1971).
7. See p. 4-139 of American Institute of Physics Handbook, edited by Dwight E. Gray (McGraw Hill, New York, 1972).
8. M. Sparks and L. J. Sham (to be published).

G. TEMPERATURE AND FREQUENCY DEPENDENCE OF  
INFRARED ABSORPTION AS A DIAGNOSTIC TOOL\*

M. Sparks

Xonics, Incorporated, Van Nuys, California 91406

Recent developments render untenable a proposed method of distinguishing between intrinsic and extrinsic infrared absorption on the basis of the proposed temperature dependence. However, when the proper temperature dependence of multiphonon absorption is accounted for and the possibility of other intrinsic processes is taken into account, the temperature and frequency dependence of the absorption of both the best available and intentionally imperfect crystals should be useful in studying extrinsic processes.

It has been suggested that the temperature dependence of the optical absorption coefficient  $\beta$  could be used to distinguish between intrinsic (characteristic of a perfect crystal) and extrinsic (caused by imperfections) infrared absorption.<sup>1</sup> Several recent developments bear on this suggestion. First, a combination of frequency  $\omega$  and temperature  $T$  dependence should be far more useful than the  $T$  dependence alone.<sup>2</sup> Second, the  $T$  dependence of  $\beta$  for multiphonon absorption deviates considerably<sup>3,4</sup> from the expected<sup>5,6,2,1</sup> result. Third, other extrinsic processes in addition to those considered in Ref. 1 should be included.

Consider the first development. The near exponential frequency dependence of  $\beta$  observed<sup>7,8</sup> in a number of materials including LiF, NaF,<sup>8</sup> NaCl, KCl, KBr, MgF<sub>2</sub>, CaF<sub>2</sub>, BaF<sub>2</sub>, SrF<sub>2</sub>, MgO, Al<sub>2</sub>O<sub>3</sub>, SiO<sub>2</sub>, TiO<sub>2</sub>, SrTiO<sub>3</sub>, and BaTiO<sub>3</sub>,

when extrapolated to  $10.6\mu\text{m}$ , gives a fair estimate of the intrinsic value of  $\beta$  at  $10.6\mu\text{m}$ . Thus, it is already known with fair accuracy whether the  $10.6\mu\text{m}$  values of  $\beta$  are intrinsic or extrinsic for a number of materials. Nevertheless, additional  $\omega$  and  $T$  measurements would be of great interest in studying the sources of extrinsic absorption and possibly new intrinsic absorption mechanisms. Intentionally introducing various types of imperfections into crystals and on their surfaces should be invaluable in such studies.<sup>2</sup> Since values of  $\beta$  of  $10^{-4}\text{cm}^{-1}$  and even lower are of current interest, standard transmission measurements are inadequate. Emissivity techniques should be capable of yielding values of  $\beta$  well below  $10^{-4}\text{cm}^{-1}$  in a carefully designed simple instrument.<sup>9</sup> Calorimetric measurements of  $\beta$ 's approaching  $10^{-4}\text{cm}^{-1}$  at the single wavelength  $10.6\mu\text{m}$  are of course now common.

Concerning the second development, the temperature dependence of the intrinsic  $n$ -phonon absorption (annihilation of one photon and creation of  $n$  phonons) is considerably weaker than the well known<sup>5,6,2,1</sup> explicit temperature dependence

$$\beta \cong \beta_0 \left(1 - e^{-\omega/\omega_T}\right) \left(1 - e^{-\omega/n\omega_T}\right)^{-n} \quad (1)$$

where  $\omega$  is the laser frequency and  $\omega_T \equiv k_B T/\hbar$ . Eq. (1), which can be written as  $\beta \sim (n_Q + 1)^n - n_Q^n$ , where  $n_Q$  is the Bose-Einstein occupation number for a phonon of frequency  $\omega/n$ , or in several other simple forms by using energy conservation, reduces to  $\beta \sim T^{n-1}$  in the high-temperature limit  $\omega_T \gg \omega$ . Experimentally, this deviation from (1) was observed by Harrington and Hass,<sup>3</sup> and it is apparent in the data of Barker.<sup>10</sup> Sparks and Sham<sup>4</sup> have explained this

deviation by including the temperature dependence of the phonon frequencies and lattice constant in their previous theory of the nearly exponential frequency dependence of  $\beta$  discussed below. In addition, the particular extrinsic processes suggested by Hardy and Agrawal<sup>1</sup> and by Rosenstock<sup>6</sup> will show similar deviations from their predicted explicit  $T$  dependence when the  $T$  dependence of the parameters is included. Until more experimental information is available to establish faith in the ability to predict the  $T$  dependence of the multiphonon and band-phonon plus localized-impurity processes, distinguishing between the two on the basis of the  $T$  dependence alone probably would be difficult.

The third development concerns a further more serious problem in distinguishing between intrinsic and extrinsic absorption on the basis of the  $T$  dependence in Ref. 1. That is, there are many possible extrinsic processes in addition to the band-phonon plus localized-impurity process suggested in Refs. 1 and 6. For example, small amounts of macroscopic inclusions can give rise to a temperature dependence ranging from  $\beta \sim T^0$  to  $T^4$  in typical cases, depending on the type of impurity.<sup>11</sup> There is also some experimental evidence, though it is not conclusive at present, for temperature independent absorption.<sup>12,3</sup>

The study of intrinsic and especially extrinsic processes, by measuring  $\beta(\omega, T)$  in ultrapure and intentionally imperfect crystals, for example, indubitably will become important if the current interest in obtaining low-absorption materials is unabated. Already there are a number of cases in which multiphonon absorption is obviously the source of  $\beta$  and others in which it obviously is not. For example, there is now little doubt that the nearly

exponential frequency dependence<sup>7,8</sup> of  $\beta$  mentioned above is the result of multiphonon absorption. The contributions of the individual n-phonon processes have been calculated and summed to obtain the nearly exponential frequency dependence.<sup>5</sup> More recently, a direct derivation of the exponential in closed form, rather than as a sum of the individual n-phonon contributions, has been given.<sup>13</sup>

The fact<sup>7</sup> that the  $10.6\mu\text{m}$  values of  $\beta$  for a number of crystals, such as KBr, CdTe, and KCl as examples, lie well above the values obtained by extrapolating longer-wavelength values to  $10.6\mu\text{m}$  surely indicates that these measured values of  $\beta$  arise from processes other than multiphonon absorption. A clear example of an extrinsic experimental value of  $\beta$  is that of a NaCl sample measured at  $10.6\mu\text{m}$  from 300 K to near the melting point by Harrington and Hass.<sup>3</sup> The room temperature value of  $\beta = 0.003\text{ cm}^{-1}$  for this sample is considerably greater than both the lowest value of  $\beta = 0.0015\text{ cm}^{-1}$  observed to date<sup>14</sup> and the estimated intrinsic value of slightly less than  $10^{-3}\text{ cm}^{-1}$  obtained by extrapolating the lower frequency data to  $10.6\mu\text{m}$ . Furthermore, the temperature dependence deviates strongly from the multiphonon value even when the T dependence of phonon frequencies and lattice constant are taken into account. In fact,  $\beta$  decreases as the temperature increases near room temperature.

## REFERENCES

\* This research was supported by the Advanced Research Projects Agency of the Department of Defense and was monitored by the Defense Supply Service - Washington, D.C. under Contract No. DAHC15-73-C-0127.

1. J. R. Hardy and B. S. Agrawal, Appl. Phys. Letters 22, 236 (1973).
2. M. Sparks, "Recent Developments in High-Power Infrared Window Research," 4th ASTM Damage in Laser Materials Symposium, Boulder, Colo., June 14-15, 1972; M. Sparks, Rand Corporation Reports WN-7243-PR, June 1971, and R-863-PR, August 1971; M. Sparks, Xonics Technical Reports on Contract DAHC15-72-C-0129, March-December 1972.
3. J. A. Harrington and M. Hass, to be published.
4. M. Sparks and L. J. Sham, to be published.
5. M. Sparks and L. J. Sham, Phys. Rev., in press; Solid State Commun. 11, 1451 (1972); AFCRL Conference on High-Power Infrared Laser Window Materials, Hyannis, Mass. Oct. 30-Nov. 1, 1972, proceedings published by Air Force Cambridge Research Laboratories, Bedford, Mass. Also see Ref. 2.
6. H. P. Rosenstock, Bull. Am. Phys. Soc. 18, 674 (1973).
7. G. Rupprecht, Phys. Rev. Letters 12, 580 (1964); T. Deutsch, to be published; American Institute of Physics Handbook, 3rd ed., Ed. D. E. Gray (McGraw-Hill, New York, 1972).
8. S. S. Ballard, private communication reported in the American Institute of Physics Handbook, 3rd ed. Calculating  $\beta(\omega)$  from the transmission data given for NaF gives an exponential frequency dependence, a fact that apparently has been overlooked previously.
9. M. Sparks, unpublished.

Sec. G

10. A. J. Barker, J. Phys. C 5, 2276 (1972).
11. M. Sparks and C. J. Duthler, J. Appl. Phys., in press; C. J. Duthler and M. Sparks, 5th ASTM Damage in Laser Materials Symposium, Boulder, Colorado, May 15-16, 1973.
12. V. O. Nicolai and G. W. Gottlieb, Technical Report AFWL-TR-69-108, Air Force Weapons Laboratory, Kirtland Air Force Base, August 1969.
13. L. J. Sham and M. Sparks, to be published.
14. J. A. Harrington, private communication.

## H. SHORT-PULSE OPERATION OF INFRARED WINDOWS WITHOUT THERMAL DEFOCUSING\*

M. Sparks

Xonics, Incorporated, Van Nuys, California 91406

The possibility of transmitting short infrared pulses through materials with little thermally induced optical distortion is shown to exist. For sufficiently short pulses, of the order of  $10^{-8}$  -  $10^{-9}$  sec, the absorbed energy does not have time to thermalize, thus avoiding heating effects until after the pulse has been transmitted.

In high-power laser systems, heating of a window or other transparent component by the laser beam causes changes in the index of refraction  $n$  and in the thickness of the window.<sup>1,2,3</sup> The resulting defocusing is one of the most serious problems in such systems. It has been pointed out that much higher intensities can be transmitted if the laser can be operated for a period of time, say of the order of a second, after which the window is cooled before the next pulse is transmitted.<sup>1,2,3</sup> Bloembergen<sup>4</sup> suggested that if the pulse duration is much shorter than a characteristic time, of the order of an acoustic velocity times a linear dimension of the window, the change in window thickness is negligible, and only changes in  $n$  (at constant strain) should be considered.

The purpose of the present note is to point out that in principle still shorter pulse durations allow the window to transmit the pulse before the

temperature rises, thus avoiding the thermal defocusing. The requirement for this effect is

$$t_{\text{puls}} \lesssim 1/\Gamma(\omega) \quad (1)$$

where  $t_{\text{puls}}$  is the pulse duration and  $\Gamma(\omega)$  is the relaxation frequency of the fundamental-phonon mode (transverse optical mode with wavevector  $\underline{k} \approx 0$ ). When (1) is satisfied, the energy absorbed from the laser field by the fundamental mode has not had sufficient time to relax out of the fundamental mode and thermalize. Thus the temperature, which corresponds to the thermal-equilibrium values of the phonon occupation numbers, remains at its initial value.

Practical values of  $t_{\text{puls}}$  depend critically on the deviation of  $\Gamma(\omega)$  from the resonant value  $\Gamma_f \equiv \Gamma(\omega_f)$ , where  $\omega_f$  is the frequency of the fundamental mode. For example, from the value of the linewidth in thin NaCl samples,<sup>5</sup>

$$\Gamma_f \approx 2.5 \times 10^{12} \text{ sec}^{-1}.$$

The corresponding value of  $t_{\text{puls}} \lesssim 4 \times 10^{-13}$  sec from (1) is smaller than values of current interest. The value of  $\Gamma(\omega)$  decreases rapidly as  $\omega$  increases above  $\omega_f$ . On resonance,  $\Gamma_f$  is large in general because there are many phonon states into which the fundamental mode can decay. As  $\omega$  increases, the lower-order processes, in which the fundamental phonon splits into only a few phonons, cannot conserve energy, and  $\Gamma(\omega)$  decreases accordingly.

In order to obtain an estimate of the size of  $\Gamma(\omega)$ , consider the optical absorption coefficient  $\beta(\omega)$ <sup>6,7</sup>

$$\beta(\omega) = A \frac{\omega \Gamma(\omega)}{(\omega^2 - \omega_f^2)^2 + \omega_f^2 \Gamma(\omega)^2} \quad (2)$$

where  $A$  is a constant. On resonance, (2) gives

$$\beta(\omega_f) = A / \omega_f \Gamma_f \quad (3)$$

At the laser frequency  $\omega$ , assumed to be high [ $\omega \gg \omega_f, \Gamma(\omega)$ ], (2) gives

$$\beta(\omega) = A \Gamma(\omega) / \omega^3 \quad (4)$$

The ratio of  $\beta(\omega_f)$  to  $\beta(\omega)$  from (3) and (4) is

$$\beta(\omega_f) / \beta(\omega) = \omega^3 / \omega_f \Gamma_f \Gamma(\omega) \quad (5)$$

which gives, with (1), the central result

$$t_{\text{puls}} \approx \frac{1}{\Gamma(\omega)} = \frac{\beta(\omega_f)}{\beta(\omega)} \frac{\omega_f \Gamma_f}{\omega^3} \quad (6)$$

Consider the materials in which distortion-free transmission is likely to be observable. In order to make  $t_{\text{puls}}$  large,  $\Gamma(\omega)$  should be small, according to (6). Since  $\beta(\omega/\omega_f)$  decreases more rapidly than  $(\omega/\omega_f)^3$  with increasing  $\omega$  in the multiphonon absorption region,<sup>7</sup> a large value of  $\omega/\omega_f$  is desirable in order to make the denominator in (6) small. However, if  $\omega/\omega_f$  is too large, other absorption processes dominate the multiphonon absorption. Thus, the

smallest value of  $\beta(\omega)$  in the multiphonon region is desired. The smallest values of  $\beta(\omega)$  measured to date at  $10.6\mu\text{m}$  are of the order of  $10^{-4}\text{cm}^{-1}$ .<sup>8</sup>

The value of  $\beta$  at  $10.6\mu\text{m}$  for KCl obtained by extrapolating from measured values<sup>8</sup> between  $\beta = 20$  and  $5 \times 10^3\text{cm}^{-1}$  is  $\beta = 10^{-4}\text{cm}^{-1}$ . In view of current interest in KCl and the fact that  $\beta = 4 \times 10^{-4}\text{cm}^{-1}$  has already been demonstrated, it is likely that  $10^{-4}\text{cm}^{-1}$  will be attained. Thus, KCl is a good candidate in which to study the effect. At other wavelengths, other materials would be more appropriate; for example, the extrapolated value of  $\beta$  equals  $10^{-4}\text{cm}^{-1}$  at  $\sim 3.5\mu\text{m}$  for LiF. If values of  $\beta$  smaller than  $10^{-4}\text{cm}^{-1}$  are attained, the choice of materials will change.

For KCl, with  $\omega_f = 2.7 \times 10^{13}\text{sec}^{-1}$ ,  $\Gamma_f \cong 0.08 \omega_f$ ,  $\omega = 1.8 \times 10^{14}\text{sec}^{-1}$  (i.e.,  $10.6\mu\text{m}$ ),  $\beta(\omega_f) \cong 5 \times 10^4\text{cm}^{-1}$ , and  $\beta(\omega) \cong 10^{-4}\text{cm}^{-1}$ , (6) gives

$$\frac{1}{\Gamma(\omega)} = 5 \times 10^{-9}\text{sec} \quad (7)$$

Such short pulses are not presently available at  $10\mu\text{m}$ . However, they are currently available at shorter wavelengths. For example, 6 TW with a pulse duration of  $10^{-11}\text{sec}$  is available at  $1.06\mu\text{m}$ . Picosecond pulse durations are theoretically possible at longer wavelengths, of course. Values of  $1/\Gamma(\omega)$  at wavelengths shorter than  $10\mu\text{m}$  can be as large as that in (7). For example, at  $3.5\mu\text{m}$  for LiF with  $\omega_f = 5.8 \times 10^{13}\text{sec}^{-1}$ ,  $\Gamma_f = 0.08 \omega_f$ ,  $\omega = 5.5 \times 10^{14}\text{sec}^{-1}$ ,  $\beta(\omega_f) = 2 \times 10^5\text{cm}^{-1}$ , and  $\beta(\omega) = 10^{-4}\text{cm}^{-1}$ , (6) gives  $1/\Gamma(\omega) = 3 \times 10^{-9}\text{sec}$ . Thus, it is possible that the no-heating short-pulse

effect could be observed over a substantial part of the near infrared region. Unfortunately, at  $1.06\text{ }\mu\text{m}$ , where  $10^{-11}$  sec-pulse-duration lasers are available, there is no material with  $\beta$  determined by multiphonon absorption. Thus, tests and applications of the theory will have to await the availability of short-pulse sources at longer wavelengths.

The analysis above applies to the case of multiphonon absorption by the anharmonic potential mechanism. The possibility of a similar no-heating effect at other frequencies and for other absorption mechanisms also exists. However, the situation is likely to be considerably more complicated. For example, for absorption in the visible and very near infrared, the absorption is likely to involve electronic excitations, such as in electric-field-induced absorption or excitation of impurity-type or surface-state levels. The time required for the energy to be transferred to the lattice varies greatly with the number of impurities, type of material, and the temperature in general. Furthermore, the direct effect on the index of refraction of the electronic processes involved in the absorption and the possibility of induced transparency from emptying the impurity levels should be considered.

In addition to being of fundamental interest, the short-pulse effect could have practical applications. It could be useful for diagnosis, as in distinguishing between multiphonon absorption and electronic-type absorption, for example. It could possibly afford a method of measuring the relaxation frequency  $\Gamma_f$  of the fundamental phonon mode directly. Its usefulness in high-power applications is limited by material breakdown at the high intensities required to obtain high

power with short pulse times. A typical value of breakdown intensity for alkali halides is  $2 \times 10^{10} \text{ W/cm}^2$ .<sup>10</sup> For  $t_{\text{puls}} = 5 \times 10^{-9} \text{ sec}$ , this gives 100 joules per pulse, or  $100 \text{ W/cm}^2$  average for a duty cycle of 1 sec. This value, which possibly could be raised by operating at lower than room temperature or further improving materials, can be compared with values of  $\sim 0.2$  to  $\sim 2 \times 10^4 \text{ W/cm}^2$  estimated to be obtainable for candidate window materials (ranging from Si to KBr) for a one second pulse, two second duty cycle, beam truncated at  $\frac{1}{3}$  its maximum intensity, and halving the intensity at the target.<sup>1</sup> If greater than half the intensity must be available at the target or if the beam is truncated at a lower intensity (as it usually is), these one-second-pulse values are reduced, by factors of a thousand or even greater in extreme cases. In such cases, the no-heating effect would be useful.

It should be mentioned that local heating of imperfections, which can lead to material failure, is a greater problem for short pulses than long ones for a given value of the energy per pulse.<sup>9</sup> The temperature rise tends to be lower for long pulses since the heat has time to diffuse away from the generation site. In this regard, notice that when (1) is satisfied, the time constant for the energy to leave the fundamental mode (after the pulse is transmitted) is  $1/\Gamma_f$ , which is considerably shorter than  $1/\Gamma(\omega)$ , since the fundamental mode oscillates at its resonant frequency after the drive field is turned off. A further limit to the high-power use of the short pulse effect is the air breakdown at the high intensities encountered in high-energy short-pulse systems.

Discussions with Dr. C. J. Duthler are gratefully acknowledged.

REFERENCES

\*This research was supported by the Advanced Research Projects Agency of the Department of Defense and was monitored by the Defense Supply Service - Washington, D. C., under Contract No. DAHC15-73-C-0127.

1. M. Sparks, J. Appl. Phys. 42, 5029 (1971).
2. M. Sparks, "Optical Distortion by Heated Windows in High-Power Laser Systems," Rand Corporation Report No. R-545-PR, September 1971.
3. M. Sparks, "Physical Principles, Materials Guidelines, and Materials List for High-Power 10.6 $\mu$  Windows," Rand Corporation Report No. R-863-PR, August 1971.
4. N. Bloembergen, "The Role of Cracks, Pores and Absorbing Inclusions on Laser Induced Damage Threshold at Surfaces of Transparent Dielectrics," to be published, Appl. Opt. 12 (April 1973).
5. R. B. Barnes and M. Czerny, Z. Physik 72, 477 (1931).
6. R. A. Cowley, Phonons in Perfect Lattices, Ed. R. W. H. Stevenson (Oliver and Boyd, Edinburgh and London, 1966). See Eq. (5.12), p. 192.
7. M. Sparks and L. J. Sham, Solid State Commun. 11, 1451 (1972), and Phys. Rev., in press.
8. T. Deutsch, J. Phys. Chem. Solids, in press.
9. M. Sparks and C. J. Duthler, J. Appl. Phys., in press.
10. D. W. Fradin, E. Yablonovitch, and M. Bass, Appl. Opt. 12, 697 (1973); NBS Special Publication 372, "Laser Induced Damage in Optical Materials," p. 27 (1972).